2013

Development of a Specialty Crop Harvester and Separation System

Kevin Lee Muell
Iowa State University

Development of a specialty crop harvester and separation system

By

Kevin Lee Muell

A thesis submitted to the graduate faculty

in partial fulfillment of the requirements for the degree of

MASTER OF SCIENCE

Major: Industrial and Agricultural Systems Technology

Program of Study Committee:
Stuart Birrell, Major Professor
Brian Steward
Steven Hoff
John Greaves

Iowa State University

Ames, Iowa

2013

TABLE OF CONTENTS

LIST OF FIGURES

LIST OF TABLES

ACKNOWLEDGEMENT

I would like to express my sincere gratitude to my major professor, Dr. Stuart Birrell, for giving me the opportunity to continue my education and study at Iowa State University under his mentorship. His understanding and optimism during stressful times and long hours are extremely appreciated. Without his patient guidance, expertise, and friendship this work could not have been completed.

The help of my committee members, Dr. Brian Steward and Dr. Steven Hoff, is also appreciated. Their guidance and expertise were invaluable throughout this work.

Kemin Industries is thanked for their support and funding of this research project. I am grateful to have been given the opportunity to partner with them on this project.

I would also like to thank Dr. John Greaves and Norman Cloud of Kemin Industries for their unwavering support and help throughout the long hours of field testing and data collection. Their ideas and contributions to the project are appreciated.

This work could not have been completed without the hard work and dedication of my friends and colleagues: Russ Hoffman, Joe Ripperger, Zach Williams, Brian McEvoy, Dustin Muell, and Ann Klein. I would like to express my gratitude for their help and assistance during the long hours of fabrication and testing.

My fiancée, Christa Scheffler, should also be thanked for her support, understanding, and love throughout this work and my life.

Lastly, I would like to thank my parents, Dale and Karen Muell, for their support throughout my education and work. They are thanked for instilling me with the work ethic, drive, and motivation to complete this work.

ABSTRACT

Mechanization has enabled many crops to be grown on a large scale due to the development and utilization of mechanical crop cultivation, harvesting, and processing technology. However, the development and utilization of specialty crops is commonly obstructed by the lack of harvesting technology available to mechanically harvest the crop. Post-harvest processing of harvested material also poses a challenge for the development of many crops. One such specialty crop that remains under-utilized due to the lack of mechanical harvesting and processing systems is *Physalis alkekengi,* or Chinese lantern.

Chinese lantern, a herbaceous perennial plant growing to heights of 30 – 110 cm, produces white flowers that result in a papery, inflated sepal that surrounds and encapsulates a berry. This arrangement, consisting of a sepal and berry, known as a lantern, has been identified as an excellent source of carotenoids. These carotenoids exist at a high concentration within the sepal, but not within the berry. A large volume of crop is required in order to realize the opportunities within these carotenoids. In order to be grown as a source of carotenoids, Chinese lantern must be grown over large productions acres with the lanterns harvested and processed mechanically.

This research focused on the development and testing of two systems: a mechanized harvesting system capable of detaching the lanterns from the plant stem and conveying them to a collection container, and a post-harvest processing system capable of separating the sepals from the berry. While several harvesting systems were developed, all were based on the same fundamental stripping method. Results from harvesting systems tests have shown that Chinese lantern can be harvested successfully by utilizing stripping elements and a header specifically designed for the crop. Two separation systems were developed and

tested as part of this research work. The results from this testing indicate that the sepals can be separated from the berry at a high efficiency through utilization of a differential drying and abrasion process.

CHAPTER 1: INTRODUCTION

1.1 Background

The invention of modern crop machinery has driven the agricultural industry to new heights. Driven by demand to produce a higher volume of product, mechanization of agricultural processes has been at the forefront of the agricultural industry. Mechanization of the harvesting process has allowed a variety of different crops to be grown on a commercial scale while reducing the overall labor and production costs. Historically, rising wages and the physical limits of hand harvesting have driven the need for mechanization in many crop industries. However, due to a lack of technology and mechanization, many specialty crops such as fruits, vegetables, tomatillos, and marigolds are still harvested and processed manually by hand. Harvesting these crops is the most labor-constrained operation in modern agriculture today. Constrained by labor needed to manually harvest crops; the size, location, and production volume of many operations is limited tremendously. The amount of labor needed for commercial hand-harvesting often approaches 50 percent of the total annual labor requirements for crop production, depending on the crop. The location of many specialty crop operations has been limited to areas where labor is abundant and relatively inexpensive. Historically, these areas have been third-world and developing countries. Hourly wages for employees and field laborers are rising around the globe, and very few areas remain where hand-harvesting of crops is economically feasible. High labor costs and low productivity of hand-harvesting has also limited the expansion and advancement of many specialty crops. To advance and utilize the potential of many specialty crops, the production process must

become economically feasible on a commercial scale. However, many opportunities within specialty crops remain unrealized due to the lack of a mechanical harvesting system. Developing safe, efficient, and cost effective mechanical harvesters is a top priority to allow for expansion of specialty crop industries.

1.2 Characteristics of Chinese Lantern

One such specialty crop that remains under-utilized due to the lack of mechanical harvesting and processing systems is *Physalis alkekengi*, or Chinese lantern. Chinese lantern is a herbaceous perennial plant growing to heights of 30 – 110 cm depending on growing conditions (Figure 1.1). Widely known as a popular ornamental plant, Chinese lantern produces white flowers, each resulting in a lantern with an average diameter of 1.72 cm. A papery, fused sepal comprised of sepals surrounds and encapsulates the berry creating a shell. This arrangement of a berry with attached sepals is commonly referred to as a lantern (Figure 1.2). Throughout plant growth, the berry and sepals change pigment and color, changing

Figure 1.1: Top portion of Chinese lantern

Figure 1.2: Typical Chinese lanterns with ruler

from green to a reddish-orange. Throughout maturity, the sepal retains strength and moisture and remaining fibrous. However, after being detached from the plant stem, the sepal begins to lose moisture and dehydrate, becoming brittle and weak.

Chinese lantern has been identified as an excellent source of specific carotenoids desired for medicinal and pharmaceutical purposes. These carotenoids exist within the reddish-orange pigment of the berry and sepals. The concentration of the carotenoids increases throughout the maturity cycle, reaching a plateau before decreasing as the plant nears the end of the growing season. It has been found that the sepal has a significantly higher concentration of desired carotenoids. These carotenoids are most easily extracted utilizing processes commonly used throughout the industry. However, Chinese lantern berries do not contain sufficient amounts of carotenoids to make extraction economical. The berries have also shown to be unsuitable for the extraction process. Therefore, effective and efficient berry/sepal separation is a vital process that must precede carotenoid extraction to achieve the required overall extraction efficiency and retain carotenoid quality.

Plant characteristics are very dependent on soil, weather, and cultivation conditions. When grown on a large scale, several methods of planting are utilized for crop establishment and expansion. Chinese lantern plants, are generally planted using a plug type transplanter machine for initial establishment during the first growing season. Inter-row spacing is set at 76.2 cm or 91.4 cm. Very little competition occurs between plants which results in a low-lying, vine type crop (Figure 1.3). Crop height is minimal as plants tend to branch and grow horizontal with respect to the ground. As the first growing season progresses, rhizomes expand and grow horizontally underground, expanding radially from each transplanted plug. If left underground, these rhizomes will survive until the following growing season and serve

as the base for new shoots and buds. The result is a second year crop of vertical, single stemmed (SVS) Chinese lantern plants (Figure 1.4). Crop height is mainly dependent on the availability of water and ranges from 30 to110 cm. The vertical structure of the second year crop is due to increased competition for soil space and sunlight.

Figure 1.3: First year Chinese lantern crop

Figure 1.4: Second year Chinese lantern crop

Rhizomes can be utilized as propagation material for establishing and expanding Chinese lantern crops. When used to expand a crop, rhizomes are dug up using a potato or rhizome digging machine. This occurs after the growing season has ended and harvest has been completed. The rhizomes are then placed into a root/rhizome transplanting machine that chops the rhizomes into smaller lengths and places them back into the ground in rows. Depending on desired planting density, effective crop area can be increased by as much a factor of 10. However, this type of trans-planting and crop expansion technique generally yields a sparse and vine type crop requiring two years before a vertical structure is obtained.

This indicates that crop geometry and density are very dependent on cultivation techniques and physiological age of the starting material.

To be grown as a commercially viable source of carotenoids, Chinese lantern plants must be grown over large productions acres with the lanterns harvested and processed mechanically. Currently, Chinese lantern is grown on minimal acres and specific areas of China where it is hand-harvested. Post-harvest separation of the berry and sepal is also done manually by hand. Hand-harvesting and manual processing over large production acres is not a feasible option for cultivation of this crop in the United States. This research focused on the development of a mechanized harvesting system and post-harvest processing system to separate the sepals from the berry. A variety of harvesting techniques were investigated including vibratory/shaking and stripping/combing systems in order to determine which harvesting technique would be best suited for harvesting Chinese lanterns. Several test stands and machines were designed and fabricated to test the concepts developed throughout this research work.

CHAPTER 2: REVIEW OF LITERATURE

2.1 Fruit Harvesting Systems and Methods

The fruit growing industry remains to be one of the few agricultural industries in which the harvesting process remains un-mechanized. Most fruit grown to be sold as fresh produce is manually harvested by hand to prevent damage to the fruit. However, many different techniques and methods are used to harvest fruit mechanically when it is feasible. Mechanical shakers have been used in many fruit crops with success. This differentiation between hand-harvesting and mechanical harvesting within a single crop can be seen in great depth within the coffee industry.

Harvesting of coffee is predominantly completed by hand-picking, similar to current Chinese lantern harvesting. Hand-harvesting allows for selectivity during the harvest process. Only ripe coffee berries can be harvested, leaving the unripen berries on the coffee tree to ripen and be harvested at a later date. This creates a higher quality end product that is highly desired and financially rewarded within the coffee industry. Other methods that have been employed to aid hand harvesting include; waiting for the berries to drop to the ground and then gathering them, beating the coffee berries off branches with long poles, or stripping berries together with leaves and winnowing later (Wrigley, 1988). Many of these methods are rarely used because of their destructive nature which reduces production and diminishes end product quality. This holds true for Chinese lantern crops as well. Carotenoids in the lanterns begin to decay once the lantern is detached from the main plant stem (Cloud, 2011). Once detached from the plant stem, exposure to sunlight increases the rate of this decay,

eliminating many alternative harvesting methods. In many cases, the high cost and short supply of labor may justify the desire for mechanical harvesters by many growers (Cargill, 1999).

Most mechanical coffee harvesters use slight variations of similar vibration technology employed throughout the fruit and nut growing industry. Coffee harvesters are generally designed to straddle a single row of trees and remove the fruit from the tree as the tree passes through the machines. As the tree enters the harvester, it is met by two vertical shaker columns with radially protruding plastic fingers (Figure 2.1). The plastic fingers impact the trees, causing an excitation force to detach the wanted coffee fruit. This harvesting method is similar to most vibration harvesting techniques utilized throughout the fruit and nut industry. The basic principle is to accelerate each fruit so that the inertia force developed is greater than the bonding force between the fruit/nut and tree (Kepner *et al*, 1987). The excitation force is typically derived from the cyclic oscillation of either a crank slider or two opposite rotating eccentric masses connected to the tree to be harvested (Thomson, 1988). As fruits are detached from the plant they drop vertically through the plant onto catching

Figure 2.1: Coffee harvester with shaker columns

Figure 2.2: Coffee harvester catch panel floor

units near ground level. The catching units used in shaker harvesting are collection surfaces below the shaker that extend under the tree, covering the drop area of the fruits (Cargill, 1999). In the case of the coffee harvester, the catching units are intricate plastic panels that individually rotate around a pivot point, allowing the trunk of each tree to pass through the machine (Figure 2.2). A conveyor system continuously transfers the harvested fruits to a collection wagon towed between the adjacent rows of trees.

There are limits to this type of mechanical harvesting process. Generally, vibratory harvesting systems perform well in crops that have low fruit detachment forces, low crop density, and require minimal vibration to detach desired crop materials. Excessive vibration is likely to cause damage to the plant/tree and reduce future production. To reduce vibration requirements, it is common practice to apply the power source to shake one tree at a time (Den Hartog, 1985). Mechanical vibratory systems also require crops to be grown in rows for several reasons including the following; machinery must be able to move throughout the crop, catch units must be placed under each plant/tree being vibrated in order to collect detached crop, the vibration columns or clamps must have ample access to the crop. These requirements limit the number or crops that can be effectively harvested using vibratory techniques.

Mechanical harvesters utilizing shaker or vibratory technology have been used to harvest a variety of other crops including; apples, peaches, pears, plums, prunes, apricots, grapes, lemons, grapefruit, olives, and many others. However, due to the non-selective nature of vibratory harvesting, all of the available fruit is generally harvested during the initial pass through the crop. This generally diminishes quality and subsequently reduces the market price received for the product. This has become a major challenge for many

producers and attempts have been made to reduce the amount of immature fruit harvested. In many crops, ripe fruits are easier to detach than unripen fruits, hence, in developing principles for a mechanical shaker, it is necessary to determine the optimal mechanical parameters.

The use of robotics has been growing steadily as technology has improved. Many harvesting systems have been developed to utilize robotics and computer vision systems. While this type of harvesting system offers a solution to many of the problems and challenges of mechanical harvesting, there are restrictions on the type of crop that can be harvested. This type of bulk harvesting requires, in addition to the canopy-like growth habit, uniform fruit ripeness at harvest, firm and tough fruit, high resistance to damage, and short/stiff limbs (Peterson, 2005). Chinese lanterns pose another challenge due to the fact that they retain a strong attachment bond while growing on flexible stems instead of trees or brushes. This arrangement makes detachment of the lantern difficult without harming the main plant stem. Crop density also impacts the efficiency of robotic harvesting systems. Robotic harvesting works well in low density crops where a limited number or large fruits are available. High density crops present challenges as the number of required operations and computing power is increased. As crop density increases, the number of harvesting cycles per second required to maintain acceptable harvesting rate also increases. While robotic and computer vision technology offer solutions for many of the problems associated with mechanical harvesting, several challenges remain. According to Sarig (1993), the major problems with robotic picking that must be solved include recognizing and locating the fruit, detaching it according to prescribed criteria without damaging the fruit or the tree. Unstructured crops present another challenge. In unstructured crops, fruits are distributed

throughout the canopy in a random manner, making it essentially impossible to explicitly model (Plebe, 2001). In addition to these challenges, the robotic system needs to be economically sound to warrant its use as an alternative method to hand picking. These limitations, coupled with the characteristics of the Chinese lantern plants reduce the possibility of a developing a successful robotic harvesting system capable of achieving desired throughput and efficiency.

2.2 Stripping Header Systems

Another approach that has been widely researched and implemented is stripping fruit or grain from the plant stem. Stripping is a very old harvesting concept that continues to challenge designers through the centuries (Tado *et al;*, 1998). These challenges include designing stripping headers that are capable of harvesting crops in a wide variety of conditions. Stripping harvesters have mainly been developed for the small grains and cereal crops. These crops are easily stripped because of their SVS and uniform grain diameters.

One of the most influential developments in stripping technology is the Silsoe stripper. Initial investigations of this design began at Silsoe Research Institute in the UK in 1984 (Tado *et al;*, 1988). The Silsoe design utilizes a rotor that is rotated about an axis perpendicular to the direction of harvester travel (Figure 2.3). Flexible arrowhead stripping elements are mounted on the rotor and essentially comb through the crop, stripping the grain from the plant stem. The arrowhead stripping elements consist of a molded thermoplastic material forming a “V” shape with a circular recess at the base (Tado *et al;*, 1988). These are commonly referred to as keyhole stripping teeth (Figure 2.3). The size of the circular recess

is directly related to the size of the crop being harvested. This parameter can be adjusted to compliment the specific crop being harvested.

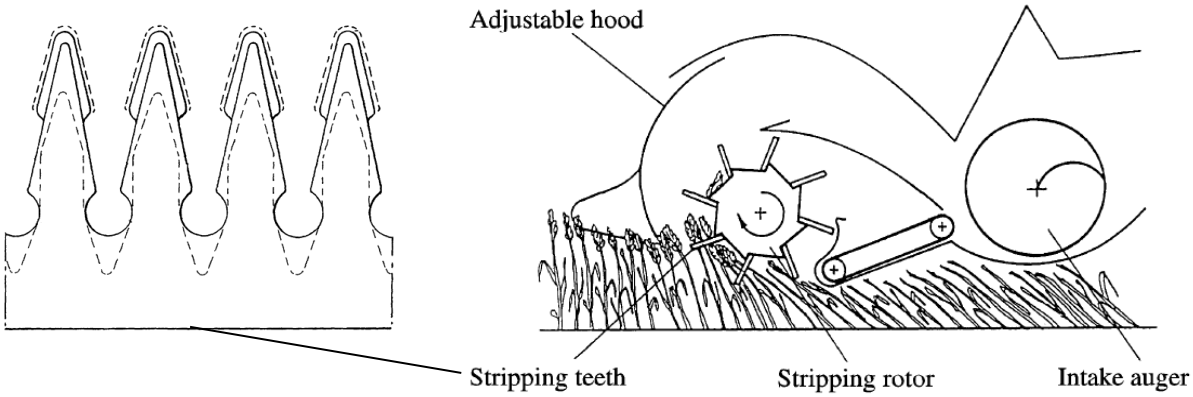

Figure 2.3: Side view of Silsoe stripping header and keyhole teeth

The efficiency of operation is directly related on the ability of the stripping elements to collect only the wanted grain, leaving behind all other material. Plant damage during stripping can cause large amounts of unwanted material to be collected with the grain. For this reason, it has been customary to make the comb plates of a thermoplastic material, which causes little, if any damage to the crop stems (Shelbourne, 2001).

The most popular production machine using this stripping technology is the Shelbourne Reynolds stripper header. This header is currently being used to harvest cereal, rice, grass seed, and other small grain crops. Shelbourne Reynolds stripper headers are attached to mainstream production combines and operated in a similar fashion to regular cutter-bar headers. This technology has shown to be very productive and efficient in widely varying conditions. In Germany, research at Halle showed that combine capacity could be increased by 70 to 90% with the stripper header (Papesch, 1995). This is mainly due to the reduced amount of material other than grain (MOG) entering the threshing components of the

combine. Reducing MOG enables grain to be cleaned better than when harvesting with conventional cutter-bar headers. However, performance of the stripper is more sensitive to machine settings as well as crop and weather conditions (Tado *et al;*, 1988).

There are many parameters to be explored when adapting stripping technology for other crops. Extensive work has shown that the application of the rotary stripping system can be extended to include the harvesting of other crops (Klinner *et al;*, 1987). Data needs to be collected from the crop to be harvested in order to design the correct stripping elements. The rotational speed of the transversely mounted rotor will need to be adjusted for different conditions existing within the crop to be harvested. Further research and development is needed in order to apply and optimize this technology for various specialty crops.

While many stripping systems have been developed for self-propelled, large scale harvesters, others have focused on creating an aid to the hand-picking laborer. Merritt (1995) developed a hand held unit with powered oscillating rake member having extending tines to strip fruit from branches. This apparatus is aimed to aid the harvest of olives and like fruit.

Figure 2.4: Cifarelli SC800 portable stem vibrator

Figure 2.5: PSV end-effector rake fingers

Similar devices have been developed such as the portable stem vibrator (PSV) for use in small fruit and berry harvesting (Figure 2.4). These types of devices aid the manual harvesting process and dramatically increase harvesting efficiencies. A small internal combustion engine creates hydraulic pressure which is utilized to oscillate an end-effector. Many types of end-effectors are utilized including c-clamps that attach to branches and also rake fingers that strip through the branches while oscillating (Figure 2.5). Oliveros (2005) has shown that the use of PSV devices to harvest coffee can increase harvest efficiencies by up to 458.3% over traditional hand harvesting methods. It was also shown that an 80% reduction in labor requirements can also be achieved by utilizing PSV's. However, although PSV devices have shown to be advantageous during the detachment phase of harvest, the collection phase remains completely manual and labor intensive.

2.3 Crop Separation Systems

While developing a mechanized harvesting system continues to be a hurdle throughout many crop growing industries, processing harvested crop material also continues to be an ever present issue. Many crops require an immediate post-harvest processing to create an end product suitable for market. These processes generally include at least one of the following; removing any unwanted material that was collected during harvesting, drying material to desired moisture content, crushing or grinding crop material to desired particle size. In the case of Chinese lantern, the post-harvest processing includes removing unwanted materials from the harvested lanterns and separating the sepals from the berry to create a dual path material stream.

Many types of systems exist to separate and process crop materials. In grain and cereal crops, threshing technology is utilized to loosen grain from the stalk and chaff that surrounds it. Both major styles of threshing mechanisms, cylinder or rotor and concave, move the crop between the surface of a rotating cylinder and an open mesh concave. Action in the threshing area detaches grain from other plant material by impact force and separates the detached free grain from other crop material (Kutz, 2007). Although most of the grain has been detached in the threshing area, it must still be removed from the MOG in order to reach performance and market criteria. There are two separation processes commonly used: gravity dependent straw walkers or rotary separation (Kutz, 2007). Straw walkers consist of sieve sections that oscillate up and down with the addition of longitudinal movement. This movement shakes the remaining grain from the crop mat consisting of grain and MOG. Rotary separation utilizes centrifugal force to move heavier grain through the concave and into collection systems. Straw walker separation systems exhibit potential for use in separating detached, harvested lanterns from unwanted materials such as stems and leaves.

Threshing systems work well when small, dense, and hard crop materials are processed. However, the physical impacts and turbulent nature would almost certainly crush Chinese lantern berries and greatly decrease extraction efficiencies. While separation systems are heavily developed and proven throughout the grain and cereal crop industries, very little work has been done to develop commercial scale separation or de-husking mechanisms in the fruit or berry industries. In order for many fruits or berries to be processed or sold, it is desirable to remove the sepals. In some cases, the sepal is of value while the berry is not desired. A fruit husking machine capable of removing the outer wrapper of onions, oranges and similar fruit was developed by Crawford (1944). Wang

(1966) investigated mechanical de-husking for *Physalis peruviana*, Cape gooseberry, also known in Hawaii as Poha. Belonging to the same genus, *Physalis*, Chinese lantern (*Physalis alkekengi*) exhibits many of the same characteristics as cape gooseberry plants. The immature green berry is relatively strong, while the mature berry is soft and easily damaged by impact or external forces. The sepal remains flexible and is able to withstand strong tensile forces throughout the maturation cycle. Because the sepals and berry possess different frictional coefficients, it was determined that removal of the cape gooseberry sepals could be accomplished using counter-rotating frictional rollers (Wang 1966). As seen in figure 2.6, counter-rotating rollers pinch the sepal, pulling it down and through the rollers while the berry remains above the rollers due to the resolution of forces. The force required to detach the husk from the berry must also be considered when analyzing this type of separation system. The frictional coefficients of the rollers and interaction with the sepal must be so that enough frictional force is generated to prevent slippage of the sepals between the rollers. It was observed that effective and efficient separation occurred when the sepal – berry pair was introduced to the rollers in a sideways orientation. However, when a sepal-berry pair was introduced with a tip-end first orientation, the entire pair was pinched and

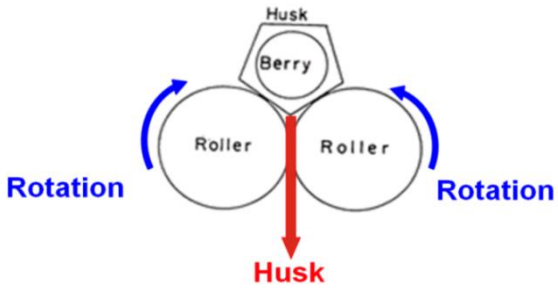

Figure 2.6: Counter-rotating friction roller separation system

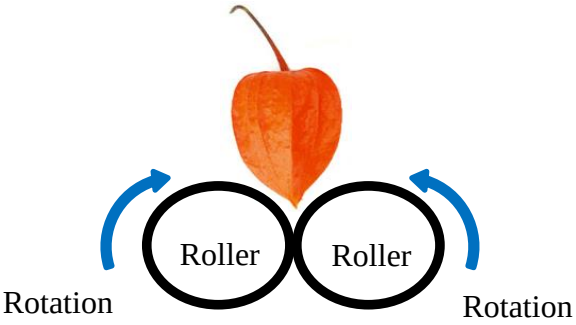

Figure 2.7: Lantern and rollers, tip-down

pulled through the roller, crushing the berry (Figure 2.7).

In the study conducted by Wang (1966), it was found that if a cut was introduced on the sepal before the sepal-berry pair was dropped on the rollers, the cut on the sepal would provide an escape for the berry, even if introduced to the rollers tip-end first. Two oxygen-acetylene torch nozzles were used to produce small flames to induce a cut or slit on the sepal. This pre-cutting method proved to be effective even when the sepal-berry pair dropped tip end first onto the rollers. However, this type of pre-cutting would most likely damage or destroy the sepals, reducing the amount of carotenoids available for extraction, which is unacceptable as it is the product of interest. A similar mechanical separation system described by Flores (2007) is designed to remove the sepals from a tomatillo (*Physalis philadelphica*). Also being from the *Physalis* genus, tomatillos exhibit many of the same characteristics as a Chinese lantern. Instead of cutting the sepals as a pre-treatment to counter-rotating rollers, the tomatillos were soaked in water for a period of time to soften the

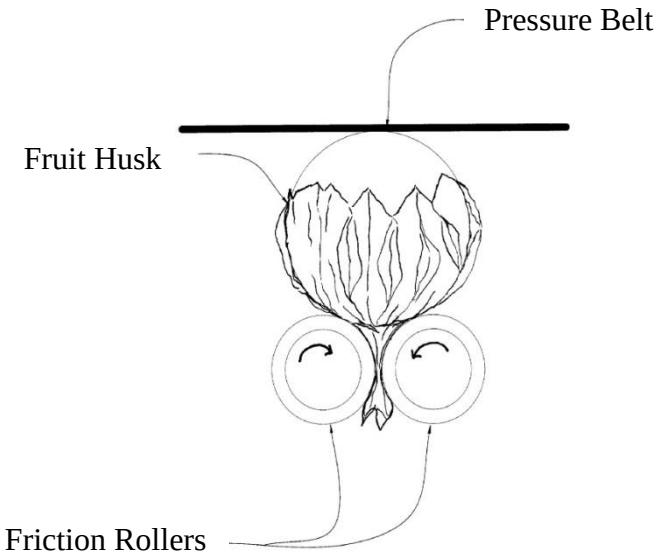

Figure 2.8: Friction rollers and pressure belt (Granger, 2002)

sepals and allow for a more efficient separation.

A similar mechanical separation system for small fruits was described by Granger (2002). Fruit and sepal pairs are soaked in water as a pre-treatment for separation by counter-rotating friction rollers. Once soaked with water, the fruit and sepal pairs are directed on top of the friction rollers and beneath a pressure belt. The pressure belt, which is comprised of a series of interlinked flaps, exerts appropriate pressure onto the fruits so they can be captured by the pinching rollers lying directly underneath (Granger, 2002). As seen in Figure 2.8, the spacing between the pressure belt and rollers must be set in accordance with the diameter of the fruit being processed. Flores (2007) utilized a similar pressure belt system that continuously engages and directs the tomatillos onto the counter-rotating rollers (Figure 2.9). Such continuous engagement with the rollers results in a more thorough removal of the sepals of the tomatillo fruit (Flores, 2007).

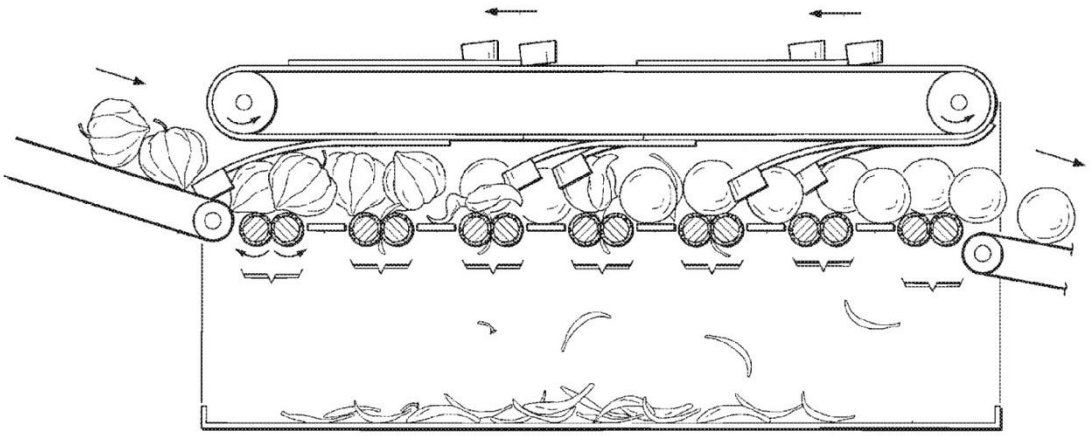

Figure 2.9: Friction rollers and engagement belt (Flores, 2007)

While all three systems described by Flores (2007), Wang (1966), and Granger (2002) utilize counter-rotating rollers to create frictional force and detach the sepals from the

berry, several differences do exist between the systems. These differences can be seen in the direction of crop material flow with respect to the counter-rotating rollers. The system developed by Granger (2002) and Wang (1966) moves crop material parallel with respect to the roller axis. Any individual cape gooseberry comes into contact with only one pair of rollers. The tomatillo husking machine developed by Flores (2007) moves crop material perpendicular to the roller axis (Figure 2.9). Tomatillos come into contact with each pair of rollers within the system. Advantages may exist within this type of system because of the increased probability of successful de-husking created by contact with multiple pairs of counter-rotating friction rollers.

CHAPTER 3: OBJECTIVES

The goal of this research project was to develop a mechanical harvesting and post-harvest processing system for Chinese lantern that will enable commercial production and advancement of the crop. To accomplish this goal, three specific objectives were derived. The specific objectives of this research project were as follows:

- Objective #1: Develop and fabricate a small scale mechanical harvest system capable of detaching the sepal and berry from the main plant stem. Tasks supporting this objective include:
    - Design and develop stripping elements capable of detaching Chinese lanterns from plant stem.
    - Determine system feasibility through field testing.
    - Analyze performance and determine improvements for scaled up harvesting system.
- Objective #2: Develop and fabricate a self-propelled mechanical harvesting system capable of continuous harvest and conveyance of crop material. Tasks supporting this objective include:
    - Conduct field tests across different field conditions and crop varieties.
    - Collect data and observations in order to make data driven decisions for improvements and modifications to the harvesting system.
    - Analyze performance of the system to determine best operating parameters and conditions.

  - Continuously improve harvesting system to achieve acceptable stripping and harvesting efficiencies.
- Objective #3: Develop a post-harvest processing system capable of mechanically separating the sepals from the berry. Tasks supporting this objective include:
  - Conduct initial system tests to investigate effects of component parameters
  - Collect data for system analysis and improvement
  - Optimize operating parameters through testing and observations

The long term focus of this research project is to develop feasible, economical systems that will allow Chinese lantern and other similar crops to be grown on a commercial scale. Having the ability to harvest and process these crops mechanically will allow for the advancement of the crops and a realization of the many opportunities they hold.

CHAPTER 4: HARVESTING SYSTEM DEVELOPMENT

For Chinese lantern to be grown on a commercial scale as a source of carotenoids, the harvesting process must be mechanized. Mechanically harvesting Chinese lantern requires: detachment of the berry and sepals from the main plant stem, and conveyance of the harvested material to a collection container or vehicle. Several agronomic characteristics of Chinese lantern were analyzed in order to determine the best approach for mechanical harvesting.

The attachment force of the lantern to the main plant stem is quite high, indicating that a large frequency and amplitude would be required to detach the lantern using vibration. The absence of stiff members or stems in the plant to transfer vibratory motion also discourages the use of vibration as a harvesting method. Vibratory harvesting methods also require the use of a catch mechanism to collect and transport harvested material. Lanterns are dispersed throughout the main plant stem, starting approximately 4-6 inches vertically above the ground. The close proximity of lanterns to the ground makes designing and developing collection mechanisms difficult. Once established, Chinese lantern is very invasive and grows randomly much like an alfalfa field. This random placement and lack of rows makes delivering vibration to each individual plant stem a challenge.

The SVS of Chinese lantern plants are very similar to grain and cereal crops which lend themselves well to mechanical harvesting by stripping methods. A stripping header harvesting system is also able to handle random placement and crop growth. Utilizing stripping fingers to comb through the stems, the berries can be used as a catch point and

allow the stripping fingers to apply a detachment force to the lantern. This section will focus on the design and development of a stripping type harvester system for Chinese lantern.

4.1 Stripping Finger Design and Development

Stripping fingers are the core of many stripping header and harvester systems. They serve several purposes during crop harvest: comb through and individualize plant stems, catch and apply detachment force to desired crop materials, and deliver detached material to a collection system. Many times, stripping fingers are individualized for each crop, designed to maximize harvest efficiency and decrease the collection of unwanted crop materials. Utilizing the correct stripping finger elements can optimize machine performance.

In order to correctly design stripping fingers for Chinese lantern several characteristics must be known about the crop. These characteristics include main plant stem and berry diameters. The stem diameter determines the size of opening leading to the keyhole component of the stripping finger while the berry diameter determines the size of the keyhole. In order to collect this data, 100 lanterns were examined and measured while 100 main plant stems were also measured. The results of this data collection can be seen in Table 4.1. All measurements were taken from 2011 crop material using a digital caliper and scale.

Table 4.1: Chinese lantern characteristics

Parameter	Berry + Calyx Weight (g)	Berry + Calyx Diameter (mm)	Berry Diameter (mm)	Berry Weight (g)	Calyx Weight (g)	Main Stem Diameter (mm)
Range	5.84	28.93	9.93	5.25	0.59	4.85
Std Dev	1.19	4.33	2.11	1.11	0.10	1.06
Average	3.22	23.87	17.42	2.84	0.36	6.99

The stripping fingers were designed using Pro-Engineer software (Parametric Technology Corporation, Needham, MA) and can be seen in Figure 4.1. Taking into account the average berry diameter and standard deviation, the keyhole diameter of the stripping fingers was set to 12.7 mm. At 4.72 mm smaller than the average berry diameter and 5.71mm larger than the average stem diameter, the keyholes were designed to catch and detach the lanterns while allowing stems to slide through freely. Assuming a normal distribution of berry diameters, the keyhole stripping fingers are capable of detaching approximately 95% of all berries. The opening leading to the keyhole was designed to be 10.41mm, slightly smaller than the keyhole itself. This smaller opening creates a "cup" and increases the surface area over which the detachment force can be applied. It also deters larger debris or weed stems from entering the keyhole and causing plugging.

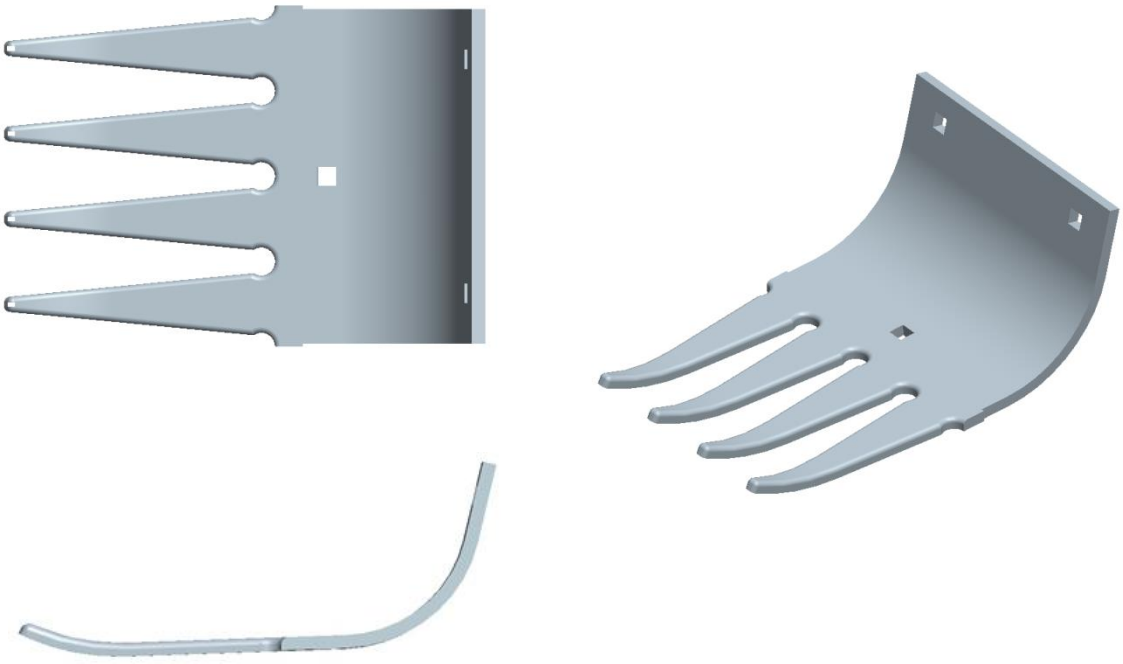

Figure 4.1: Keyhole stripping finger

As is with most cutting or stripping elements, the stripping fingers were designed to be modular and interchangeable. This design allows all stripping elements to be identical and easily interchanged in case of breakage. At 15.25 cm wide, the fingers are designed to be attached directly next to each other on a reel or other harvesting mechanism. The stripping units were designed to meet at the center of the keyhole, retaining strength in the narrow, extending fingers. This mating design is very similar to the stripping elements used in the Silsoe and Shelbourne stripping systems. However, the design differs greatly in the curved nature of the stripping finger. The curvature is modeled much like a human hand when stripping fruit or berries off stems. Utilizing a curved stripping finger allows the detachment force applied to the Chinese lantern berry to be directed into the curved, cupping portion of the stripping finger. In order to minimize stripping fingers digging into the soil, the tips of the protruding fingers were designed with a slight curvature.

Several manufacturing methods were considered to fabricate the stripping fingers. However, due to the curved nature and multiple radii along the keyholes and fingers, machining and other metal forming methods were found to be time-consuming and cost-inefficient. Several rapid prototyping methods offered solutions to produce small quantities without incurring significant investment costs. Through analysis of these rapid prototyping methods, selective laser sintering was chosen to produce the first batch of stripping fingers.

Selective Laser Sintering (SLS) is an additive manufacturing technology that uses a high power laser to fuse plastic, ceramic, or glass powders into a 3-dimensional object. Cross-sections of the part are scanned using data generated from a 3-D CAD file. The laser then selectively sinters material together to form the part structure as indicated in the CAD file. After each cross-section is scanned the powder bed is lowered by one layer

thickness, a new layer of material is applied on top, with the process repeated until the part is completed. This process is capable of producing working prototypes that can endure field testing. In order to build strength into the stripping fingers, glass filled nylon was selected as the material for fabrication. This type of manufacturing process and material resulted in a robust stripping finger. The stripping fingers were manufactured by GPI Prototype and Manufacturing Services in Chicago, IL. SLS proved to be very cost-efficient when producing small quantities of the stripping fingers. However, as this project progress a larger quantity of stripping fingers was required.

Injection molding, a process designed for high volume and throughput, was chosen as the process to produce the higher quantities of stripping fingers required. Zytel 70G33 HSIL NC010 was injected into an aluminum mold to produce the stripping fingers. Zytel, a 33% glass-reinforced nylon, produced a very rigid stripping finger required by the crop stripping and detachment process. This manufacturing was also conducted by GPI Prototype and Manufacturing Services.

4.2 Rotary Harvester Design

While a mechanical harvesting system has never been developed for Chinese lantern, several other harvesting systems have been developed utilizing stripping technology. These systems utilize a horizontal, rotating reel to which stripping elements are attached. Using the principles established by these systems, a small hand- powered mechanical harvesting system was developed. The goal of this system was to test the feasibility and performance of the stripping fingers.

The keyhole stripping fingers were designed to be attached to a horizontal rotating reel, allowing them to comb through the crop while detaching Chinese lanterns. Attaching the fingers to a reel was accomplished by welding six attachment plates to a length of 6.35cm OD tubing. These attachment plates were placed in 60 degree increments around the reel. During rotation, the stripping fingers enter the crop and direct plant stems into the keyhole portion of the stripping finger. Once in the keyhole portion, detachment force can be applied to the berry of the Chinese lantern as the plant stem slides through the keyhole. The detachment force can be described as perpendicular to the surface of the stripping finger at the keyhole.

When attached to a rotating reel, the detachment force is quickly directed toward the center of the reel as the stripping fingers are rotated through the crop. Directing the detachment force towards the center of the reel assists with the collection of detached fruit

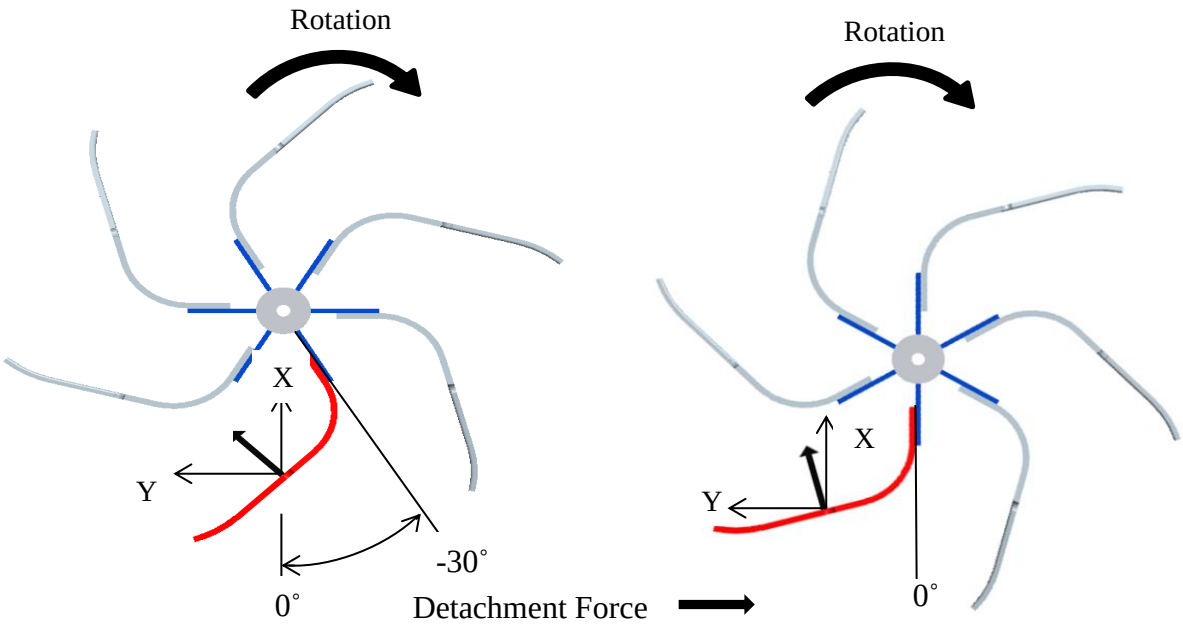

Figure 4.2: Rotation of stripping finger reel, -30 to 0 degrees

and reduces harvesting losses due to detached fruit falling out of the stripping fingers. As the stripping fingers and reel are rotated approximately 30 degrees, -30 to 0 degrees, the stripping fingers are inserted into the crop material (Figure 4.2).

Through this portion of reel rotation the detachment force is directed slightly away from the center of the reel. However, when rotated from 0 degrees to 30 degrees, the detachment force becomes directed into the reel (Figure 4.3). The curvature of the stripping fingers creates this change direction of the detachment force and attempts to reduce collection losses occurring after detachment. As the reel and stripping finger rotation approaches 60 degrees the detachment force continues to be directed towards the center of the reel (Figure 4.4). Past 60 degrees the stripping fingers begin to exit the crop and plant stems. The curvature of the stripping fingers also becomes critical throughout this portion of rotation. The stripping fingers are curved in order to retain the detached Chinese lanterns and convey them to a collection system or hopper.

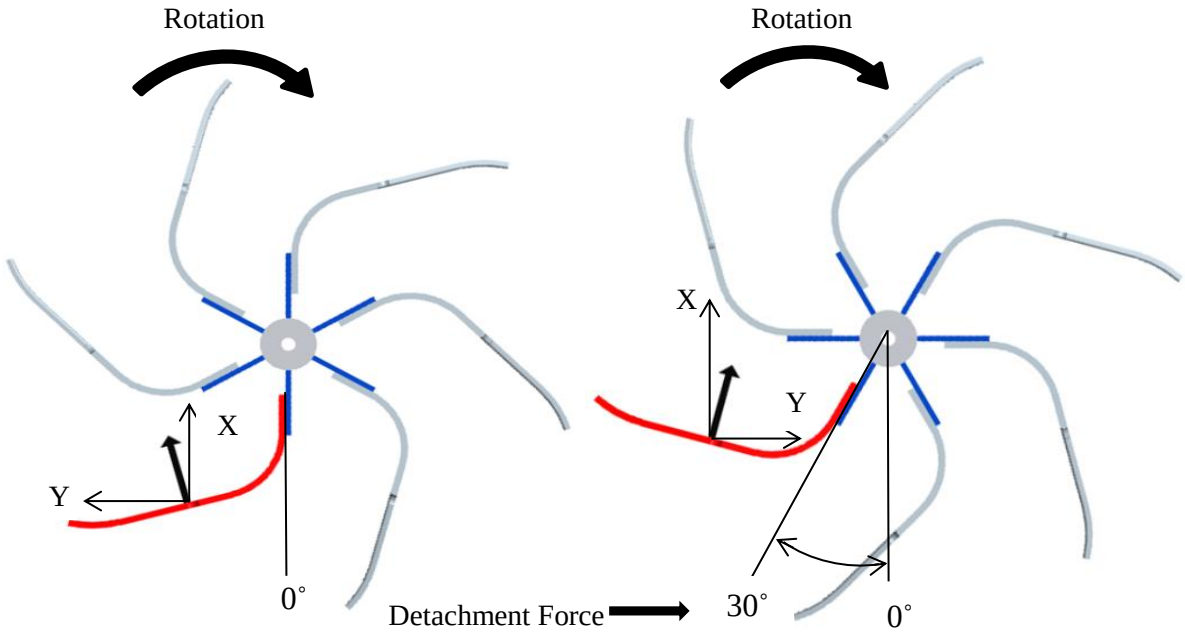

Figure 4.3: Rotation of stripping finger reel, 0 to 30 degrees

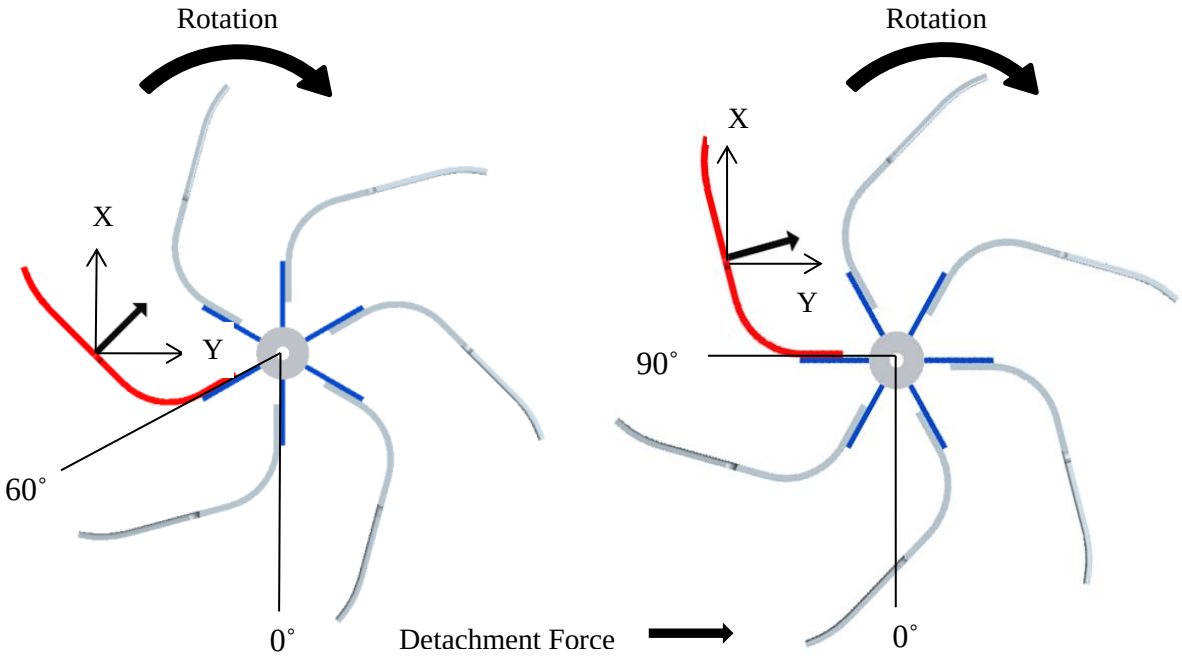

Figure 4.4: Rotation of stripping finger reel, 60 and 90 degrees

Depending on rotational speed of the stripping fingers and reel, two methods were developed to remove the detached Chinese lanterns from the reel and fingers. When a high rotational speed is utilized, the harvesting system is designed to utilize centrifugal force to convey the detached lanterns to a collection system. A set of dislodging fingers were designed to help remove detached lanterns when a low rotational speed is required. The dislodging fingers are a mirror image of the stripping finger geometry. Offsetting the dislodging fingers horizontally places them between the stripping fingers and dislodges any stuck material. These were mounted using adjustable brackets to allow for horizontal, vertical, and angular adjustment. Integration of the dislodging finger mounts into the stripping reel mounts enables a single adjustment of vertical height for the entire harvesting system. The stripping fingers were also developed to accommodate deflection shields to

keep detached Chinese lanterns from falling too far in-between successive rows of stripping fingers. These deflection shields simply bolt on to successive rows of stripping fingers and can be easily added or removed as needed. Figure 4.5 and 4.6 display Pro-Engineer models of the dislodging fingers and deflection shields respectively.

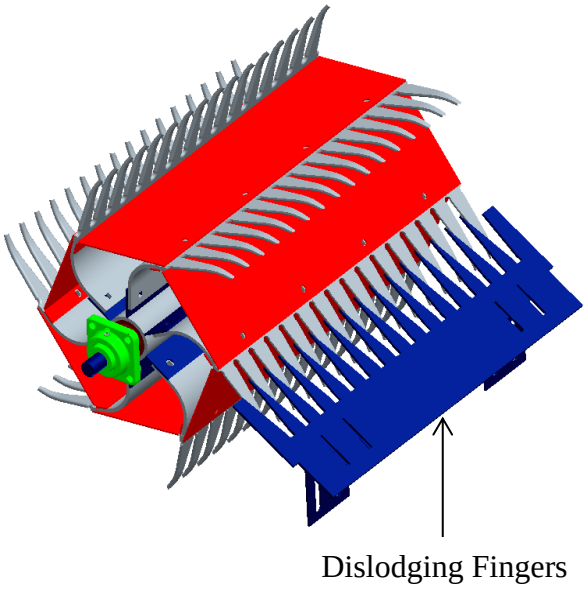

Figure 4.5: Dislodging fingers and stripping reel

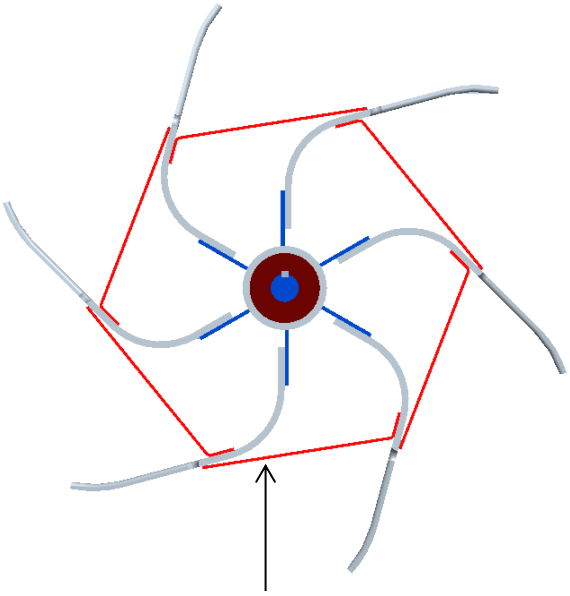

Figure 4.6: Deflection shields and stripping reel

A small test platform was fabricated using these principles for testing and validating the stripping fingers during the fall 2011 harvest. The stripping reel utilized six rows of four stripping fingers, equally spaced around the reel center tube. This arrangement resulted in an effective harvesting width of 53.34 cm. The reel was hand-powered using a crank to permit variable rotational speed. A 1:1 gear ratio was utilized between the hand-crank and stripping reel. The stripping reel height was made to be adjustable with a range of finger to ground

clearance of 0 to 30 cm. A cross section view of this harvesting system can be seen in Figure 4.7.

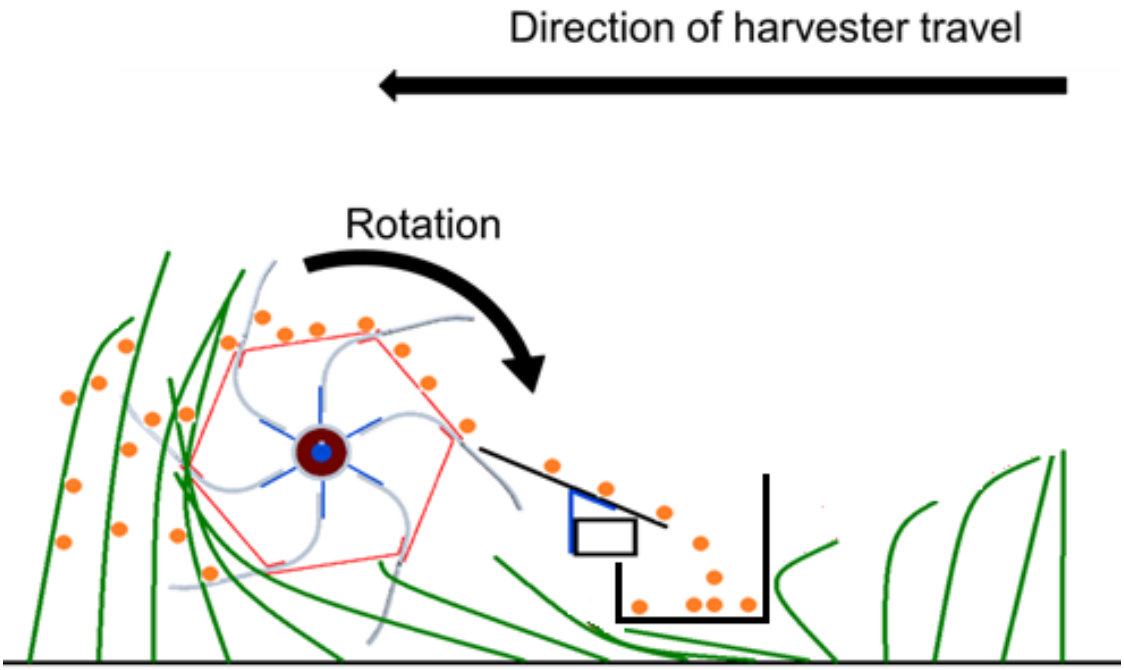

Figure 4.7: Rotary harvester cross-section view

4.3 Integrated Harvesting and Conveyance Design

During initial testing of the rotary system, significant loss of harvested material was seen in the transition portion of the harvester, between the stripping finger reel and collection hopper. In order to combat these losses, another small test platform was developed alongside the rotary reel harvester during the first year of testing, fall 2011. This design integrated crop harvesting and conveyance into one singular system. Stripping fingers were attached to a conveyor belt system comprised of roller chain, attachment links, angle iron cross bar slats, and rubber belting. Attachment links, inserted every 25.4 cm into two lengths of roller chain, provided attachment points for angle iron cross bar slats. Stripping fingers were then

attached to the slats while rubber belting was attached between slats. The chain and slat system was then positioned on a pair of shafts and sprockets. Rotating one of the shafts propelled the conveyor belt, moving the keyhole stripping fingers through the crop and conveying the detached crop to a collection hopper or material handling system. In order to keep standing crop material engaged with the stripping fingers a rotating reel was added to the front of the system. This reel comprised of six strip brushes equally spaced around a center cylinder. Rotating opposite of the stripping fingers, the reel fed standing crop material into the stripping finger conveyor belt. A cross section view of this harvesting system can be seen in Figure 4.8. Attaching the stripping fingers to a chain and rubber belting system creates a conveyor that elevates the detached Chinese lanterns. Elevating the harvested crop material also allows the collection hopper to elevated, resulting in higher ground clearance. Similar to the rotary system previously discussed, the rotation of the stripping fingers around

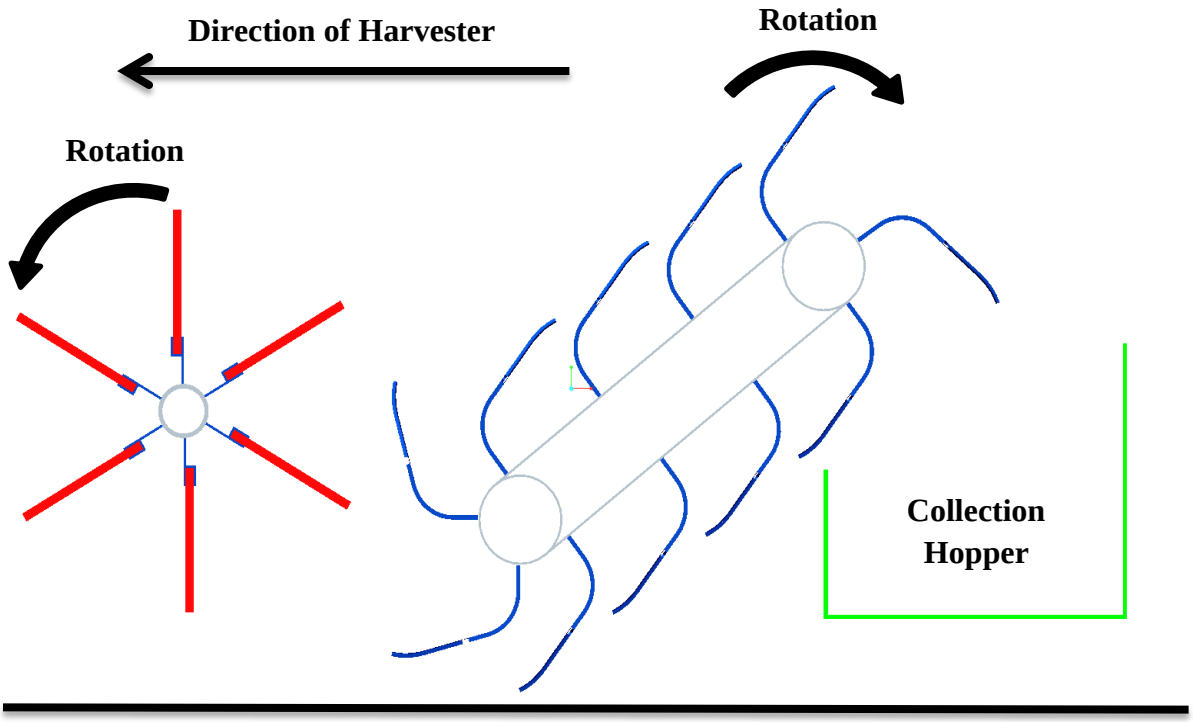

Figure 4.8: Integrated harvester and conveyance system

the lower shaft causes the detachment force to be directed into the conveyance and rubber belting system. Harvesting width was also the same as the rotary system, 53.34 cm, or 4 stripping finger units wide. Figure 4.9 displays this machine in a Chinese lantern test plot.

In order to achieve constant harvesting system rotation speed, the stripping finger belt and conveyor system was powered by a 12 VDC high torque right-angle gear motor (Buyers Products, Mentor, Ohio). An internal 90:1 gear ratio reduced the rotational speed of the output shaft to 40 revolutions per minute (RPM). Capable of producing a maximum of 213.54 N·m of torque, this motor proved to be more than adequate to power the harvesting system. Power was supplied to the motor via a 12 VDC battery mounted on top of the harvesting unit. An extension cord was used as a tether between the battery on the harvester and a battery in a pickup truck. The pickup truck engine was left running during harvesting

Figure 4.9: Integrated harvesting and conveyance test platform

to charge the batteries and provide a constant source of power to the battery on the harvester. The front reel was also powered by this electric motor. Forward motion of the harvester was achieved by manually pushing the harvester or towing it behind a small tractor. When towed behind a tractor, forward speed was limited to 1 mile per hour (MPH).

Due to the output shaft speed of the motor already being reduced, no further reduction was necessary. A 1:1 gear ratio was utilized to drive the stripping finger conveyor belt system. Using #60-15 tooth sprockets to drive the stripping finger belt system resulted in a belt linear velocity of 12.7 meters/minute. To keep crop material firmly engaged with the stripping fingers, a 1.60:1 gear ratio was used to drive the front reel from the stripping finger belt system. This gear ratio resulted in a rotational speed of 64 RPM. 25.4 cm strip brushes and a 5.08 center tube were used to fabricate the front reel, resulting in an overall diameter of 30.48cm and linear velocity at the outer edges of 61.28 meters/minute.

To account for a variety of crop conditions, the front reel mounting system was designed so that the reel itself could be adjusted in both the vertical and horizontal directions. The vertical proximity of the stripping fingers to the ground could also be adjusted by raising or lowering the lower shaft of the stripping finger belt system. The front reel and stripping finger belt speeds can be adjusted by swapping out drive sprockets and subsequently changing the gear ratios. However, these speeds were never changed during testing.

The collection hopper was designed to be removable from the main harvesting unit. This allowed for the hopper to be easily emptied and cleaned out. The removable hopper design also provided easy access to the stripping finger belt system for any necessary maintenance or repairs.

4.4 Self-Propelled Harvester Design and Development

In order to scale up the harvesting system and conduct larger scale tests, a self-propelled harvesting platform was required. The design and development of this machine took place after the initial testing of the stripping fingers and harvesting system was completed in fall 2011. The self-propelled harvesting platform was designed to facilitate continuous harvest and conveyance of Chinese lantern crop material. This section includes and explains details about the design and development of the self-propelled harvester test platform and header.

4.4.1 Power Unit Design and Development

The driving factor behind the power unit design was a fully customized machine capable of meeting the requirements of the harvesting system. Designing a custom machine allowed for several key features to be integrated, resulting in better flexibility and machine performance. These factors drove the decision to build a custom machine rather than utilize a power unit already manufactured and available in the equipment industry. The design is fully flexible and allows for custom headers to be attached to the front and material hopper s or trailers to be connected to the rear (Figure 4.10). The self-propelled power unit consisted of a 4 wheeled vehicle that includes an operator station, 3-point header attachment and lift mechanism, trailer and material handling attachments, and front mounted auxiliary hydraulic hookup. Power unit and header width were limited to 1.52 m to allow for compatibility when working with first year Chinese lantern crop transplanted on 0.76 m row spacing. The wheelbase of the power unit was designed to be relatively short, 1.01 m, to allow for easy maneuvering and a tight turning radius.

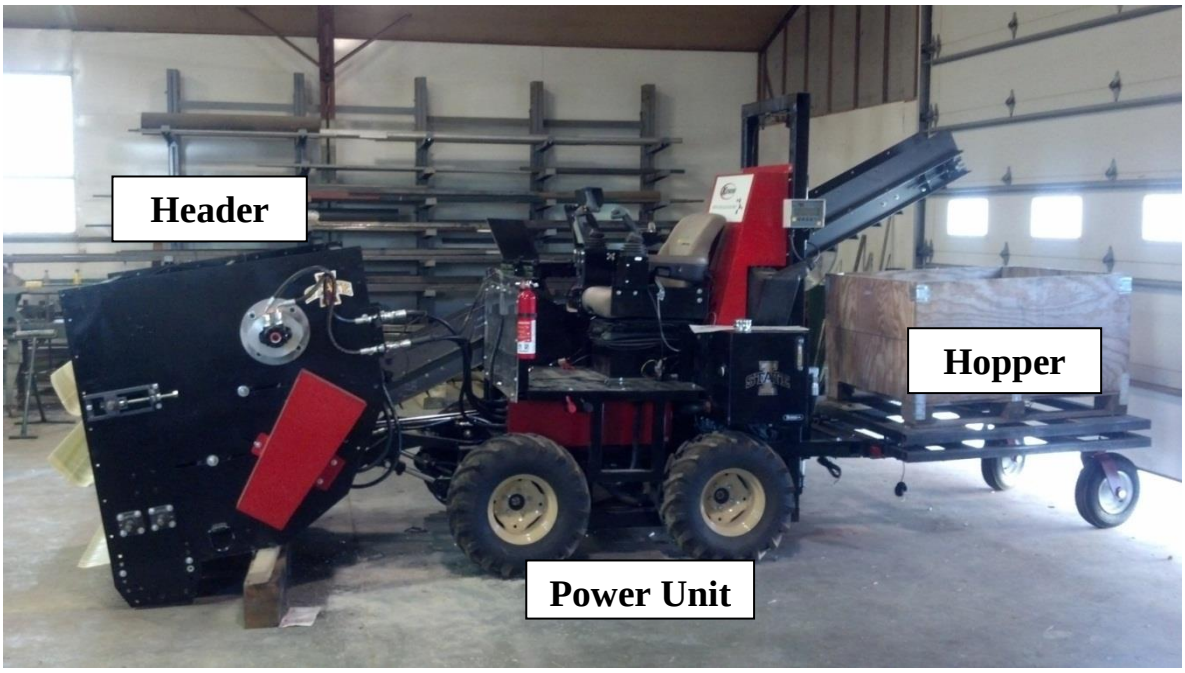

Figure 4.10: Self-propelled power unit, header, and hopper trailer

Figure 4.11: 3-Point header attachment system

Two hydraulic cylinders provide approximately 45.72 cm of vertical header lift while a third hydraulic cylinder acting as a top link provides 45degrees of fore-aft header tilt and rotation (Figure 4.11). This range of motion allowed the header to be adjusted for varying crop height and conditions.

A conveyance system was also designed into the power unit. This system consisted of two separate conveyors designed to remove material from the header at the front of the power unit and transfer it to a hopper located at the rear of the power unit. The first and forward mounted conveyor floats with the header throughout the vertical height range and header tilt rotation. Harvested material is collected from the header and conveyed along the forward mounted conveyor. Material is then transferred to the second, rear mounted conveyor that moves the material to the collection hopper at the rear of the machine. The elevation of the rear conveyor spout can be adjusted via a hydraulic cylinder. The forward mounted conveyor is powered by a hydraulic motor, allowing for variable speed. The rear mounted conveyor is powered by the driveshaft of the forward mounted conveyor. Both conveyors utilize the same size belting drive pulleys. A gear ratio of 0.90:1 was achieved using sprockets and roller drive chain to ensure that material would not accumulate in the transition between conveyors.

Power for the entire self-propelled harvesting system was provided by a 3 cylinder Lombardini LDW1603 diesel engine (Lombardini, Reggio Emilia, Italy). With a displacement of 1,649 cm^3, this engine provided approximately 29.5 kW (40.1HP) and 111.9 N·m (82.5 ft-lb) at 1600 RPM. This engine was mounted rear-facing and slightly behind the rear wheels to distribute weight and account for the weight of the header.

4.4.2 Hydraulic System Design

The self-propelled power unit utilized a hydraulic pump to power all machine functionality including propulsion, steering, conveyor drives, and header functions. Sauer Danfoss (Neumünster, Germany) hydraulic components were utilized for the majority of the hydraulic system. A full hydraulic component list can be seen in Appendix A. A series 45 axial piston pump was mated directly to the Lombardini engine using a SAE B – 2 bolt bellhousing mount. A hydraulic schematic for the self-propelled harvester is shown in figure 4.12. Reference numbers and descriptions are listed for each major component. The model L25C hydraulic pump had a displacement of 25 cm^3 / revolution that provided hydraulic flow to a bank of PVG 32 load independent proportional valves.

The PVG 32 valve block included a number of different modules. A closed center pump side module was attached to the valve bank to manage hydraulic flow from the pump. This pump side module included a pressure port (P) and tank return port (T) as well as a load sensing (LS) port. During operation oil flowed from the pump (10) to the pump side module (11). Oil was provided to the valve bank (9) and returned through the tank port on pump side module. The load sensing port on the pump side module allowed pump output flow to be adjusted in order to maintain constant pressure. The valve bank provided hydraulic flow to various hydraulic cylinders and motors throughout the self-propelled harvester. The valves were controlled using proportional valve electric actuation modules. Individual hydraulic wheel motors were used drive each of the four wheels. Each set of two hydraulic motors, right and left side, were connected in series to conserve hydraulic flow. With a displacement of 463.75 cm^3/rev, the White Hydraulic (White Drive Products Hopkinsville, Kentucky) RE series wheel motors provided a theoretical torque of 1272.2 N·m at 17.2 MPa

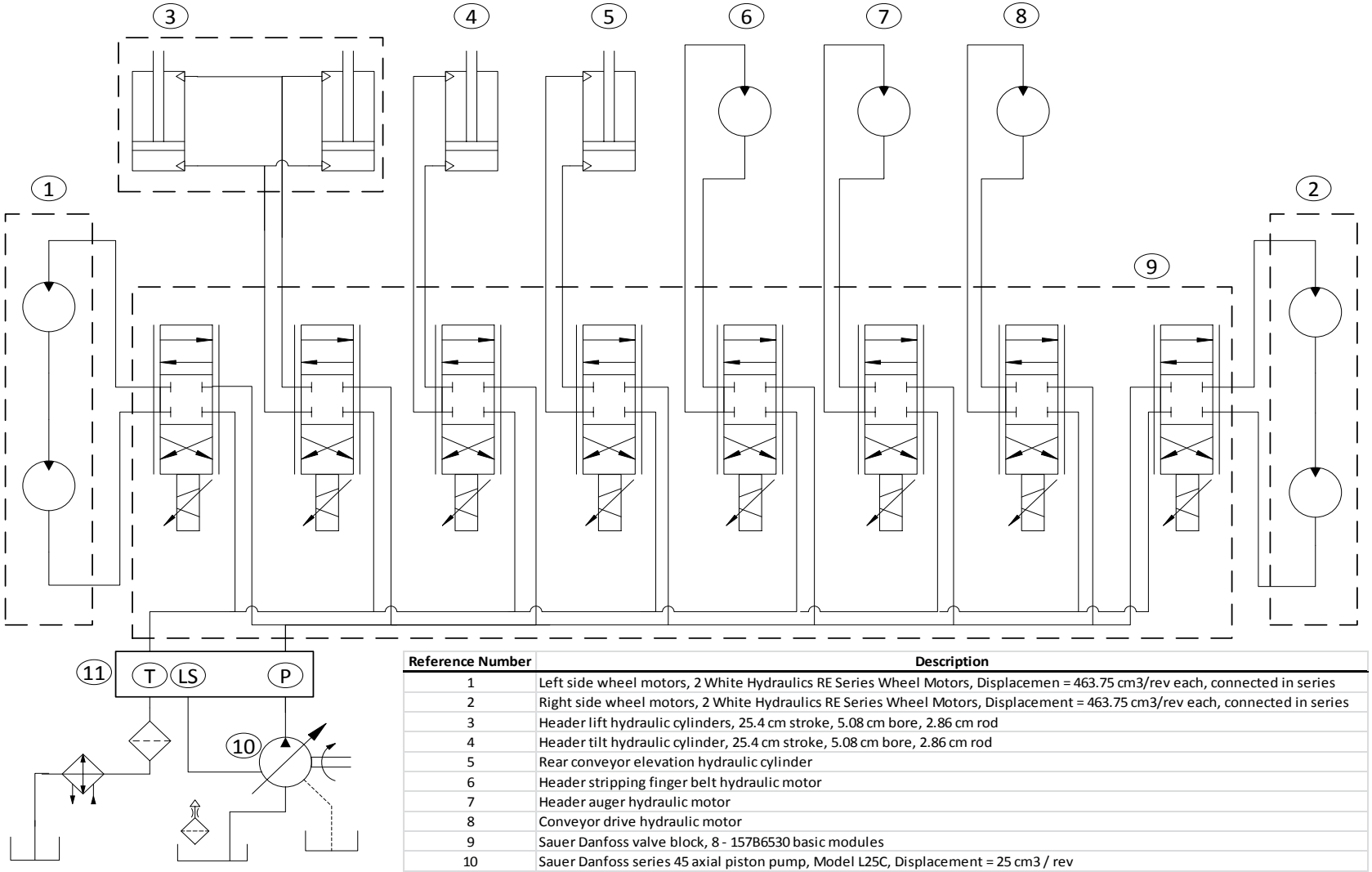

Reference Number	Description
1	Left side wheel motors, 2 White Hydraulics RE Series Wheel Motors, Displacemen = 463.75 cm3/rev each, connected in series
2	Right side wheel motors, 2 White Hydraulics RE Series Wheel Motors, Displacement = 463.75 cm3/rev each, connected in series
3	Header lift hydraulic cylinders, 25.4 cm stroke, 5.08 cm bore, 2.86 cm rod
4	Header tilt hydraulic cylinder, 25.4 cm stroke, 5.08 cm bore, 2.86 cm rod
5	Rear conveyor elevation hydraulic cylinder
6	Header stripping finger belt hydraulic motor
7	Header auger hydraulic motor
8	Conveyor drive hydraulic motor
9	Sauer Danfoss valve block, 8 - 157B6530 basic modules
10	Sauer Danfoss series 45 axial piston pump, Model L25C, Displacement = 25 cm3 / rev
11	Sauer Danfoss 157B5914 pump side module, pressure, tank, load sensing ports

Figure 4.12: Self-propelled power unit hydraulic schematic

4.4.3 Controls System Design

The operator station of the self-propelled power unit provided controls for propulsion, steering, header lift and tilt, auxiliary hydraulics, and conveyor functions. The self-propelled power unit utilized Sauer Danfoss Plus +1 compliant electronics and software to establish a fully integrated controls package. Two JS700 joysticks, one right handed and one left handed, were utilized to provide operator control of all machine functionality. A DP600 provided a user interface. This interface provided real time machine information and also allowed for machine operating parameters to be adjusted. The JS7000 joysticks and DP600 display interfaced with a MC088-015 microcontroller. A detailed component list for all mobile electronics utilized can be seen in Appendix A. The MC088-015 microcontroller was also utilized to interface with the Sauer Danfoss PVE electric actuators and control hydraulic flow for each valve. Header height and speed sensors were also connected to the MC088-15. A controls program for the power unit was developed using Sauer Danfoss PLUS +1 Guide software. This program was then downloaded to the MC088-15 microcontroller.

A CAN bus network was developed for communications between the MC088-015 microcontroller, JS7000 joysticks, and DP600 display. A service port was added to allow software changes to be made using a laptop computer and CAN to USB converter. An overview of this CAN bus network can be seen in figure 4.13.

Several safety features were built into the machine control program. A “propel engage” function was utilized in order to stop any unexpected movement of the power unit.

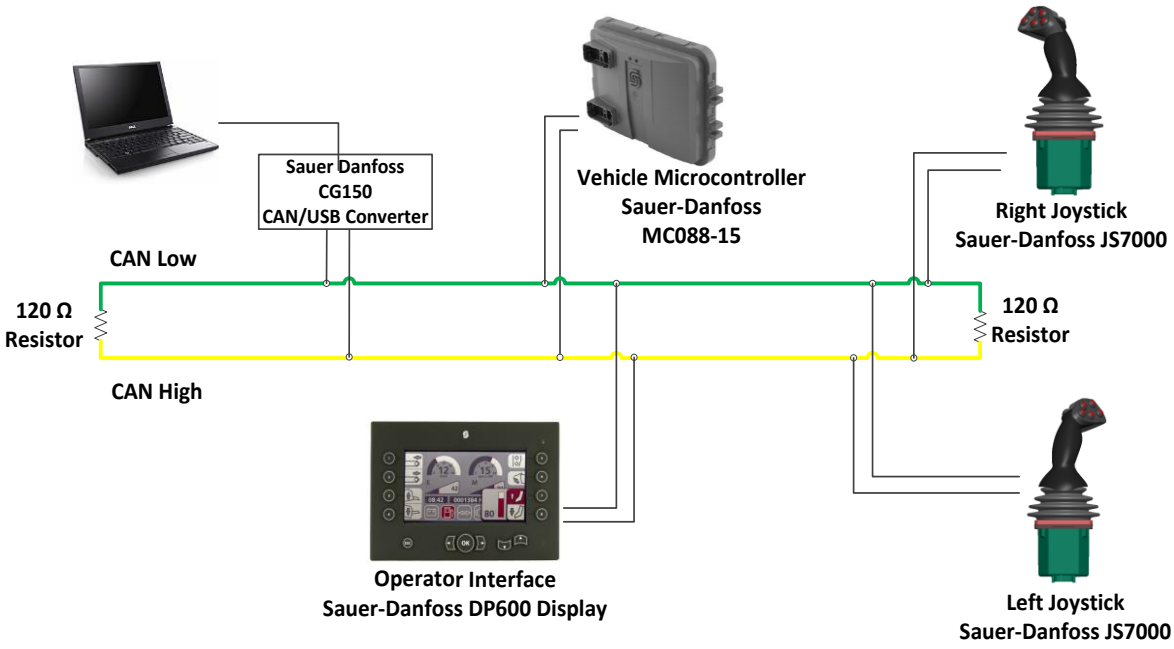

Figure 4.13: CAN bus network overview

This button must be pressed momentarily in order to engage propulsion, and allow hydraulic flow to be directed to the wheel motors. Using this function prevented movement of the power unit if either of the joysticks is bumped when climbing in or out of the power unit operator station. All electrical power to the controls network was directed through a master electrical power disconnect that could be disconnected easily if unpredicted machine movement or equipment failure was experienced. A vehicle speed limiter function was also utilized not only for safety reasons, but also to act as an aid while harvesting. When engaged, this limiting function allowed the operator to push the joysticks full forward to achieve a preset, constant speed. The maximum vehicle speed parameter could be set through the operator interface. A full list of machine functionality control can be seen in table 4.2. Explanations and locations of joystick buttons and functionality can be seen in figure 4.14.

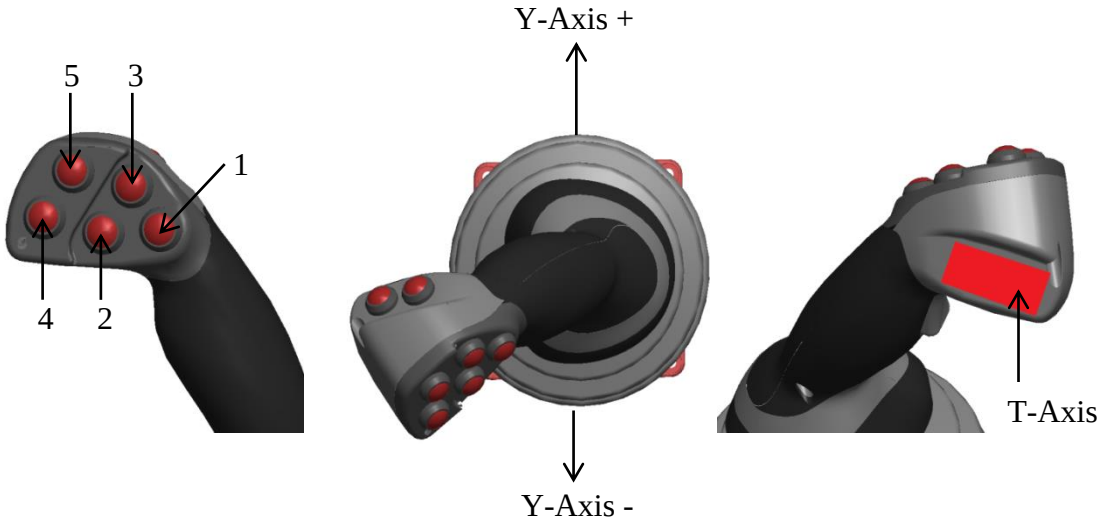

Figure 4.14: Sauer Danfoss JS700 joystick buttons

Table 4.2: Joystick functionality

Left Joystick JS7000

Input	Function	Notes
Y-Axis Position	Left wheels forward/reverse	Y-Axis is forward/reverse on joystick
Button 1	Conveyor on/off	Latched function
Button 2	Conveyor elevation down	Momentary function
Button 3	Conveyor elevation up	Momentary function
Button 4	Vehicle speed limiter on/off	Latched function
Button 5	Propel on/off	Latched function, "on" allows wheel movement

Right Joystick JS7000

Input	Function	Notes
Y-Axis Position	Right wheels forward/reverse	Y-Axis is forward/reverse on joystick
T-Axis Position	Header up/down	Proportional roller switch
Button 1	Header on/off	Latched function
Button 4	Header tilt back	Momentary function
Button 5	Header tilt forward	Momentary function
Button 8	Auto header height engage	Latched function

Automatic header height control was designed into the control system in order to maintain correct header height during harvesting. This was accomplished by utilizing a rotary potentiometer and linkage arm. A skid was fabricated to contact and run along the ground to provide positive indication of header height (Figure 4.15) Automatic header height could be engaged by the operator pressing button #8 on the right joystick. The header would then adjust to the correct height accordingly. The height of the header during automatic mode could be adjusted through the DP600 operator interface. The rotational speed of the header stripping finger belt was determined utilizing a Cherry GS100102 magnetic pickup sensor (Cherry, Auerbach, Germany) and sprocket (Figure 4.16). The rotational speed of the stripping finger belt drive shaft and also the linear velocity of the stripping finger belt were calculated and displayed on the operator interface screen. Rotational speed and therefore linear velocity of the stripping finger belt could be adjusted through the user interface.

+5 VDC sensor power, ground, and sense line inputs were provided by the microcontroller. A complete wiring schematic of the power unit can be seen in figure 4.17.

Figure 4.15: Automatic header height sensor and skid assembly

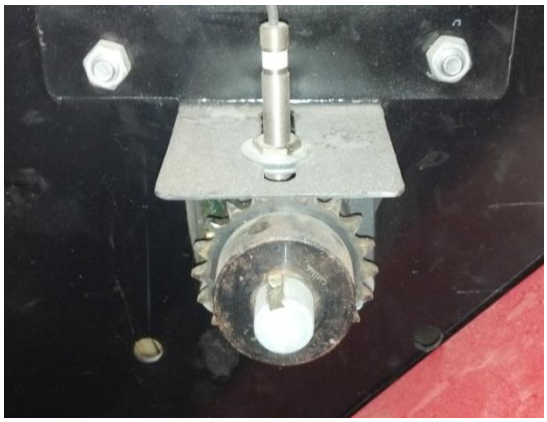

Figure 4.16: Header rotational speed sensor and sprocket

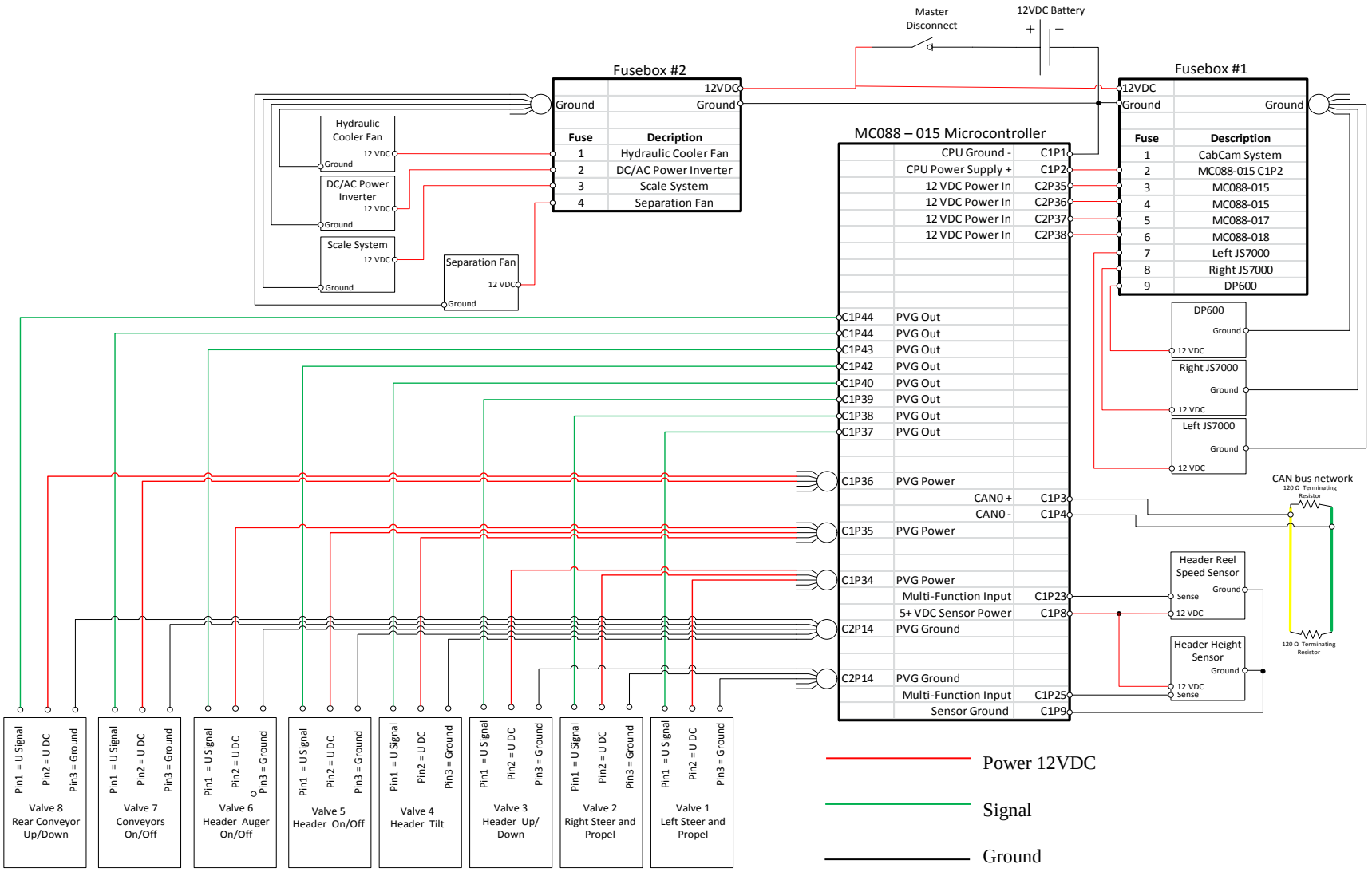

Figure 4.17: Self-Propelled power unit wiring schematic

4.4.4 Header Design and Development

In order to harvest Chinese lanterns a header was designed and fabricated. The header utilized several key features identified during fall 2011 testing of the smaller hand-propelled harvester units previously discussed. This header was designed to be attached to and powered by the self-propelled power unit. Based on a 1.52 m working width, the header was designed to harvest first year crop transplanted on 0.762 m row spacing, or second year and older crops resembling an alfalfa type crop. Stripping fingers designed for the smaller test platforms were utilized on the header. However, due to the larger width and size of the header a larger volume of stripping fingers were required. In order to manufacture the large volume of fingers required, an injection molding process was utilized to produce high quality, functional stripping fingers.

The header system was designed to integrate the harvesting, collection, and conveyance systems. A stripping finger belt system with a modified geometry was utilized as the main harvesting portion of the header. The stripping finger belt system comprised of three sets of roller chain and attachment links routed around a set of four drive shafts and sprockets. Diamond Chain (Diamond Chain Company, Indianapolis, Indiana) B2 attachment links were installed into #60 roller chain every 30.48 cm. This style of attachment link can be seen in figure 4.18. Angle iron was then attached to the attachment links on each of the three

Figure 4.18: B2 attachment links in roller chain

chains to serve as attachment point for the stripping fingers. As the drive shafts and sprockets were rotated the stripping fingers moved with the roller chain around the drive shaft geometry and through the Chinese lantern crop. The drive shaft and roller chain geometry can be seen in figure 4.19. Figure 4.20 displays a Pro-Engineer cut away model of the header. Rubber belting was installed between successive sets of stripping fingers to act as a conveyor and catch harvested material. After stripping material off the crop stems, detached crop material was conveyed to the rear of the head by the stripping finger belt system. Harvested crop material was then transferred to a latitudinal screw auger that conveyed material to the left side of the header. Upon reaching the left side of the header, material dropped through a cutout in the auger trough onto the forward mounted conveyor of the power unit. Material was then transferred to the collection hopper by the power unit conveyors.

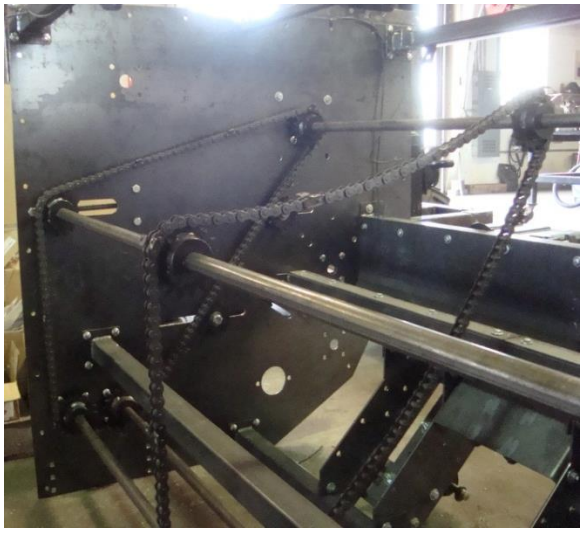

Figure 4.19: Side view of stripping header roller chain geometry

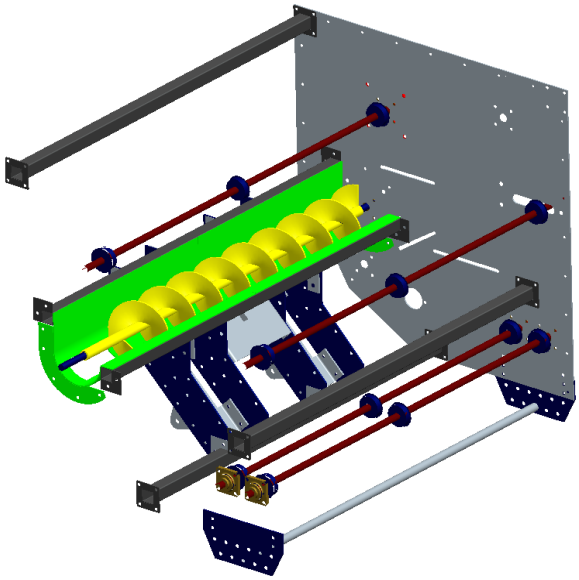

Figure 4.20: Header cut away CAD model

The geometry of the roller chain and stripping finger belt system was designed to accomplish several objectives. An annotated cut-away side view of the harvesting header can be seen in figure 4.21. In order to capture and detach the low lying lanterns, the harvesting portion of the geometry was designed to insert the fingers into the crop at a minimal vertical distance from the ground (1). After insertion into the crop, the stripping finger belt system makes a 90 degree rotation around a drive shaft and sprocket (1). The stripping fingers are rotated through the crop, effectively combing and detaching the Chinese lanterns. The fingers are then elevated vertically through the crop stems, detaching and capturing the detached material by creating a "cup" between the stripping fingers and rubber belting (2). Cylinder brushes (3) are rotated against the backside of the stripping fingers to dislodge any material stuck in the fingers. As the stripping fingers reach the rear of the header they are rotated over a screw auger (5) and the harvested crop material is transferred to the auger (4).

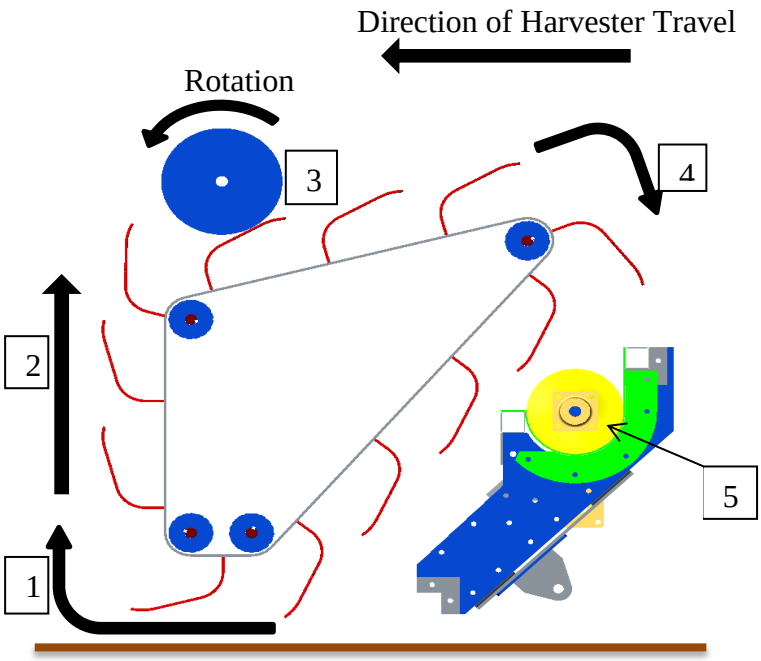

Figure 4.21: Annotated side view of harvesting header

After initial testing several modifications and improvements were made to the stripping header. Rotating cylindrical brushes were added to the top portion of the header in order to dislodge material that had become stuck in the stripping fingers. These brushes are located in the top portion of the header as seen in Figure 4.22. The drive system for these brushes was tied directly to the stripping finger belt drive shaft. Utilizing a direct drive maintained the correct gear ratio throughout the range of stripping finger belt speeds. A pin and guide system was developed and installed on the header to prevent deflection of the angle iron stripping finger mounts and roller chains themselves. Two pins were added to each end of the angle iron stripping finger mounts, spaced approximately 6.35 cm apart. A guide system was fabricated from 2.54 cm thick ultra-high molecular weight (UHMW) plastic (Figure 4.23). The guide channel system was designed to accept the guide pins and prevent deflection throughout the insertion into the crop and stripping portions of the stripping finger belt geometry. Both of these modifications improved the harvesting reliability of the header.

Figure 4.22: Stripping header with cylindrical dislodging brushes. Without guide pin system.

Figure 4.23: Stripping header with guide channels installed

CHAPTER 5: SEPARATION SYSTEM DESIGN AND DEVELOPMENT

Chinese lantern sepals serve as a primary source of carotenoids, containing a high concentration of carotenoids while the berry does not. Carotenoid extraction requires the berry and sepals be separated to streamline the process and increase efficiencies. Therefore, for commercial extraction of the carotenoids to be economically feasible, a mechanized system to separate the sepals from the berry must be integrated into the post harvesting process. To be effective, the system must be capable of accepting recently harvested lanterns and separating the sepals from the berry with minimal material loss and damage. A modular, self-contained system is also desired to minimize dependency on support systems or material handling. With these objectives, two separation systems were developed and fabricated. One system utilized counter-rotating frictional rollers to mechanically separate the sepals from the berry. Multiple rollers were placed next to each other to create a multi-channel separation bed. Two material handling and feeding systems were developed to deliver lanterns to the roller bed. The other system consisted of two processes, differential drying of the sepals and berry and an abrasion process to remove the dried sepals from the berry. Several aspects of each system will be discussed throughout this section.

5.1 Frictional Roller Separation System Design

After analysis of previous crop separation work concerning plants within the *Physalis* genus, a system was designed utilizing many of the same principles previously developed. The frictional coefficients of the berry and sepals were determined to be significantly different, indicating separation could be accomplished using frictional rollers. The

berry/sepal separation system developed consisted of a bank of counter-rotating rollers mounted in a frame. This frame was designed hold the rollers with the ability to rotate 45 degrees around a pivot point located at one end of the roller bank. Lantern stems and sepals are pinched by the rollers and pulled down through the rollers into a sepal collection system, and allowing the berries to be collected in a secondary collection container.

5.1.1 Roller Design

In order to correctly size the counter-rotating rollers, several interactions were examined. The forces acting on a Chinese lantern berry when resting on counter-rotating rollers can be seen in figure 5.1 as examined by Wang (1966).

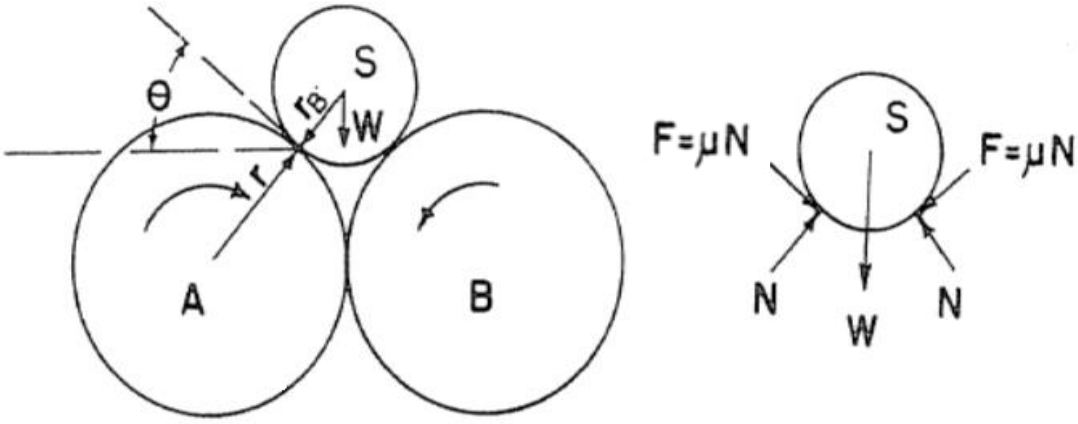

Figure 5.1: Roller and berry free body diagram (Wang, 1966)

Where:

A, B = counter-rotating rollers

S = Chinese lantern berry

W = weight of berry, S

r = radius of rollers, A and B

r_B = radius of berry, S

θ = angle between berry S and rollers A and B

F = frictional force between berry and rollers

μ = kinetic frictional coefficient between berry S and rollers A and B

The balanced vertical forces of the berry and rollers results in equation 5.1:

$$2(Fsin\theta) + W = 2(Ncos\theta) \quad \textbf{Equation 5.1}$$

Considering the frictional coefficient μ and the normal force N yields:

$$F = \mu N \quad \textbf{Equation 5.2}$$

Because the weight of the berry is greater than 0, combining equation 5.1 and 5.2 results in:

$$2F\left(\frac{cos\theta}{\mu} - sin\theta\right) = W > 0 \quad \textbf{Equation 5.3}$$

$$cot\theta > \mu \quad \textbf{Equation 5.4}$$

And:

$$cot\theta = \frac{\sqrt{((r + r_B)^2 - r^2)}}{r} = \sqrt{\frac{r_B}{r}(2 + \frac{r_B}{r})} \quad \textbf{Equation 5.5}$$

Combining equation 5.4 and 5.5 yields:

$$\sqrt{\frac{r_B}{r}\left(2 + \frac{r_B}{r}\right)} > \mu \quad \textbf{Equation 5.6}$$

As seen in equation 5.5, r_B is the radius of the Chinese lantern berry and is not variable. The kinetic frictional coefficient μ is positive and determined by the surface of the counter-rotating frictional rollers. Therefore, equation 5.6 determines the maximum radius of the frictional rollers. The values of frictional coefficients between the Chinese lantern berry and the surfaces of the frictional rollers become of interest. These values can be estimated utilizing cape gooseberry data obtained by Wang (1966). Cape gooseberry plants belong to

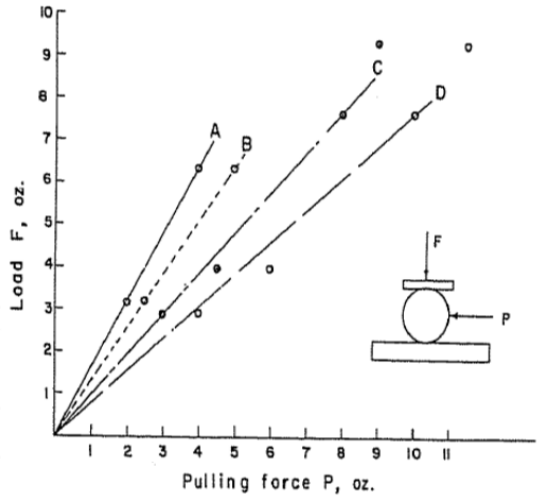

Figure 5.2: Load force vs. pulling force on cape gooseberry (Wang, 1966)

the same genus, *Physalis*, and also exhibit characteristics similar to Chinese lanterns. The frictional coefficient data collected by Wang (1966) can be seen in figure 5.2 and table 5.1.

Table 5.1: Frictional coefficient data for cape gooseberry and sepal (Wang, 1966)

Line	Test	Kinetic Friction Coefficient, μ_x
A	Berry and Neoprene (Durometer 60, Shore A)	$\mu_A = 0.78$
B	Berry and Neoprene (Dry Cell)	$\mu_B = 0.625$
C	Sepal and Neoprene (Durometer 60, Shore A)	$\mu_C = 1.3$
D	sepal and Neoprene (Dry Cell)	$\mu_D = 1.04$

Equation 5.6 was utilized to determine the maximum radius of the frictional rollers. The lower value of r_B and the kinetic frictional coefficients of the berry and neoprene, μ_A and μ_B, should be used. Using the data collected previously, as shown in table 4.1, the minimum berry diameter was found to be 12.37 mm (0.487 in). Therefore r_B = 6.185 mm (0.2435 in) and $\mu = \mu_B = 0.625$. Substituting these values into equation 5.6 where X = $\frac{r_B}{r}$ yields equation 5.7:

$$X^2 + 2X > (0.625)^2$$ **Equation 5.7**

Solving for X results in the maximum roller diameter that will satisfy the limiting conditions of $r < 34.03\ mm$ (1.34 in). However, the horizontal forces must also be considered. Wang (1966) found that the maximum horizontal force, $F_{H\text{-}Max}$, that berries could withstand to be approximately 8.9 – 11.1 N (2-2.5lb_f). As seen in figure 5.2, the horizontal forces can be explained by equation 5.8, where F_H represents the horizontal force applied to the berry by the rollers.

$$F_H = 2(Fcos\theta = Nsin\theta)$$ **Equation 5.8**

Combining equations 5.1, 5.2, and 5.58 results in equation 5.9:

$$F_H = W\frac{\mu\ cot\theta + 1}{cot\theta - \mu}$$ **Equation 5.9**

However when considering $F_{H\text{-}Max,}$ equation 5.9 can be expressed as:

$$F_{H-MAx} = W\frac{\mu\ cot\theta+1}{cot\theta-\mu}>0$$ **Equation 5.10**

Due to the fact that $F_{H\text{-}Max}$ must be greater than zero and μ cannot be negative, equation 5.9 can be determined as true. Equation 5.10 can be rewritten:

$$\frac{\mu\ cot\theta + 1}{cot\theta - \mu} < \frac{F_{H-MAX}}{W}$$ **Equation 5.11**

While W in equation 5.11 is usually expressed as the weight of the berry, the downward force of separation must also be considered during the instant the sepal is being pulled off the berry. This force of separation is highly influenced by the rotational speed of the rollers and the speed at which the sepal is detached. Thus, satisfying the conditions of equation 5.11 must be determined through experimental testing of different frictional roller rotational speeds. This testing will be discussed in future chapters.

The rollers for the separation system were sized to satisfy the constraints of equation 5.7. The initial separation system was built with 20.63 mm (0.8125 in) radius steel rollers. 12.7 mm diameter drive shafts were utilized to for each roller. Steel endplates were machined to accept 2 bolt flange bearings that held the roller drive shafts. The bearings could be adjusted to vary the distance between successive rollers. However, due to the design of the spur gear drive system, adjustment was limited to a range of 41.275 – 42.545 mm roller center to successive roller center distance. Suction was provided to an air box fabricated underneath the rollers in an attempt to pull lanterns into the rollers. A cut-away isometric view of the initial separation system can be seen in figure 5.3.

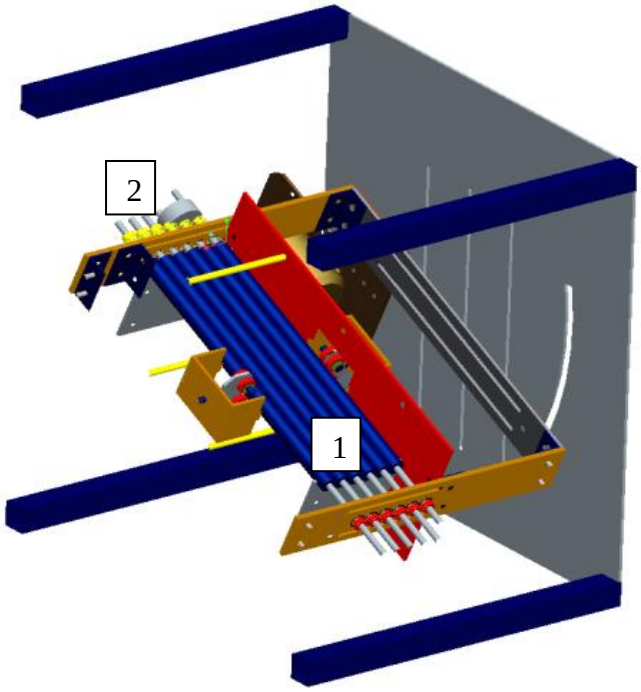

1: Frictional Rollers

2: Spur gear drive bank

Figure 5.3: Cut-away isometric view of the initial separation system

Figure 5.4: Separation system spur gear bank and drive sprocket

The drive system for the rollers consisted of a bank of spur gears, with each individual spur gear located at the end of a roller driveshaft (Figure 5.4). The bank of spur gears was driven by a roller chain sprocket attached to a roller driveshaft in the center of the bank of rollers. Power was provided by a Dayton (Dayton Electric Mfg. Co., Niles, Illinois) 3N017BD industrial electric motor. A Schneider Electric (Schneider Electric, Rueil-Malmaison, France) ATV12HO75M2 variable frequency drive was utilized to provide rotational speed control. This separation system was developed for validation and proof of concept testing that was completed during spring 2011.

Utilizing the results and experience from the initial separation system and testing a second system was developed and fabricated for further testing and commercial use in fall 2012. This system comprised of a similar frictional roller bank and drive system. The rollers were machined from steel bar stock and had a radius of 15.875 mm (0.625 in). Machining the frictional rollers allowed for tighter tolerances to be held between successive rollers. The outside surface of the frictional rollers was knurled to increase the kinetic friction coefficient. The rollers were spaced 31.75 mm (1.25 in) center to center in the roller bank, making successive roller touch. The steel endplates of the roller bank were machined to accept

flange bearings with a spacing tolerance of 31.75 ± 0.127 mm center to center distance. A similar spur gear drive system was utilized to rotate the frictional rollers. Power to the spur gear bank was again provided by a Dayton 3N017BD industrial electric motor and Schneider Electric ATV12HO75M2 variable frequency drive. However, several additions were made in order to increase throughput and ease material handling. A 1:8.64 gear reduction ratio between the electric motor and main roller drive sprocket increased the torque applied to the spur gear bank to handle the increased material throughput. A material hopper and feeder system was also added above the roller bank.

5.1.2 Feeding System Design

Two feeding systems were designed to deliver lanterns to the frictional roller bed. The initial system comprised of two sets of conveyor belts. These belts attempted to singulate the lanterns and deliver them individually to the frictional roller bed. A hopper was fabricated on top of the first set of conveyor belts to provide a steady supply of material. An alternative feeding system was developed in an attempt to orient the lanterns before delivering them to the roller bed. This system utilized a feeding tube and vibratory table to orient and direct lanterns. Both feeding systems will be discussed throughout this section.

In order to increase material throughput and separation efficiency a material feeder was developed and attached on top of the bank of frictional rollers. The feeder consisted of two sets of five conveying belts mounted above the frictional rollers. John Deere (John Deere, Moline, Illinois) A67976 seed delivery belts were utilized to singulate and convey the Chinese lanterns (Figure 5.5). The lugs on the conveyor belts assisted with singulation of the lanterns due to their spacing with respect to the average length of a lantern. The first set of conveyor belts conveyed lanterns from the material hopper to the top of the frictional roller

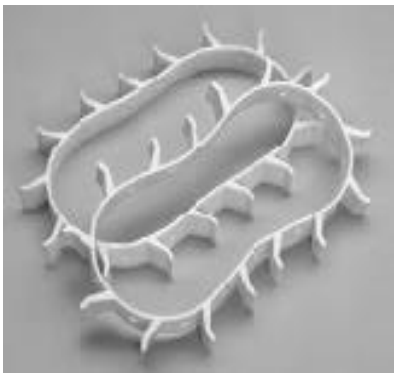

Figure 5.5: Feeder system conveying belts

Figure 5.6: Roller and feeder system variable speed drives

bank, dropping the lanterns onto the rollers individually. The conveyor belt lugs moved the lanterns and separated berries along the first half of the roller bank. The second set of conveyor belts, located toward the rear of the roller bank, conveyed lanterns and separated berries down the remainder of the rollers. The second set of conveyor belts were positioned closer to the rollers in an attempt increase separation efficiency by providing down pressure on any un-separated lanterns. The conveyor belt system was powered by a Dayton 3N017BD electric motor and Schneider Electric ATVHO75M2 variable frequency drive (Figure 5.6).

A material hopper was attached to the conveying belt frame and allowed Chinese lanterns to be loaded and conveyed to the rollers by the belts. The belts were separated by dividers positioned to guide the lanterns into the correct roller channels for separation. Correct belt spacing was also maintained by these dividers. A diagram of the feeder and material hopper system can be seen in figure 5.7.

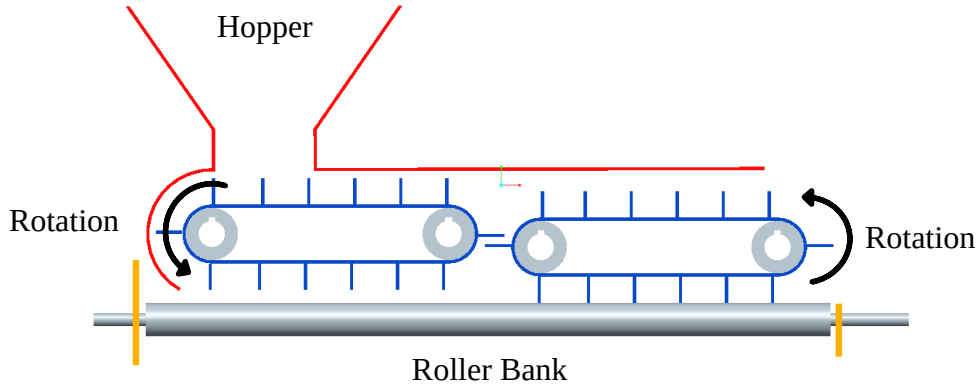

Figure 5.7: Material feeder, conveying belts, and roller bank diagram

An alternative method of feeding the lanterns onto the roller bed was also developed. During several preliminary tests it was noted that Chinese lanterns had a tendency to orient stem first when on a vibration table. Therefore a vibration table was set up to orient and feed lanterns onto bed of frictional rollers. A chute was fabricated to bridge the gap between the vibration table and roller bed. To maintain correct orientation and positioning, channels were added directly to the chute. Chinese lanterns were fed onto the table with a tube positioned perpendicular to the vibration table (Figure 5.8). An Eriez (Eriez Manufacturing Company, Erie, Pennsylvania) series HI-VI model 15A vibration unit was utilized to provide vibration. A custom table top was fabricated to match the width of the existing frictional roller bed. 220-grit sandpaper was glued to the top of the table to assist with orientation and movement of the lanterns. The vibration unit controls provided user input control of the vibration amplitude. Testing and analysis of this system as a feeding mechanism will be further discussed in the following chapters.

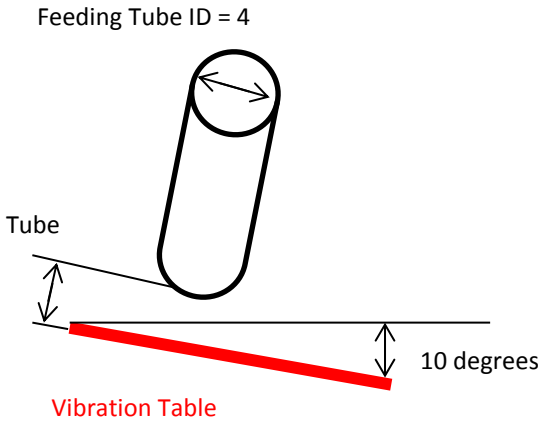

Figure 5.8: Diagram of vibration table and feeding tube set up

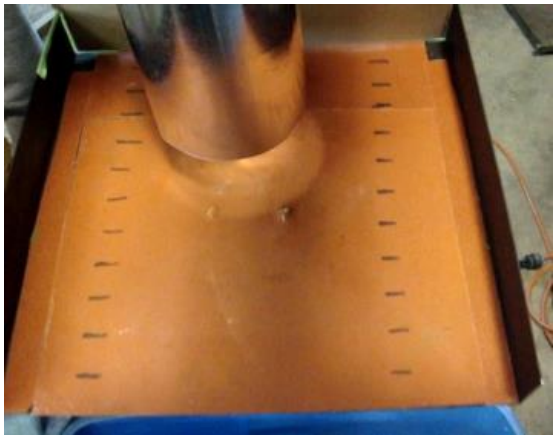

Figure 5.9: Vibration table and feeding tube

5.3 Drying and Abrasion Separation

Through interaction with Chinese lanterns it was observed that the sepal begins to dry out and become brittle once the lantern is detached from the plant stem. The sepals can then be easily crumbled away from the berry and stem. The berry retains moisture and remains intact during this process. However, the berry does begin to shrivel up after extended periods of time, similar to a raisin. The difference in the moisture retaining characteristics between the berry and sepals spurred discussions that led to the development of an alternative method for berry/sepal separation. This method includes drying the whole lantern to a specific point, at which the sepal is brittle while the berry retains moisture and strength. After drying, the lanterns are subjected to an abrasion process to fragment the sepal and detach it from the berry and stem. While very little work exists that investigates differential drying and abrasion as a process to remove and separate sepals from fruit, it was decided to investigate this method further.

While there is a multitude of commercially available drying equipment, a majority use the same basic principles to dry material; heat and aeration. Aeration, passing air through material, allows water to be removed and carried away from the material. Heating air lowers the relative humidity of the air, increasing the drying rate and water carrying capacity. Air temperature and airflow rate, primary drying system parameters, become of interest when developing a drying system for Chinese lantern. However, moisture content of the sepals and berry become the primary value to quantify drying efforts. Because different drying techniques can be applied to achieve similar results, moisture content of the sepals and berry becomes the measure to base the amount of actual material drying achieved by the system.

A variety of abrasion processes exist for separation of crop and commercial products. Many of these systems are designed to separate and classify different materials of different shape or size. For this application, an abrasion process to remove the dried sepals from the berry is required. The goal of the abrasion process is to completely separate the sepals from the berry effectively creating two separate component streams, while minimizing berry damage and cross contamination between the two components.

CHAPTER 6: METHODS AND MATERIALS

6.1 Harvester Testing, Experimental Runs

The harvesting units were tested over the course of two harvest seasons, fall 2011 and fall 2012. The manual rotary harvesting prototype and electric motor powered integrated system were tested on small test plots throughout the late summer and fall 2011 harvest season. These units were tested on small test plots, approximately 6 m wide and 30 m in length. The plots contained first year crop material that had been transplanted the in spring 2011. All the test plots were generally located in the central Iowa, in the Des Moines vicinity. Kemin Industries, the industry sponsor for this project, was responsible for the cultivation and agronomic details of the crop. The exception to this was the initial testing of the rotary harvester system completed at the Franzenburg location near Van Horne, Iowa.

The self-propelled harvester was tested during fall 2012 in large scale plots, generally 0.4-1.0 ha in size. These were second year growth plots, established from rhizomes left in the ground after the first year harvest. The rhizomes were left untouched since initial transplanting and plot establishment in spring 2011.

6.1.1 Rotary Harvester Testing

The manually powered rotary harvester prototype was tested on third year crop material at the Franzenburg residence near Van Horne, Iowa. Approximate GPS coordinates for the testing location are as follows: N 42.017736, W 92.126284. The crop was originally being grown for ornamental purposes, but was discovered by Kemin Industries staff and

offered to our research team for validation testing purposes. The data collected during this testing was not done in a manner that permitted statistical analysis of operational parameters. This was due to the hand-powering of the unit and inability to maintain a distinct constant reel speed and forward ground speed. However, the data collected did serve as validation of the stripping finger concept and very meaningful insight was gained into the harvester development.

The third year growth plot was dense and very well established (Figure 6.1). The plant structure consisted of SVS plants. Stem branching was very minimal throughout the plot. Average plant height was measured to be approximately 45-61 cm. Lantern growth started approximately 10 cm above ground level and populated the plant stems at a rate of 2-4 lanterns per individual stem. Due to the nature of the crop, no evidence of crop rows was observed throughout the test plot. Plant and stem density very closely resembled an established alfalfa crop. A complex and very well established rhizome system was observed when individual plants were dug up.

Testing of the rotary harvesting system consisted of two sets of three runs, for a total of six recorded test runs. Three test runs were completed without the deflection shields

Figure 6.1: Franzenburg third year test plot

installed, while the other three runs were completed with them installed. Several other small test runs were initially completed to get a feel for the system and observe the harvester-crop interactions. The six recorded runs were completed on sub-sample test plots that were marked out of the larger plot. The width of the six test plots was dictated by the width of the rotary harvester, 0.60m. The overall size of the six test plots was 0.60m wide by 5.0 m long.

Before testing, the test plot to be harvested was examined for lanterns lying on the ground. These were carefully removed from the plot so that data collection would not be skewed. After making a single pass through the test plot, the collected lanterns were counted (M). The lanterns that were not collected were also counted, with a distinction made between those on the ground and those still attached to the stem. The lanterns lying on the ground after testing was completed were ruled as harvesting losses (D), being detached from the stem but lost in harvesting process. The lanterns still attached to the plant stem were denoted as left on plant (LOP). The stripping efficiency (SE) was then calculated as seen in equation 6.1:

$$SE = \left(\frac{M + D}{M + D + LOP}\right) * 100 \qquad \textbf{Equation 6.1}$$

Where:

M = number of lanterns harvested by the machine

D = number of lanterns detached by the machine, but lost or dropped

LOP = number of lanterns left on the plant stem

How well the rotary header conveyed the detached lanterns to the collection hopper was another important factor when evaluating the performance of the overall system. The overall efficiency (OE) was calculated utilizing equation 6.2.

$$OE = \left(\frac{M}{M + D + LOP}\right) * 100 \qquad \text{Equation 6.2}$$

Several figures of this testing can be seen below.

Figure 6.2: Testing of the rotary harvesting system

Figure 6.3: Rotary harvester validation testing

6.1.2 Integrated Harvesting and Collection System Testing

The integrated harvesting and collection system prototype was tested in the fall 2011on several different test plots throughout central and south-central Iowa. These test plots were first year growth plots, grown rhizomes transplanted in spring 2011. Grown and managed by Kemin Industries, the plots were designated for harvesting system research as well as agronomic and genetic research purposes. Overall plot size was approximately 6.0 m by 30.0 m. However, smaller sub-sample plots were used for data collection in a similar fashion as done with the rotary harvester testing. A description and location for each test plot can be seen in Table 6.1.

Table 6.1: Test plot names, locations, and landscape descriptions for integrated harvesting system

Test Plot Name	Latitude	Longitude	Landscape Description
Kemin Summerset	41.440736	-93.554555	Bottom Ground
Kemin North Summerset	41.47452	-93.534818	Hilltop/Hillside
McGinnis Location	41.354233	-93.491394	Hilltop/Hillside
Kerber Location	41.309343	-95.648932	Bottom Ground

The first year growth of these plots differed greatly from the third year growth observed at the Franzenburg location. The crop consisted of sparse, low lying plants with excessive branching from the main stem. Plant growth was horizontal and spread radially from the main stem along the ground. This type of growth was mainly due to a lack of intra and inter-row competition between plants. Plants were not forced to grow vertical in order to reach the necessary sunlight. Plant height averaged less than 30 cm. Lantern population per plant was very dependent on location and weather experienced throughout the growing season. Several images of the first year crop can be seen below.

Three tests runs were completed at each location, with the exception being the Kerber location. No data was collected at the Kerber location due to the poor plant quality. Data collections procedures were identical to those used during testing of the rotary harvesting

Figure 6.4: First year crop test plots

Figure 6.5: First year test plot plants in rows

system. System efficiencies were calculated using equations 6.1 and 6.2.

6.1.3 Self-Propelled Harvester Testing

The self-propelled harvesting system was tested throughout the fall 2012 harvest season. Second-year growth test plots were utilized for all testing. The harvesting system was tested at two locations seen in table 6.2. The test plots utilized for testing were cultivated for harvester testing and development as well as agronomic and genetic research. The second-year crop growth consisted of mainly vertical, single stemmed plants. Due to a lack of precipitation throughout the 2012 growing season, the Kemin Summerset location was irrigated using a lateral move irrigation system. Irrigation of this test plot resulted in a tall, dense, and lush crop (Figure 6.6). The Kemin Walter location was not irrigated, resulting in a shorter, less dense crop (Figure 6.7). The test plot also started to become very dry and brittle at the end of the growing season.

Table 6.2: Test plot names, locations, and landscape descriptions for self-propelled harvester testing

Test Plot Name	Latitude	Longitude	Landscape Description
Kemin Summerset	41.440736	-93.554555	Bottom Ground
Kemin Walter Location	41.387384	-93.626572	Hilltop/Hillside

Figure 6.6: Kemin Summerset location test plot

Figure 6.7: Kemin Walter location test plot

Initial testing of the self-propelled harvesting system was completed at the Kemin Walter location. Due to the lack of precipitation throughout the growing season, the crop matured earlier than the crops at other test locations. Crop height also suffered due to a lack of moisture. Average crop height for the test plot was approximately 60 cm. The plant stems contained very few leaves, most of which had turned brown and shriveled up. Several small validation tests were run to gain familiarity with the harvesting system and interactions with the crop. No data was collected on these tests. Before data collection testing, six allotments measuring 1.52 m by 30.48 m were marked out for each test run. Each plot was harvested and data was collected on harvested lanterns, dropped lanterns, and lanterns left on the plant stem. These tests were completed using the initial header design, without the guide pins and channels installed. The maximum vehicle speed function was utilized during this testing to minimize errors and losses due to irregular harvester speed. Approximate forward vehicle speed during tests was measured to be 1.0 km/h. A wooden box hopper was placed on the harvester trailer to collect the harvested lantern from the conveyor system. In order to improve collected lantern cleanliness a fan was added to the spout of the rear conveyor. Debris and unwanted materials were blown out of the harvested material stream and directed away from the collection hopper.

Further testing of the self-propelled harvester was completed at the Kemin Summerset location. Irrigation of the crop resulted in a SVS plants. Average crop height for the test plot was approximately 81cm. A large volume of leaves were present throughout the crop. However, the leaves tended to be in the top ¼ of the plant stems, leaving the lower ¾ of the plants stems bare of leaves. Lanterns populated the plant stems at a rate of 6-12 lanterns per stem, starting approximately 15cm from the ground. Several challenges arose during

testing at the Kemin Summerset location. Due to the dense and lush crop, the header had difficulty effectively combing through the crop material. The thick crop material and stems created an immense resistance and caused deflection of the roller chain stripping finger system. As a result several header components failed or bent, causing multiple machine shutdowns for repairs. Therefore, only two tests were completed with data collection at the Kemin Summerset location. Small test plots measuring 1.52 m by 20 m were measured out for these tests. Data collection procedures were identical to those followed during testing of the rotary harvesting system. During this testing the guide pin and channel header concept was developed.

The guide pins and channels strengthened the stripping finger drive system and reduced deflection dramatically. A small portion of the crop was saved for testing once modifications and improvements had been made. Several short tests were completed after the guide system was installed. No header breakage of failure was experienced during these tests. Several figures of the self-propelled harvester testing can be seen below.

Figure 6.8: Test plots after initial testing at Kemin Walter location

Figure 6.9: Testing at the Kemin Summerset location, without guide system installed

6.3 Roller Separation System Initial Testing, Experimental Runs

Several initial tests were completed using the frictional roller separation system. These tests were completed with open rollers, before the feeding system was developed or fabricated. The rollers utilized for these tests had a smooth, finished steel surface and an outer diameter of 41.28mm. A total of 12 runs were completed, with runs #10-12 utilizing the optimum settings. Two different lantern orientations were used for test runs 1-9. Five lanterns were placed on the rollers with a random orientation while another five were placed with a stem-down orientation, inserting the stem into the pinch point created by the rollers. The number of successful separations was then recorded. A successful separation was defined as a complete separation of the sepals from the berry, without crushing the berry. The test parameters for test runs 1-9 can be seen in table 6.3. Separation efficiencies were calculated for random and stem down orientations. Overall separation efficiency was also calculated.

Table 6.3: Machine parameters, experimental tests 1-9;l

Run	Roller Angle (Degrees)	Air Suction (in/water)	Roller Speed	Roller RPM
1	30	0	Low	20
2	30	25	Low	20
3	30	25	Low	20
4	30	0	Medium	40
5	30	25	Medium	40
6	30	25	Medium	40
7	30	0	High	60
8	30	25	High	60
9	30	25	High	60

After analysis of the results, three additional test runs were completed using the optimum machine parameters to maximize overall separation efficiency. These tests were completed by placing ten lanterns stem down on the roller bed. The results from these tests were analyzed in a similar fashion.

6.4 Roller Separation System, Design of Experiments

A larger separation system was developed for further testing. Frictional rollers were machined from steel bar stock specifically for the separation system. Several changes were made to the roller design to improve functionality. The frictional roller outer diameter was reduced to 31.75 mm in an attempt to reduce crushing of the berry. A diamond pattern knurling was machined into the outer surfaces of the roller to increase the frictional force on the stem and sepals. (Figure 6.10) A feeder belt and hopper system was developed to increase machine throughput and control feeding rate. After completion of the preliminary experimental test runs a complete design of experiments (DOE) was developed for the complete separation system. The DOE was based on two experimental factors, roller speed and feeder belt speed. Three levels of each factor were used to create the 3x3 full factorial DOE. Two additional center point runs were added to the DOE to provide a measure of

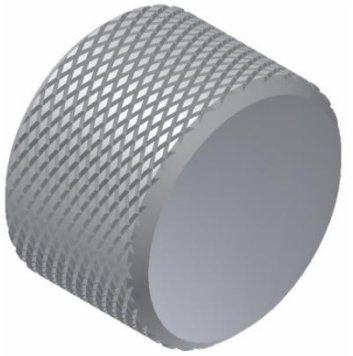

Figure 6.10: Diamond pattern knurling added to frictional roller shafts

process stability and inherent variability. Each test run was replicated three times, resulting in 44 total test runs. (Table 6.4)

Table 6.4: DOE separation machine parameters

Test Run	Factor Level Pattern	Roller Speed (RPM)	Roller surface linear speed (cm/min)	Feeder Belt Linear Speed (cm/min)
1	31	30	298.6	375.4
2	21	20	199	375.4
3	0	20	199	750.8
4	31	30	298.6	375.4
5	12	10	99.5	750.8
6	23	20	199	1126.2
7	32	30	298.6	750.8
8	13	10	99.5	1126.2
9	13	10	99.5	1126.2
10	21	20	199	375.4
11	13	10	99.5	1126.2
12	32	30	298.6	750.8
13	21	20	199	375.4
14	12	10	99.5	750.8
15	32	30	298.6	750.8
16	32	30	298.6	750.8
17	33	30	298.6	1126.2
18	22	20	199	750.8
19	0	20	199	750.8
20	22	20	199	750.8
21	11	10	99.5	375.4
22	21	20	199	375.4
23	33	30	298.6	1126.2
24	0	20	199	750.8
25	12	10	99.5	750.8
26	0	20	199	750.8
27	11	10	99.5	375.4
28	12	10	99.5	750.8
29	0	20	199	750.8
30	13	10	99.5	1126.2
31	31	30	298.6	375.4
32	0	20	199	750.8
33	11	10	99.5	375.4

Table 6.4 (cont.): DOE machine parameters

Test Run	Factor Level Pattern	Roller Speed (RPM)	Roller surface linear speed (cm/min)	Feeder Belt Linear Speed (cm/min)
34	23	20	199	1126.2
35	33	30	298.6	1126.2
36	31	30	298.6	375.4
37	0	20	199	750.8
38	0	20	199	750.8
39	22	20	199	750.8
40	23	20	199	1126.2
41	33	30	298.6	1126.2
42	22	20	199	750.8
43	23	20	199	1126.2
44	11	10	99.5	375.4

A test consists of setting the variable frequency drives to the correct output, feeding 50 lanterns into the hopper and feeder system, allowing the machine to process the material. Once through the machine, the separated berries and un-separated lanterns were counted to determine machine performance. Due to an inability to successfully re-process partially crushed berries, partial crushage of the berry was recorded as a crushed berry. The separation efficiency for the frictional roller system can be described by equation 6.3.

$$Separation\ Efficiency\ (SE_{FR}) = \left(\frac{F}{T}\right) * 100 \qquad \text{Equation 6.3}$$

Where:

F = number of fully separated, intact berries

T = number of total lanterns in test run

The number of crushed berries was determined by equation 6.4.

$$Crushed\ berries\ (CB) = (T - (F + U)) \quad \text{Equation 6.4}$$

U = number of un-separated lanterns

After the conclusion of each test the separation machine was cleaned out and allowed to run for approximately 5 minutes to clear any remaining lanterns or material. The roller and feeder belt speed was increased outside of the test parameters to ensure all material had been cleared before beginning the next test run.

6.5 Vibration Orientation and Feeding

Several initial tests were completed to gain a familiarity with the vibration table and the effects on Chinese lanterns. It was through this testing that a range of acceptable vibration amplitudes for lantern orientation was discovered. Along with several other observations, a primitive DOE was developed to test lantern orientation and feeding capabilities of the system. This DOE consisted of two variables: feeding tube height from vibration table and vibration table amplitude. The full DOE can be seen in table 6.5. While table 6.5 shows tests arranged according to test number, during actual testing the tests were completed in a random order. A test consisted of loading 25 lanterns into the feeding tube, setting the vibration table characteristics, and allowing the lanterns to feed out of the tube and down the vibration table. A slide was fabricated at the bottom of the feeding tube to stop the flow of lanterns until the vibration amplitude was set, at which time the slide was then opened so that the feeding tube was completely unobstructed. Lanterns were then allowed to flow freely out of the feeding tube and onto the vibration table.

Table 6.5: Vibration orientation and feeding DOE parameters

Test #	Tube Height (cm)	Amplitude (mm)
1	2.54	0.61
2	2.54	0.61
3	2.54	0.61
4	2.54	0.91
5	2.54	0.91
6	2.54	0.91
7	2.54	1.22
8	2.54	1.22
9	2.54	1.22
10	3.18	0.61
11	3.18	0.61
12	3.18	0.61
13	3.18	0.91
14	3.18	0.91
15	3.18	0.91
16	3.18	1.22
17	3.18	1.22
18	3.18	1.22
19	3.81	0.61
20	3.81	0.61
21	3.81	0.61
22	3.81	0.91
23	3.81	0.91
24	3.81	0.91
25	3.81	1.22
26	3.81	1.22
27	3.81	1.22
28	4.45	0.61
29	4.45	0.61
30	4.45	0.61
31	4.45	0.91
32	4.45	0.91
33	4.45	0.91
34	4.45	1.22
35	4.45	1.22
36	4.45	1.22

For analysis and data collection, each test was videotaped. During analysis, the orientation of each lantern as it exited the vibration table was recorded. The orientation of each lantern was classified as an angle, with 0° being defined as completely stem first. Classification angles for each individual lantern were: 0°, 45°, 90°, 135°, and 180°. Lanterns that were orientated 0° and 45° were also denoted as having "correct" orientation and able to orientated stem first into the rollers. Lanterns having an orientation of 90°, 135°, or 180° were denoted as having "random" orientation. The number of lanterns stuck in the feeding tube and the number of lanterns stuck on the vibration table, not orientated, were also recorded for each test. The vibration table was allowed to operate for 2:00 minutes during each test before it was shut off and the results analyzed. Throughput time for the 25 lanterns was also extracted from the video of each test. These results were then utilized to calculate estimated separation efficiency and throughput for a separation system comprised of a vibration table feeding a bed of frictional rollers. Estimated separation efficiency(EST) for each test was calculated as described by equation 6.4.

$$EST = \left((C * SE_C) + (R * SE_R)\right) * 100 \qquad \textbf{Equation 6.4}$$

Where:

EST = Estimated separation efficiency, %

C = number of correctly orientated lanterns

R = number of randomly orientated lanterns

SE_C = separation efficiency for correctly orientated lanterns, stem first*

SE_R = separation efficiency for randomly orientated lanterns*

*SE_C and SE_R were determined from previous testing

The feed rate (FR) for each test was calculated using the time extracted from the video analysis. Feed rate is defined as the amount of material that could be supplied to the system per amount of time. Feed rate is described by equation 6.5.

$$FR = \left(\left(\frac{L}{T}\right) * 3600\right) * WL \qquad \text{Equation 6.5}$$

Where:

FR = Feed rate, kg lanterns/hour/foot of system width

L = number of lanterns in test, constant, 25

T = time required for lanterns to move out of feeding tube and across vibration table

WL = Average weight of a lantern

Separated throughput (ST) for each test was calculated by utilizing the EST and FR values as seen in equation 6.6

$$ST = (FR * EST) \qquad \text{Equation 6.6}$$

Return throughput (RT), the fraction of the federate that does not get separated on the first pass through the system, was calculated as seen in equation 6.7.

$$RT = 1 - (FR * EST) \qquad \text{Equation 6.7}$$

Each test was also analyzed for feasibility. This analysis identified sets of parameters that could possibly be implemented into a large scale separation process. Feasibility was defined by the following set of parameters.

- Estimated separation efficiency above 60.00%
- Less than 5.00% of lanterns stuck in tube
- Correct orientation above 30.00%

After the conclusion of each test the lanterns were collected and reloaded into the feeding tube for the next test. The same lanterns were utilized for all vibration orientation tests in order to minimize variation caused by irregularities in lantern characteristics.

6.6 Drying and Abrasion Separation Testing

Due to the lack of Chinese lantern material, initial testing of the drying and abrasion separation system was completed utilizing Cape gooseberry material. Cape gooseberries, belonging to the same family, are very similar to Chinese lanterns and exhibit many of the same characteristics. Cape gooseberries are readily available on the market and can be purchased through a commercial distributer year-round. While a small amount of Chinese lantern material was available during testing, it was determined that the concept could be validated before testing any Chinese lanterns. The drying and abrasion testing requires a relatively large volume of material to complete each test, while also being destructive. Once a sample is dried and sent through the abrasion process it is unusable for any future testing. After the concept was validated using Cape gooseberry material, tests were conducted using Chinese lanterns material to validate the process and optimize the parameters for Chinese Lanterns.

Testing consisted of two separate processes, drying and abrasion. The drying process for all testing was completed utilizing a Thermo-Scientific (Thermo Fisher Scientific, Waltham, Massachusetts) Heratherm OGS750 gravity convection oven. A single layer of material was spread evenly over the drying racks and allowed to dry for the specified amount of time. The abrasion process was completed using a Seedburo (Seedburo Equipment

Company, Des Plaines, Illinois) pellet durability tester, product code PDT. (Figure 6.11 and 6.12) This tester is generally used to predict the amount of fines produced by handling pellets before feeding time. However, the tester was utilized to provide a standard method of abrasion, utilized for all abrasion tests. Compliant with ASAE standard S269.5 (ASABE Standards, 2007), this machine consists of four chambers measuring 25.4cm long * 13.97 cm wide * 25.4 cm deep. The chambers are rotated by an electric motor at 50 RPM.

Each test consisted of drying 50 whole Cape gooseberries or Chinese lanterns. The drying parameters, temperature and residence time, were specified for each test by the DOE that was being completed. After drying, the material was removed from the dryer and allowed to cool. The material was then loaded into one of the pellet durability tester chambers with five rubber balls. The rubber balls had an outside diameter of 33.50 mm. The hardness of the rubber balls was determined using a Durometer. The hardness of the outside surface was found to be 35A while the hardness of the inner rubber material was determined to be 30A. For concept validation testing, the tester was allowed to rotate for five minutes. The abrasion residence time was varied during optimization of the process for Chinese

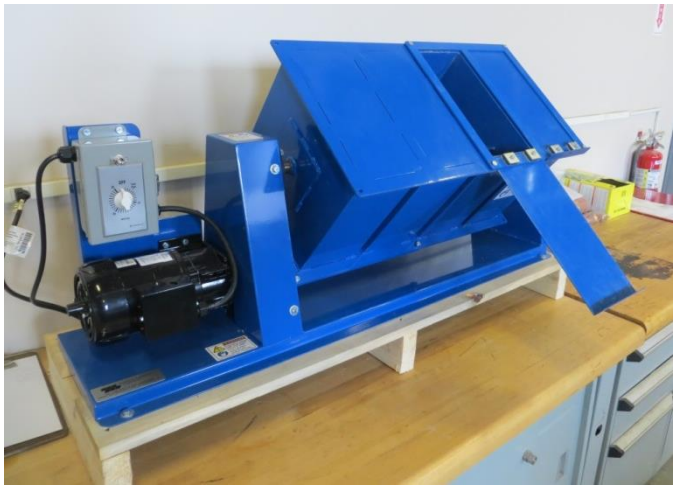

Figure 6.11: Seedburo pellet durability tester

Figure 6.12: Inside of Seedburo tester chamber

lantern. Material was then collected from the chamber and sorted. Intact, full berries were removed from the material and counted. The remaining material was sieved to produce three portions of different particle size: above 7.62 cm, between 7.62 and 5.08 cm, and fines consisting of material below 5.08 cm particle size. The material used in each test was weighed before and after each step in the drying and abrasion processes, drying and abrasion. Analysis was also completed on material that had been dried, but not put through the abrasion process. The material was manually separated into three distinct portions: berry, sepal, and stem. The resulting portions were weighed individually to determine the ratio of each portion to the total gooseberry or lantern. These ratios were then used to estimate and predict results of the drying and abrasion process. The ratios were also used to determine contamination of the sepal portion, the amount of berry material that had broken down during abrasion and remained with the sepal material. The same can be said for estimating the amount of sepal still attached to the berries and stem after abrasion.

When optimizing the system for Chinese lanterns, the amount of sepal remaining on the berry and stem was determined by manually removing the sepal by hand and weighing the removed material. This allowed for actual separation efficiency for the differential drying and abrasion to be calculated using equation 6.8.

$$SE_{DA} = 1\text{-}(SA/(SA+SD)) \qquad \textbf{Equation 6.8}$$

Where:

SE_{DA} = Separation efficiency of differential drying and abrasion system

SD = Total sepal weight detached during abrasion

SA = Total sepal weight still attached to berry after abrasion

Initial testing of the drying and abrasion separation process consisted of four different tests, each replicated three times for a total of 12 tests. Two drying temperatures, 85 and 100˚ C were used along with two drying residence times, 6 and 18 hours. The DOE for this set of tests can be seen in table 6.6. While the test runs in table 6.6 are organized by test number, tests were completed in a random order during actual testing. These tests were completed using Cape gooseberry material to validate the overall process as a method for separating an outer sepal from an inner berry.

Table 6.6: Drying and Abrasion Process, Initial Testing Parameters, completed with cape gooseberry material

Test #	Repetition #	Temperature (˚C)	Residence Time (hour)
1	1	100	6
2	2	100	6
3	3	100	6
4	1	100	18
5	2	100	18
6	3	100	18
7	1	85	6
8	2	85	6
9	3	85	6
10	1	85	18
11	2	85	18
12	3	85	18

Optimization of the process parameters was completed using Chinese lantern material. In order to optimize the process parameters, results needed to be collected over a wide range of parameters, requiring many tests. These tests were also designed to define a relationship between moisture content of both components and separation efficiency, also requiring testing over a wide range of moisture contents. Due to these requirements and the

small amount of Chinese lantern material, each test was limited to 10 lanterns. 26 total tests were completed over a wide range of parameters as seen in table 6.7.

Table 6.7: Differential drying and abrasion process testing, validation testing completed with Chinese lantern material

Test #	Drying Temp (˚C)	Drying Residence Time (hours)	Tumbling Time (min)
1	55	6	N/A
2	55	6	N/A
3	55	6	N/A
4	70	6	N/A
5	70	6	N/A
6	70	6	N/A
7	85	1	5
8	85	2	5
9	85	2	15
10	85	4	5
11	85	4	5
12	85	4	15
13	85	6	5
14	85	6	5
15	85	6	15
16	100	2	5
17	100	4	5
18	100	6	5
19	115	0.5	5
20	115	0.5	15
21	115	1	5
22	115	2	5
23	115	2	5
24	115	4	5
25	115	4	5
26	115	4	15
27	115	4	15
28	115	4	15
29	115	6	5
30	115	6	5
31	115	6	15
32	115	6	15

These tests were conducted and analyzed in a similar fashion to the concept validation tests completed with cape gooseberries. However, due to being in cold storage for an extended period, the Chinese lantern material was significantly drier than freshly harvested material. In order to counteract this effect, the Chinese lantern material was re-hydrated to moisture contents similar to those recorded during harvest before the differential drying process. These moisture contents were approximately 40.00 and 75.00% for the sepals and berry, respectively. No separation tests were completed for Tests 1-6. Due to limited material, material that had been dried at 55 and 70˚C was utilized solely for the investigation of cis-zeaxanthin formation as a result of the drying process.

These tests were aimed not only to define a relationship between moisture content and separation efficiency, but also to investigate the effects of temperature and time on the formation of cis-zeaxanthin and degradation of usable product. Re-hydrating the Chinese lantern material and simulating recently harvested material also allowed for a more realistic analysis of cis-zeaxanthin formation to be completed. Due to the molecule formation, cis-Zeaxanthin is considered unusable and a direct loss of product. It is understood that exposing Chinese lantern material to high temperatures tends to cause trans-zeaxanthin to convert to the higher energy cis-zeaxanthin state. However, the relationship between drying temperature, drying residence time and the rate at which trans-zeaxanthin converts to cis-zeaxanthin remains to be investigated and defined. This work aims to define this relationship and determine the significant factor in cis-zeaxanthin formation. The formation of cis-zeaxanthin was analyzed by an outside laboratory. The testing results were analyzed using extraction and analysis procedures developed specifically for the analysis of zeaxanthin and

the molecular characteristics. These results were then communicated between research teams for further analysis and discussion.

CHAPTER 7: RESULTS AND DISCUSSION

7.1 Harvester Experimental Runs

Testing of the various harvesting systems yielded good data as well as a number of observations. While a formal DOE was never completed for the harvesting systems, a good amount of data was collected in order to validate the stripping system and components as a viable option for mechanized harvesting of Chinese lantern. The following section will discuss the results and observations collected during testing of the harvester systems.

7.1.1 Rotary Harvester Testing

The rotary harvesting system testing took place September 9, 2011 at the Franzenburg farm near Van Horne, Iowa. The rotary system performed very well in the 3rd year, single stemmed vertical crop. The stripping fingers were able to comb through the plant stems and detach the lanterns with ease. The results from the six test runs completed can be seen in table 7.1.

Table 7.1: Test results, rotary harvesting system

Test #	Deflection Shields Installed	Harvested Lanterns (M)	Dropped Lanterns (D)	Lanterns left on plant (LOP)	Stripping Efficiency (SE) %	Overall Efficiency (OE) %
1	No	49	53	4	96.23	46.23
2	No	42	63	2	98.13	39.25
3	No	41	44	7	92.39	44.57
Tests 1-3 Average		44.00	53.33	4.33	**95.58**	**43.35**
4	Yes	67	38	5	95.45	60.91
5	Yes	64	32	0	100.00	66.67
6	Yes	70	32	2	98.08	67.31
Tests 4-6 Average		67.00	34.00	2.33	**97.84**	**64.96**
Overall Average		55.5	43.66	3.33	**96.71**	**54.16**

During tests 1-3 it was observed that lanterns were falling into the center of the stripping reel after being detached from the plant stem. The lanterns become lodged near the center of the reel and would fall out until they rotated past the collection hopper system. These lanterns would subsequently fall onto the ground and be counted as dropped lanterns. While the stripping efficiency of the rotary system was very high during these tests, averaging 95.58%, the overall efficiency suffered due to losses of dropped lanterns.

After tests 1 through 3 it was determined that deflection shields could be fabricated to reduce losses. Deflection shields were quickly fabricated and installed on the rotary stripping finger reel. Tests 4 through 6 were completed after the fabrication and installation of the deflection shields. A significant improvement in overall efficiency, approximately 21.61%, resulted from the use of deflection shields. The deflection shields reduced the number of dropped lanterns while having no negative effect on stripping efficiency.

The stripping finger concept was validated through this initial testing. The stripping fingers performed very well, reaching a stripping efficiency of 97.84%. The single-stemmed vertical crop structure was very conducive to harvesting by means of stripping and combing. The complex and robust rhizome root system of the crop prevented plants from being up-rooted during stripping. The harvested material in the collection hopper was relatively clean, containing very few leaves and other debris. The maturity and canopy structure of the crop limited foliage and leaves. In this test plot, the crop structure allows leaves to slide through the keyhole section of the stripping fingers without being detached.

Due to the stripping finger reel being powered by manually by hand, a constant rotational speed could not be achieved. However, during preliminary testing it was evident that a faster rotational speed did not increase stripping or overall efficiency. A very slow

rotational speed tended to increase dropping losses due to a lack of centrifugal force to transport the lanterns into the collection hopper.

7.1.2 Integrated Harvesting and Collection System Testing

Testing of the integrated harvesting and collection system took place throughout September and November 2011, and at several locations. All of the testing was completed on first year, plug transplanted crop. The crop structure was very short and branched, creating a vine like structure horizontal to the ground. Throughout testing it became evident that plant structure has a direct impact on stripping efficiency. This was seen in all tests completed on the first year crop. The stripping fingers would catch the plants underneath a branch node, resulting in the plant being ripped from the ground and entangled in the stripping fingers. The vine like branches also became tangled in the stripping fingers, decreasing stripping efficiency. (Figures 7.1, 7.2) During testing it was noted that snoots may be capable of elevating the low lying branches, making them more suitable for harvesting. Several iterations of snoots were fabricated and tested on various occasions with no increase in stripping or overall efficiency. The observations collected through testing on

Figure 7.1: Chinese lantern branches tangled in stripping fingers

Figure 7.2: Chinese lantern branches tangled in stripping fingers

first year crop material confirmed that a single-stemmed, vertical crop structure is ideal for stripping harvester systems.

Insect control also became an issue throughout the 2011 harvesting season. Several of the test plots became infested with fruit worms that damaged or completely ate the berry inside of the calyx. Without berries upon which to apply detachment force, the stripping fingers were incapable of detaching the lanterns. A significant reduction in stripping efficiency was seen in these areas. Quantitative results from the testing of the integrated harvesting and collection system can be seen in table 7.2.

Table 7.2: Test results, integrated harvesting system

Location	Test #	Harvested Lanterns (M)	Dropped Lanterns (D)	Lanterns left on plant (LOP)	Stripping Efficiency (SE) %	Overall Efficiency (OE) %
Kemin Summerset	1	39	9	26	64.86	52.70
	2	25	10	21	62.50	44.64
	3	24	4	20	58.33	50.00
Average		29.33	7.67	22.33	**61.90**	**49.12**
Kemin North Summerset	1	35	12	27	63.51	47.30
	2	33	9	22	65.63	51.56
	3	27	7	19	64.15	50.94
Average		31.67	9.33	22.67	**64.43**	**49.93**
McGinnis Location	1	43	9	29	64.20	53.09
	2	47	12	31	65.56	52.22
	3	39	7	27	63.01	53.42
Average		43.00	9.33	29.00	**64.26**	**52.91**
Overall Average		34.67	8.78	24.67	**63.53**	**50.65**

Average stripping efficiency of the integrated harvesting system was reduced approximately 33.18 % due to the branched, vine like crop structure. Overall efficiency also

decreased slightly relative to the rotary system due to the reduction in stripping efficiency. However, collection system losses were reduced dramatically. Collection system losses due to dropped lanterns were calculated as a percentage of stripped lanterns lost during the collection process, described by equation 7.1. Table 7.3 displays and compares the collection losses between the rotary and integrated harvesting systems due to dropped lanterns or lanterns detached but not collected. Observations during testing on very dry crop conditions concluded that lanterns can become detached from the plant stem if the stem is impacted with a strong force or subjected to harsh vibration. Many times lanterns detached by these methods would be lost and not collected. During testing of the rotary harvesting system, collection losses were reduced from 52.46 to 62.90 %, a reduction of 19.56% due to the installation of the deflection shields. The integrated harvesting and collection system further reduced collection losses from 32.90 to 12.89%, a 20.01% reduction. This reduction in collection losses proved the advantage of utilizing a stripping finger belt to harvest and transfer crop material to a collection hopper

$$Collection\ Losses\ (CL)\ \% = \left(\frac{D}{M + D + LOP}\right) * 100 \qquad \textbf{Equation 7.1}$$

Table 7.3: Comparison of average collection losses for 2011 harvesting systems

Machine	Average Collection Losses (CE) %
Rotary harvester without deflection shields	52.46%
Rotary harvester with deflection shields	32.90%
Integrated belt harvesting and collection system	12.89%

The results from testing of both the rotary and integrated harvesting systems influenced the design and development of the self-propelled harvesting header. The stripping fingers were proven to be capable of combing through plant stems and detaching lanterns,

provided that the crop structure is suitable for stripping. While the rotary system experienced high collection losses, the integrated harvesting and collection system reduced collection losses. The stripping finger belt system proved to be efficient at conveying the harvested material to a collection or hopper system. All of these factors and observations were taken into account during the development of the self-propelled harvester and header. Many aspects of the integrated harvesting system, such as the stripping finger belt system, were designed into the harvesting header in an attempt to maximize overall efficiency.

7.1.3 Self-Propelled Harvester Testing

Testing of the self-propelled harvester took place September through November 2012. The tests were completed on second year growth test plots. The crop structure was mainly vertical, single stemmed plants throughout the test plots.

Preliminary tests were completed at the Walter location with the self-propelled harvester. The purpose of these tests was to gain familiarity with the system and identify any areas of the system in need of major improvement. Several areas of improvement were identified during this initial testing. The conveyor drive and mount system was damaged during transport due to vibrations and road turbulence. The mounting and drive systems were improved and strengthened. A stand was designed and fabricated to stabilize the conveyor system during transport. It was also determined that a steady forward ground speed was necessary to minimize losses due to dropped lanterns. Abrupt changes in forward ground speed caused the stripping fingers to impact the plant stems violently, detaching the lanterns off the plant stem and onto the ground. The forward ground speed limiting function was developed and integrated into the machine control program as a result of this testing. Observations during preliminary testing also indicated that header height had a significant

impact on stripping efficiency. In order to successfully strip and collect the low lying lanterns the header was required to be as low to the ground as possible. Controlling header height manually proved to be a difficult task. Automatic header height control was developed to keep the header at a constant distance from the ground without relying on operator input during actual crop harvesting. This feature also eliminated abrupt changes that occurred when the operator manually adjusted header height.

After preliminary testing was completed, test runs were completed at the Walter location on August 14, 2012. The crop at the Walter location was very "poor", meaning short stems and a low density of stems. The header had no problems combing the stripping fingers through the second year, vertical stemmed crop and detaching lanterns, resulting in an average stripping efficiency of 95.50%. Losses were seen when lanterns were close to the ground, below what the header could strip. Losses were also seen when the fingers impacted the lanterns harshly and threw them forward, out of the header. On average, 13.49% of the harvested lanterns were lost due to these problems and determined to be collection losses. A full set of quantitative results from this testing can be seen in table 7.4.

Table 7.4: Test results, self-propelled harvester, Walter location

Test #	Harvested Lanterns (M)	Dropped Lanterns (D)	Lanterns left on plant (LOP)	Stripping Efficiency (SE) %	Collection Losses (CL) %	Overall Efficiency (OE) %
1	920	138	50	95.49	12.45	83.03
2	813	306	58	95.07	26.00	69.07
3	1314	244	70	95.70	14.99	80.71
4	1190	104	51	96.21	7.73	88.48
5	975	92	27	97.53	8.41	89.12
6	1405	207	121	93.02	11.94	81.07
Average	1102.83	181.83	62.83	**95.50**	**13.49**	**81.92**

A second round of testing was attempted at the Kemin Summerset location on August 20, 2012. The second year crop at the Kemin Summerset location was very dense due to irrigation throughout the growing season. The crop had a very high plant stem density and large volume of leaves attached to the stems. The stripping header had multiple problems combing through the dense crop. The large volume of stems and leaves tended to become lodged in the keyhole portion of the stripping finger, creating an immense amount of drag and resistance. The drag on the stripping fingers caused deflection in the roller chain drive system, damaging several drive shafts and components. The plant stems also remained in the combing and stripping area of the header even after they had been completely stripped of lanterns. These stems contributed to the drag and resistance.

The harvester was moved to an area of the test plot that had a less dense crop structure. Two test runs were completed before the stripping finger belt drive system experienced a major failure. The results from this testing can be seen in table 7.5. Although both stripping and overall efficiency suffered due to the dense crop, several key observations were made during this testing. It was evident that several improvements and modifications were necessary to handle the increased load created by the dense crop.

Table 7.5: Test results, self-propelled harvester, Kemin Summerset location - 8-20-12

Test #	Harvested Lanterns (M)	Dropped Lanterns (D)	Lanterns left on plant (LOP)	Stripping Efficiency (SE) %	Collection Losses (CL) %	Overall Efficiency (OE) %
1	1327	194	243	86.22	11.00	75.23
2	1282	306	369	81.14	15.64	65.51
Average	1304.50	250.00	306.00	**83.68**	**13.44**	**70.37**

The modifications and improvements that were made:

- The drive system was strengthened by adding braces and carrier bearings to the drive shafts. These bearings were added to minimize deflection of the drive shafts and increase the load carrying capacity.
- A larger displacement hydraulic motor was utilized to drive the stripping finger belt. Throughout testing it was observed that more torque was necessary to power the stripping fingers through the dense crop. This motor effectively increased the available torque without requiring a higher hydraulic pressure.
- The stripping finger belt system was redesigned with more robust components. Larger roller chain was utilized to drive the system. The rubber belt mounting system was redesigned for greater flexibility and functionality.
- A guide and pin system was developed and installed on the header. This system utilized guide pins and channels to stabilize and control the orientation of the stripping fingers through the harvesting portion of the header geometry. This system minimized deflection of the entire stripping finger belts system and created a very robust harvesting header.
- A push bar was added to the front of the harvesting header to remove stripped plant stems from the stripping fingers and reduce system load. The push bar was mounted approximately 7.62 cm from the ground and spanned the width of the header.

After the changes were completed, the self-propelled harvesting system was tested again at the Kemin Summerset location on October 16, 2012. The harvesting system performed relatively well throughout these tests. No breakages were experienced during this testing. The modifications to the header allowed the stripping fingers to pull through the thick crop, combing the plant stems and detaching lanterns. Deflection was minimized as a result of the guide pin and channel system. Results of the two tests completed after the modifications can be seen in table 7.6. The stripping efficiency of the harvester decreased slightly after the modifications were made. This is most likely due to the reduced flexibility of the stripping finger belt system. Before the guide pin and channel system were installed, deflection was allowed in the stripping finger belt. This deflection allowed the fingers bend with the crop load, resulting in more lanterns being stripped. After the modifications were made to the header, deflection of the stripping finger belt was minimized, resulting in a more forceful movement of the stripping fingers through the crop. The increased impact from this movement likely impacted the plant stems harshly, detaching the lanterns before they could be collected by the stripping fingers. The crop was also past maturity and consisted of very dry and brittle plant and lantern stems. The dry and brittle lantern stems were easily broken by impacting the plant stem, resulting in many lanterns being dropped on the ground. Collection losses increased during these tests, likely due to the brittle crop and plugging of the header cross auger. The cross auger became plugged with weeds and grass stems, causing lanterns to be thrown over the front lip of the auger tube and onto the ground.

Table 7.6: Testing results, self-propelled harvester, Kemin Summerset location - 9-16-12

Test #	Harvested Lanterns (M)	Dropped Lanterns (D)	Lanterns left on plant (LOP)	Stripping Efficiency (SE) %	Overall Efficiency (OE) %	Collection Losses (CL) %
1	864	211	245	81.44	65.45	15.98
2	1163	306	425	77.56	61.40	16.16
Average	1013.50	258.50	335.00	**79.50**	**63.43**	**16.09**

7.2 Harvester Systems Testing Observations

While the different harvesting systems were tested at different times and locations, their performance can still be evaluated by comparing stripping efficiency, collection losses, and overall efficiency. This comparison can be seen in table 7.7 and figure 7.3. Table 7.7 contains the averages for each system, over all the test runs completed by the system.

Table 7.7: Harvesting systems comparison, testing results

Harvesting System	Stripping Efficiency (SE) %	Collection Losses (CL) %	Overall Efficiency (OE) %
Rotary Harvester w/o deflection shields	95.58	52.46	43.35
Rotary Harvester with deflection shields	97.84	32.90	64.96
Integrated harvesting and collection system	63.53	12.89	50.65
Self-propelled Harvester	89.48	14.53	74.95

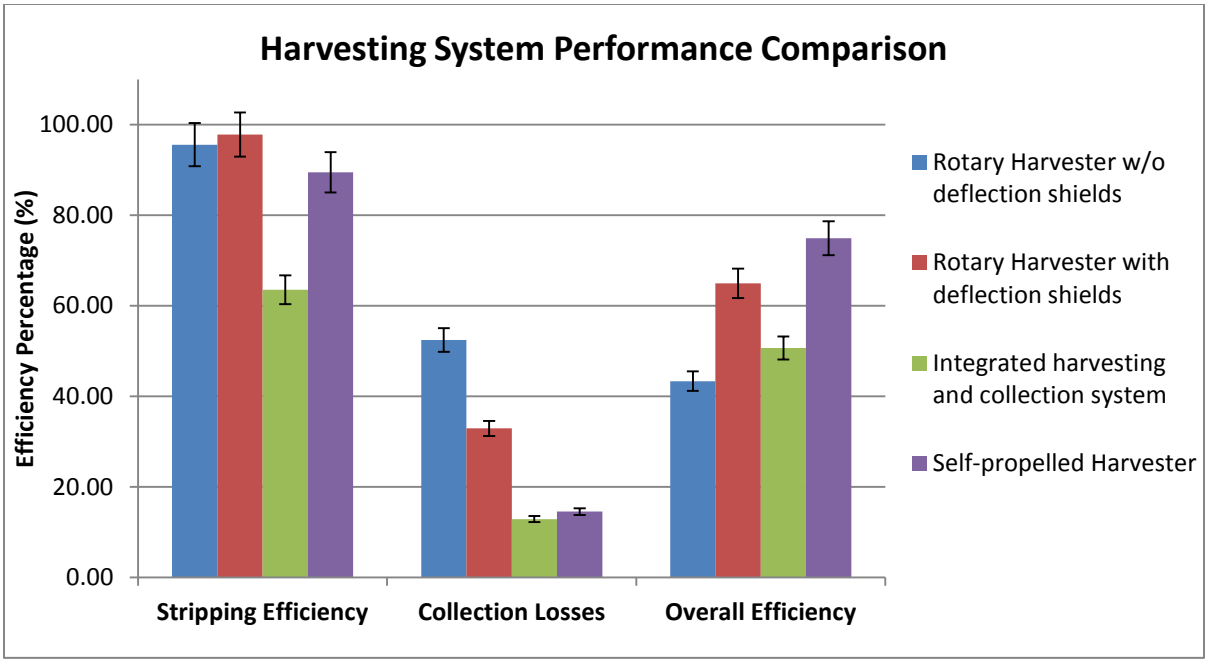

Figure 7.3: Harvesting systems performance comparison

When comparing the harvesting systems, it can be seen that stripping efficiency remained fairly constant across all systems. The exception to this comparison is the integrated harvesting and collection system. The stripping efficiency of this system was likely reduced by the short, branched crop structure of the tests plots used during testing. The harvesting system was improved with each new development and iteration of the system. This can be clearly seen by the decrease in collection losses. The collection losses of the rotary system decreased drastically when deflection shields were utilized. Collection losses were further decreased by the integrated harvesting and collection machine through the use of the stripping finger belt system. Collection losses for the self-propelled harvester were slightly higher, on average, than the integrated harvesting and collection machine. This may be partially due to the challenges of the dense and lush crop structure of the test plots used

for testing of the self-propelled harvester. Lanterns lost to plugging of the header cross-auger also had a negative impact on collection losses. However, when comparing overall efficiencies, a steady increase can be seen with each new harvesting system. Once again, the exception to this increase is the overall efficiency of the integrated harvesting and collection machine. The overall efficiency of this machine was significantly impacted by the reduction in stripping efficiency previously discussed.

7.3 Roller Separation System, Experimental Tests

The experimental tests of the separation system were completed to validate the frictional roller concept and provide insight into several important parameters such as roller diameter, roller rotational speed, and roller surface characteristics. Nine initial tests were completed using three roller speed levels. As seen in table 7.8, a roller speed of 30 rpm yielded the highest overall separation efficiency. However, it became very evident that orientation of the lanterns as they were introduced to the rollers had a very significant impact on separation efficiency. Orientating the lanterns "stem down" resulted in an average separation efficiency of 69%. Random orientation of the lanterns yielded an average separation efficiency of 40%, 29% lower than the separation efficiency of stem down orientated lanterns. Three more test runs were completed using the optimum machine parameters identified in test runs 1-9. Results from the optimized parameter testing are displayed in table 7.9. All ten lanterns were orientated stem down in tests 10-12 in order to develop optimum parameter scenario separation efficiency. The results from the experimental runs indicated that introducing the lanterns stem-down to the rollers yielded the highest separation efficiency.

Table 7.8: Testing results, separation system parameter investigation - roller bed angle, roller rpm

Run	Roller Angle (Degrees)	Air Suction (in/water)	Roller RPM	Stem Down % Separation	Random Orientation % Separation	Overall % Separated
1	30	0	15	60%	0%	60%
2	30	25	15	80%	40%	60%
3	30	25	15	60%	60%	60%
Average				**67%**	**33%**	**60%**
4	30	0	30	40%	80%	60%
5	30	25	30	100%	60%	80%
6	30	25	30	80%	20%	50%
Average				**73%**	**53%**	**63%**
7	30	0	45	80%	60%	70%
8	30	25	45	80%	0%	40%
9	30	25	45	40%	40%	40%
Average				**67%**	**33%**	**50%**

Table 7.9: Testing results, separation system – optimized parameters

Run	Angle (degrees)	Air Suction (in/water)	Roller RPM	Guards	Stem Down % Separation	Overall % Separated
10	30	25	30	Yes	90%	90%
11	30	25	30	Yes	100%	100%
12	30	25	30	Yes	90%	90%
Average					**93%**	**93%**

Several other experimental tests were completed to test other machine parameters. During one group of these tests the frictional rollers were spaced so that a 0.254 mm gap existed between adjacent rollers. The idea behind the spacing was to allow the sepals to pass between the rollers without become crushed and torn apart. However, the gap between the rollers reduced the frictional force and pinching ability of the rollers, drastically reducing separation efficiency. This idea was subsequently discarded.

Another set of tests were completed using polyurethane rollers. These rollers were fabricated using polyurethane tubes and an inner drive shaft. The polyurethane tubes were sized to fit tightly over the steel drive shafts so that no epoxy or fixing method was necessary. The polyurethane tubes were manufactured with to a 60A Durometer hardness rating. During testing, the polyurethane tubes proved to be too soft to pinch and pull the sepals from the berry and stem. The lack of frictional force created by the polyurethane rollers resulted in very few lanterns being successfully separated. The polyurethane rollers were discarded in favor of steel rollers. This testing eventually led to the machining of steel rollers and knurling of the outer surface.

The knurled outer surface of the rollers increased the kinetic frictional coefficient. This increased friction was necessary to effectively pull the outer sepal material into the roller pinch point. The knurled steel rollers achieved the best separation efficiency of any of the rollers tested. These rollers were utilized for testing and completion of the full DOE designed to optimize system parameters.

7.4 Roller Separation System, Design of Experiments

A full factorial DOE was completed to investigate the performance of the frictional rollers and feeder separation system. The effect of the factors, roller speed and feeder belt speed, on % un-separated lanterns and % full berries recovered was examined. Three levels of each factor were utilized for the testing. Roller speed levels of 30, 20, and 10 rpm were utilized for testing. Feeder belt linear velocity levels of 112.62, 75.08, and 37.54 m/min

Table 7.10: Roller Separation System full DOE results

Pattern	Roller Speed (rpm)	Feeder Belt Linear Velocity (cm/min)	% Un-separated Lanterns	% Full Berries	% Crushed Berries
0	20	75.08	10.00%	30.00%	60.0%
0	20	75.08	24.00%	30.00%	46.0%
0	20	75.08	12.00%	38.00%	50.0%
0	20	75.08	12.00%	44.00%	44.0%
0	20	75.08	18.00%	48.00%	34.0%
0	20	75.08	18.00%	56.00%	26.0%
0	20	75.08	24.00%	64.00%	12.0%
0	20	75.08	18.00%	66.00%	16.0%
11	10	37.54	12.00%	48.00%	40.0%
11	10	37.54	34.00%	66.00%	0.0%
11	10	37.54	22.00%	68.00%	10.0%
11	10	37.54	12.00%	72.00%	16.0%
12	10	75.08	24.00%	30.00%	46.0%
12	10	75.08	4.00%	34.00%	62.0%
12	10	75.08	20.00%	40.00%	40.0%
12	10	75.08	12.00%	42.00%	46.0%
13	10	112.62	24.00%	36.00%	40.0%
13	10	112.62	12.00%	52.00%	36.0%
13	10	112.62	24.00%	54.00%	22.0%
13	10	112.62	24.00%	56.00%	20.0%
21	20	37.54	24.00%	18.00%	58.0%
21	20	37.54	22.00%	44.00%	34.0%
21	20	37.54	28.00%	46.00%	26.0%
21	20	37.54	46.00%	54.00%	0.0%
22	20	75.08	16.00%	38.00%	46.0%
22	20	75.08	18.00%	42.00%	40.0%
22	20	75.08	16.00%	46.00%	38.0%
22	20	75.08	18.00%	60.00%	22.0%
23	20	112.62	32.00%	42.00%	26.0%
23	20	112.62	14.00%	44.00%	42.0%
23	20	112.62	12.00%	46.00%	42.0%
23	20	112.62	18.00%	66.00%	16.0%
31	30	37.54	16.00%	16.00%	68.0%
31	30	37.54	26.00%	30.00%	44.0%
31	30	37.54	14.00%	42.00%	44.0%
31	30	37.54	18.00%	60.00%	22.0%
32	30	75.08	14.00%	24.00%	62.0%
32	30	75.08	16.00%	26.00%	58.0%
32	30	75.08	22.00%	46.00%	32.0%
32	30	75.08	34.00%	54.00%	12.0%
33	30	112.62	22.00%	30.00%	48.0%
33	30	112.62	28.00%	32.00%	40.0%
33	30	112.62	26.00%	44.00%	30.0%
33	30	112.62	20.00%	44.00%	36.0%

were also used for testing. Each parameter combination was replicated there times, with an additional two center point runs added as a measure of process stability. A full set of quantitative results can be seen in table 7.10. Percentages of un-separated lanterns and full berries are both provided on the right side of the table. While table 7.10 is sorted according to pattern, the tests were completed in a randomized order.

A statistical analysis was conducted to ascertain any statistical significance among the data and factor levels. The analysis was completed utilizing JMP (SAS Institute, Cary, North Carolina) software. A standard least squares model analysis was applied to the data. This analysis provides a least square fit with an analysis of variance for the model. The results of the ANOVA analysis can be seen in table 7.11.

Table 7.11: ANOVA results for un-separated lanterns and full berries response. Roller speed and feeder belt speed utilized as factors.

Response	Effect	DF	SS	F Ratio	p > F
Un-Separated Lanterns	Roller Speed	1	10.667	0.691	0.4105
	Feeder Belt Speed	1	3.375	0.2188	0.6425
	Roller Speed *Feeder Belt Speed	1	5.0625	0.3283	0.5699
Full Berries	Roller Speed	1	234.375	5.5022	0.024*
	Feeder Belt Speed	1	3.375	0.0792	0.779
	Roller Speed *Feeder Belt Speed	1	52.562	1.234	0.273

*Significant at 0.10 level

When utilizing a p value ≤ 0.10 to signify statistical significance, it is seen that only roller speed become significant in relation to the number of full berries recovered after each test. This indicates that roller speed has a statistically significant effect on the severity and level of berry crushage. Therefore, all insignificant effects were removed in order to examine roller speed as the only main effect. A t-test was also performed to compare the means of every treatment to the means of every other treatment. The t- test examined the differences in roller speed levels and their effect on the number of full berries recovered.

The confidence coefficient, α, was set to 0.10 for this analysis. The results of this analysis can be seen in tables 7.12 and 7.13. As seen in table 7.13, roller speed levels 30 and 10 are not connected by any level. This indicates that roller speed 30 and 10 are statistically different from each other, the difference between their means is larger than the expected standard error. The results also conclude that there is no statistical difference between roller speeds 30 and 20. There is also not a statistical difference between 20 and 10. However, the analysis did recognize a statistical difference between 30 and 10. The conclusion from this analysis is that a larger range of roller speeds may need to be tested in order to obtain a larger range of means and overall variation. The effect of roller speed on full berries can also be graphically depicted as seen in figure 7.4

Table 7.12: Separation system model utilizing roller speed as single main effect

Source	DF	SS	Mean Square	F Ratio	p < F
Model	1	17.273	17.235	5.594	0.0227*
Error	42	1742.533			
C. Total	43	1759.807			

*Significant at 0.10 level

Table 7.13: Roller speed t-test results effect on full berries

Roller Speed Level	Level	Mean
10	A	24.917
20	A B	23.05
30	B	18.667

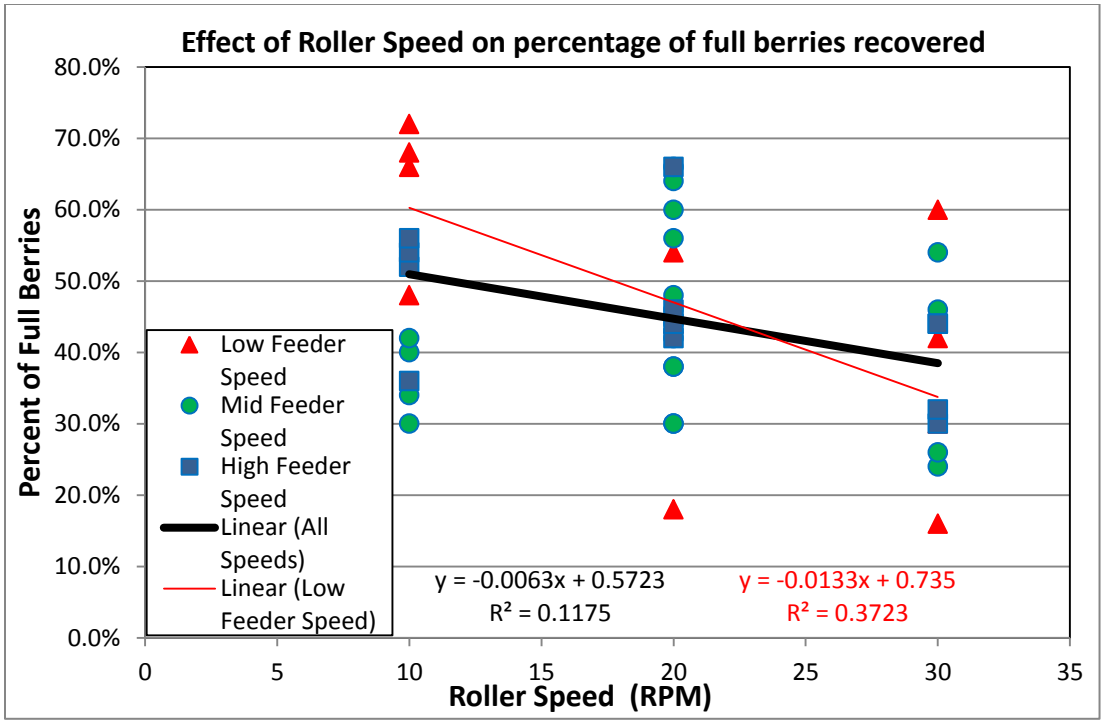

Figure 7.4: Effect of roller speed on berry damage, roller speed vs. Percent full berries recovered

Figure 7.4 displays the effect of roller speed on the percentage of full berries recovered. Due to the fact that crushed berries are unacceptable for further downstream processing, this data can also be recognized as the effect of roller speed on separation efficiency.

An important point to emphasize in this data is that one of the main goals of this testing is to maximize separated lanterns, while minimizing crushed berries. Due to the fact that crushed berries cause many downstream processing problems, reducing berry damage and crushage becomes a major point of interest. The amount of crushed berries is explained previously be equation 6.4. The effects of roller speed on percent crushed berries can be seen in figure 7.5. While these effects were not found to be statistically significant, the data does display slight trends that may explain some of the interactions. As seen, the percentage of

crushed berries is minimized when feeder belt and roller speeds are reduced. However, when roller speed is held constant at 10 rpm, berry damage is reduced as feeder belt speed is increased from 75.08 to 112.62 m/min. This is most likely caused by the reduction of roller bed exposure time of the lantern. A higher feeder belt speed also has a tendency to cause tumbling of the lanterns, which may increase the possibility of the stem getting caught in the rollers, increasing the chances for a successful separation.

Further analysis of the data leads to the investigation of the factor effects on the percentage of un-separated lanterns (Figure 7.6). Again, these effects were not found to be statistically significant at the $\alpha = 0.10$ level, but several trends are displayed in the data. This analysis also displays evidence that a relatively slow roller speeds and feeder belt speed yield the best results. In this case, the desired result is to minimize the percentage of un-separated lanterns.

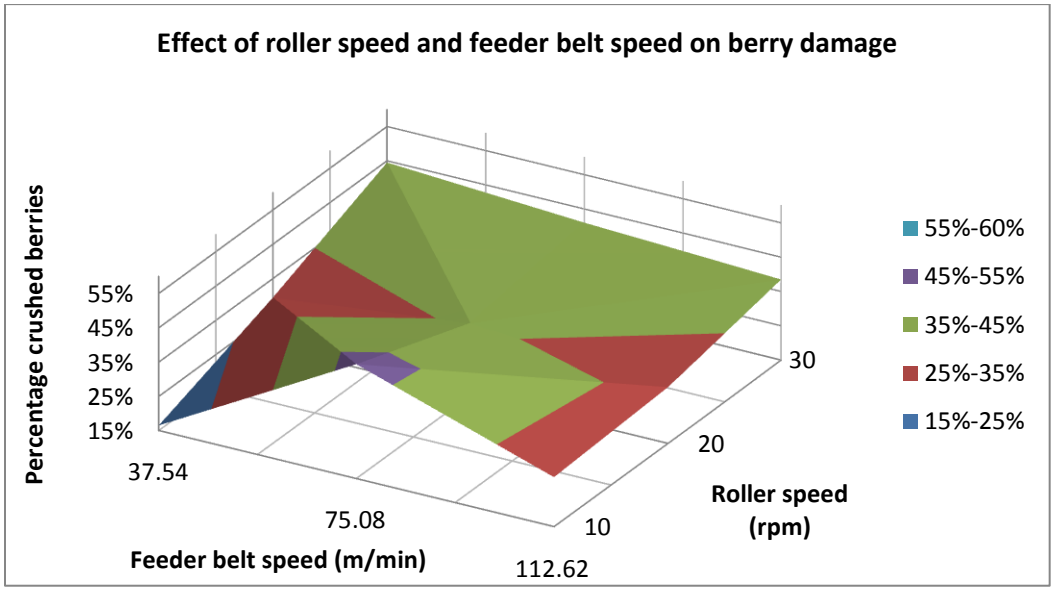

Figure 7.5: Effect of roller speed and feeder belt speed on percentage of crushed berries

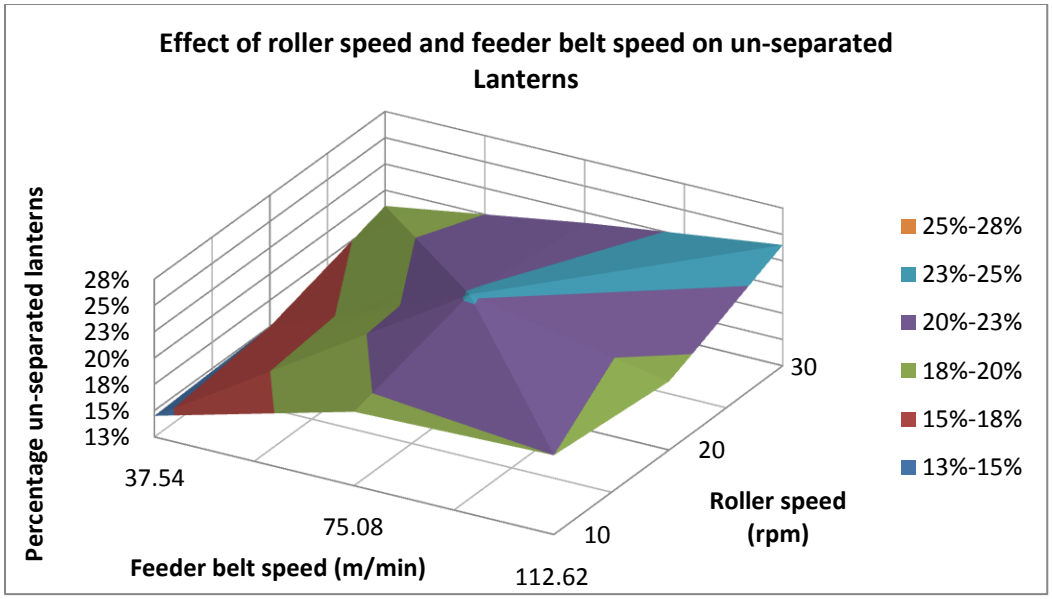

Figure 7.6: Effect of roller speed and feeder belt speed on percentage of un-separated lanterns

Overall, for the separation system developed and tested for this project, the data indicates that separation efficiency, the percentage of full berries recovered, can be maximized by utilizing relatively slow roller speeds, below 20 rpm, and feeder belt linear velocities below 75.08 m/min.

7.5 Vibration Orientation and Feeding Testing

Testing of the vibration table feeding system was completed to investigate an alternative feeding mechanism to deliver lanterns to the frictional roller bed. The goal of the vibration feeding system was to orient the lanterns stem first, in order to maximize separation efficiency. Preliminary testing identified three vibration amplitudes with potential for orientating lanterns. These amplitudes were tested in conjunction with a feeding tube in order to test feeding tube height and feasibility of the system. The feeding tube was utilized to simulate a bulk feeding environment and investigate any bridging issues. The resulting

lantern orientation for each tube height can be seen in figures 7.7 through 7.10. Average orientation and separation efficiency data for each set of three tests from the vibration orientation and feeding testing can be seen in table 7.14. The raw data and orientation data collected from this testing can be seen in Appendix A. A total of 36 tests were completed for this set of tests. During several of the tests lanterns remained trapped between the bottom of the feeding tube and vibration table. The lanterns were unable to move from out under the feeding tube and continue down the vibration table. These lanterns were denoted as "stuck in tube" during data collection. Severe material grouping and bunching was observed during two of the tests. Data was not able to be collected for these tests. Each test was evaluated for feasibility according to the benchmarks defined previously. Three parameter combinations were found to produce results that met or exceeded the feasibility benchmarks. The tests that were found to feasible can be found in table. The data from these tests was further investigated in order to derive estimated feed rate and throughput values.

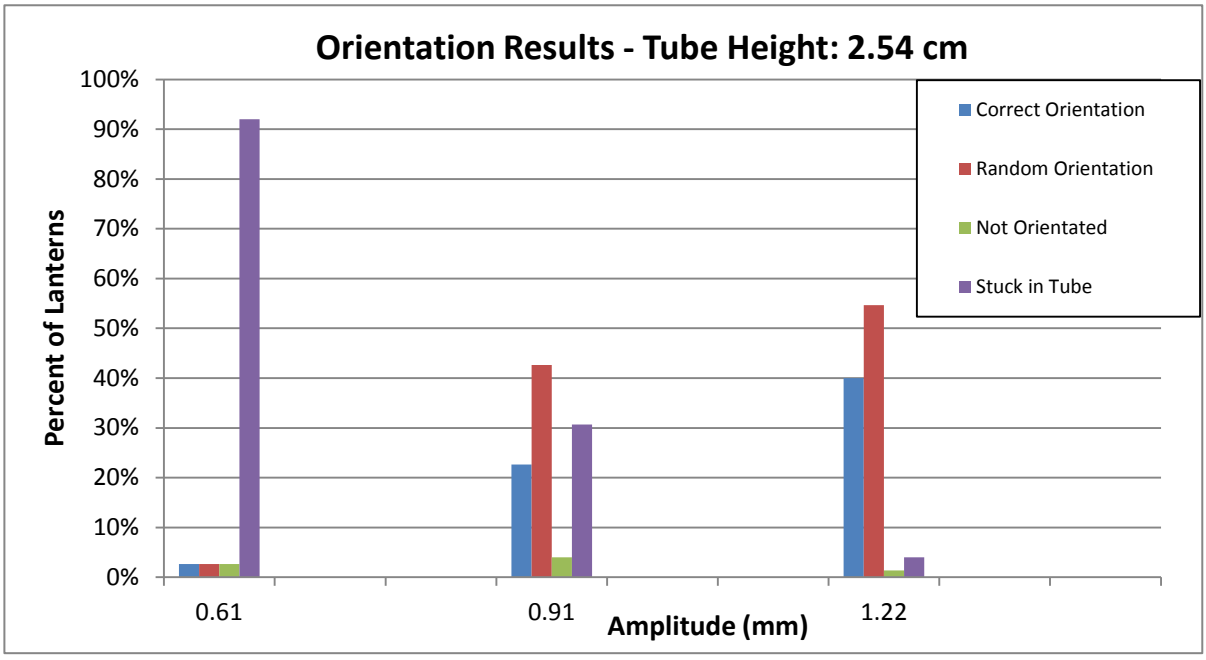

Figure 7.7: Orientation results, 2.54cm tube height

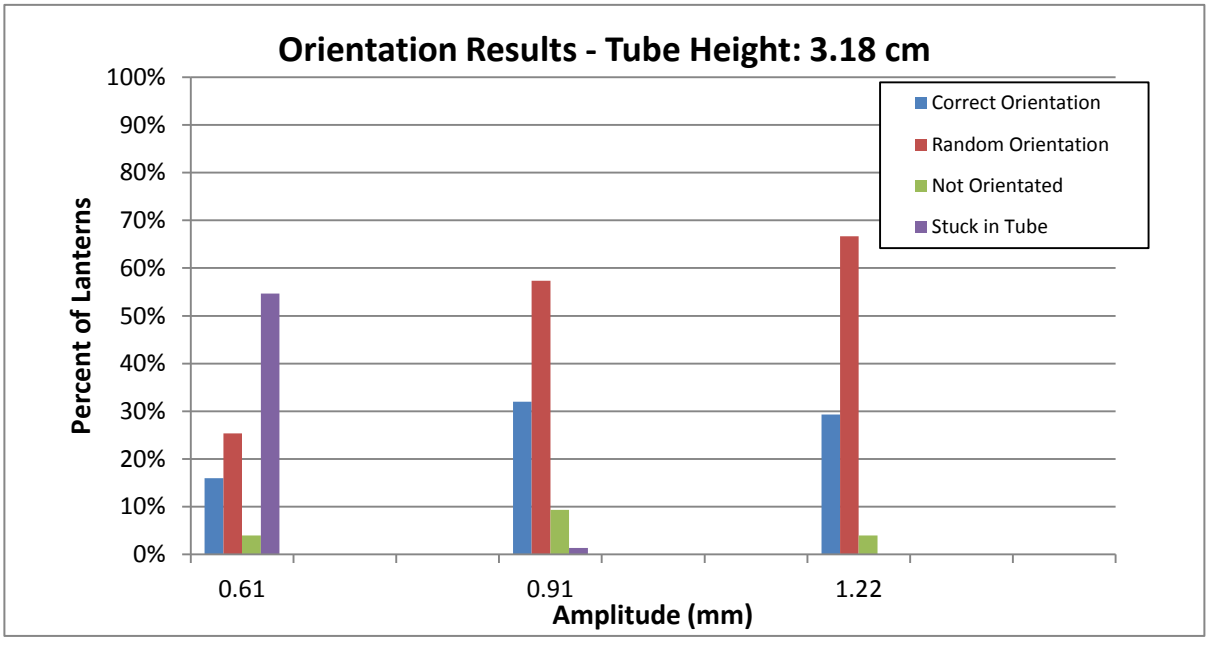

Figure 7.8: Orientation testing results, 3.18 cm tube height

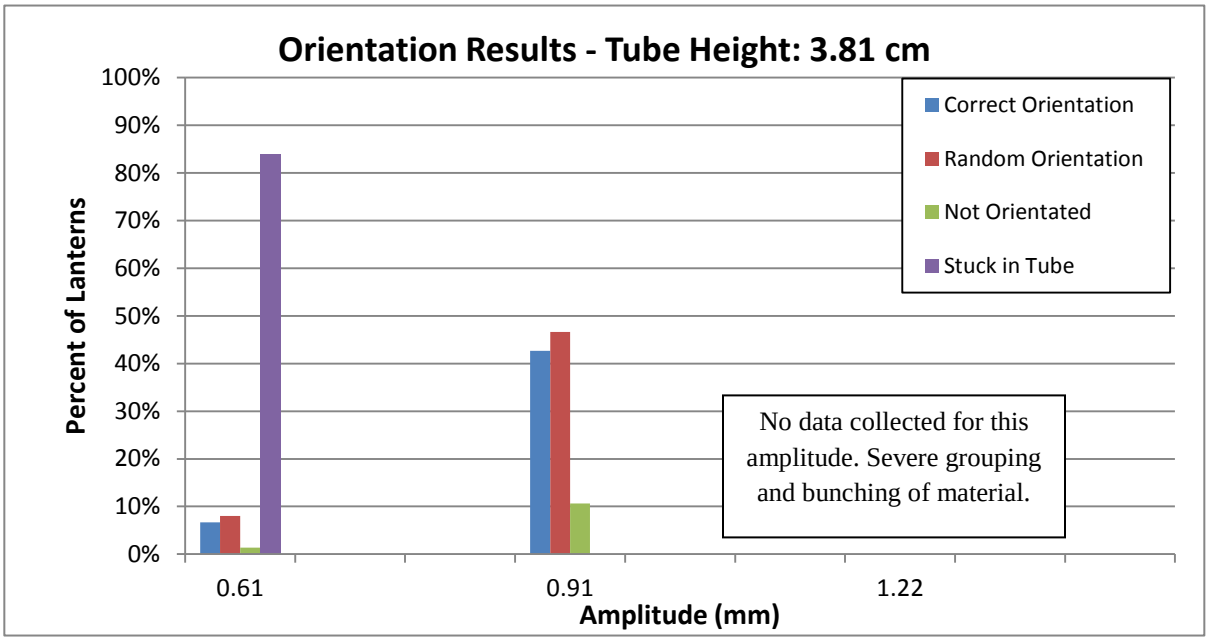

Figure 7.9: Orientation testing results, 3.81 cm tube height

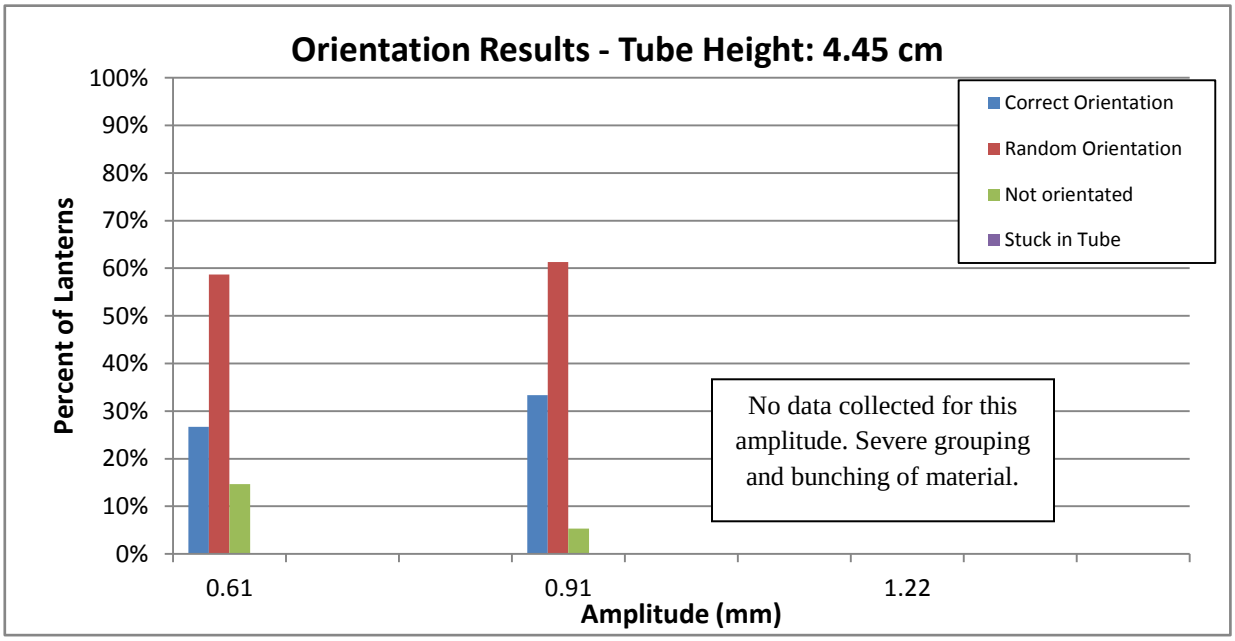

Figure 7.10: Orientation testing results, 4.45 cm tube height

Table 7.14: Vibration orientation and feeding test results including: average lantern orientation, estimated separation efficiency, and overall feasibility

Parameter combination set	Tube Height (cm)	Amplitude (mm)	Average % Lanterns Correct Orientation	Average % Lanterns Random Orientation	% Lanterns stuck in tube	% Lanterns not orientated	Estimated Average Separation Efficiency %, First pass	Feasible
1	2.54	0.61	2.67%	53.30%	92.00%	2.67%	23.81%	NO
2	2.54	0.91	25.33%	44.00%	30.67%	4.00%	41.23%	NO
3	2.54	1.22	41.33%	54.67%	4.00%	1.33%	60.43%	YES
4	3.18	0.61	18.67%	26.67%	54.67%	4.00%	28.09%	NO
5	3.18	0.91	38.67%	60.00%	1.33%	6.67%	60.08%	YES
6	3.18	1.22	32.00%	68.00%	0.00%	4.00%	57.06%	NO
7	3.81	0.61	6.67%	93.30%	84.00%	1.33%	43.54%	NO
8	3.81	0.91	48.00%	52.00%	0.00%	10.67%	65.58%	YES
9	3.81	1.22	Not feasible, severe grouping and bunching of material.					NO
10	4.45	0.61	32.00%	68.00%	0.00%	14.67%	57.06%	NO
11	4.45	0.91	36.00%	64.00%	0.00%	5.33%	59.19%	NO
12	4.45	1.22	Not feasible, severe grouping and bunching of material.					NO

Table 7.15: Vibration orientation and feeding testing results, feed rate and throughput analysis for feasible parameters

Tube Height (cm)	Amplitude (mm)	Estimated Sep. Efficiency %	Estimated Average Sep. Efficiency %	Separation Efficiency Standard Deviation	Feedrate (kg/hr/footwidth)	Separated Throughput, First Pass (kg lanterns/hr/foot width)	Un-Separated Return Throughput (kg lanterns/hr/footwidth)
2.54	1.22	58.12%			15.11		
2.54	1.22	61.85%	60.43%	2.02%	28.70	13.64	8.93
2.54	1.22	61.32%			23.92		
3.18	0.91	55.46%			35.88		
3.18	0.91	61.32%	60.08%	4.14%	26.09	21.99	14.61
3.18	0.91	63.45%			47.84		
3.81	0.91	67.72%			35.88		
3.81	0.91	61.32%	65.58%	3.69%	47.84	25.27	13.26
3.81	0.91	67.72%			31.89		
Overall Average			**62.03%**		**32.57**	**20.30**	**12.27**

The three sets tests that were identified as feasible were analyzed to determine estimated feed rate and separated throughput under optimum operating parameters. These values can be seen in table 7.15. The feedrate seen in table 7.15 values correspond to the amount of material that could be provided to the vibration table in order sustain a steady flow of material to the frictional roller bed. The estimated separated throughput values define the amount of material that will be successfully separated by the vibration table and frictional roller system, on the first pass through the system. The material that is not separated on the first pass and requires multiple passes through the system is represented by the un-separated return throughput column. These values can also be seen in figure 7.11.

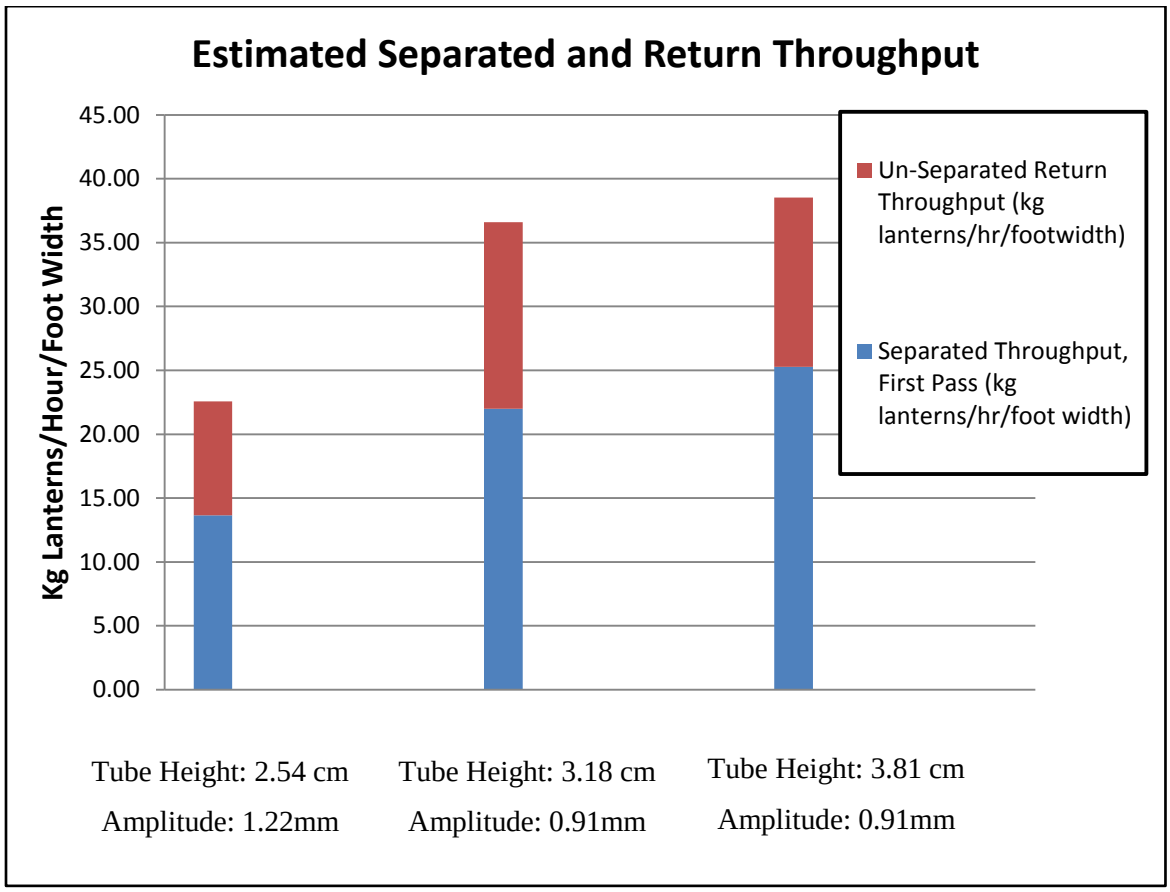

Figure 7.11: Estimated separated (blue) and return throughput (red), feasible separation system parameters

As seen in figure 7.11, the estimated separated throughput increases as tube height increases. This trend is caused by the ability for material to flow more easily out of the feeding tube onto the vibration tube. This decreases the time required for material to clear the feeding tube, subsequently increasing the throughput. However, un-separated throughput also increases as a result. The larger volume of return material requires a larger material handling system to recycle the un-separated material for multiple passes through the separation system. It has also been noted, through observations that separation efficiency decreases for material after the first pass. While no data has been formally collected to validate this claim, this decrease in separation efficiency presents many areas of investigation in the future.

Overall, several challenges have been presented through this testing. It has been found that lantern orientation is difficult to maintain from the vibration table to the frictional roller bed. This is a result of lanterns tending to tumble down an incline, rather than sliding neatly. As a result, the percentage of lanterns orientated correctly could be reduced during the transition from vibration table to frictional roller bed, decreasing separation efficiency. While higher vibration amplitudes have shown to improve correct lantern orientation, a threshold does exist for vibration amplitudes. At amplitudes above 1.22mm lanterns tend to bounce around the vibration table, rather than orientating. This effectively negates the purpose of the vibration table and attempt at orientating the lanterns. The physical characteristics have also shown to affect efforts to orient the lanterns using vibration. While no tests have been focused at formally explaining these interactions, the interactions between size, weight, and shape were apparent during testing. The variation that all these challenges present create an orientation system that is very susceptible to changing crop conditions and

also operating conditions. The physical characteristics of the harvested lanterns not only introduce variation that affects the orientation, they also introduce variation to and affect the friction roller bed surface. Different size lanterns and berries may require rollers of different sizes and surface frictional coefficients. However, the system has proven to be successful at orientating and separating lanterns at certain efficiency levels.

7.6 Differential Drying and Abrasion Concept Validation Testing

Concept validation of the drying and abrasion separation process was accomplished by completing the simple 2x2 DOE outlined in table 6.6. The results of this testing were very promising and provided a good understanding of the system and interactions between the two processes, drying and abrasion. A full set of quantitative results from this testing can be seen in table 7.16.

Table 7.16 displays several results for each test completed. The weight after abrasion represents the total weight of all material recovered after abrasion. The percentage of intact berries recovered indicates the percentage of the total number of full berries that were recovered from the material after abrasion testing. Any partial or broken berries were not included in this assessment and were included in the sepal and other material fraction weights. Total sepal weight displays the total weight of all material after the intact berries were removed. The three fractions of sepal material can also be seen in table 7.16.

Table 7.16: Drying and abrasion initial testing results, % berries recovered intact and fraction weights

Repetition #	Temp (˚C)	Residence Time (hours)	Weight after abrasion (g)	% of berries recovered intact	Berry weight (g)	Total sepal weight (g)	Fraction above 3/16 weight (g)	Fraction 3/16 - 2/16 weight (g)	Fraction below 2/16 weight (g)
1	85	6	70.34	100.00%	65.14	5.17	2.45	0.87	1.81
2	85	6	68.27	100.00%	63.52	4.64	2.16	0.76	1.61
3	85	6	76.99	98.00%	72.02	4.85	1.92	1.04	1.80
Average			**71.87**	**99.33%**	**66.89**	**4.89**	**2.18**	**0.89**	**1.74**
1	100	6	53.22	98.00%	47.83	5.27	2.74	0.68	1.77
2	100	6	49.50	100.00%	45.82	3.69	1.73	0.63	1.24
3	100	6	53.70	100.00%	48.62	5.06	2.02	0.84	2.10
Average			**52.14**	**99.33%**	**47.42**	**4.67**	**2.16**	**0.72**	**1.70**
Residence time group average			**62.00**	**99.33%**	**57.16**	**4.78**	**2.17**	**0.80**	**1.72**
1	85	18	41.02	84.00%	26.55	14.47	2.47	1.40	10.56
2	85	18	43.04	90.00%	29.95	13.15	2.65	1.03	9.34
3	85	18	45.55	96.00%	32.72	12.78	2.25	1.04	9.40
Average			**43.20**	**90.00%**	**29.74**	**13.47**	**2.46**	**1.16**	**9.77**
1	100	18	41.24	74.00%	10.53	30.70	2.67	1.39	26.56
2	100	18	40.92	70.00%	11.15	29.66	3.34	1.96	24.13
3	100	18	41.36	50.00%	8.6	32.60	3.52	2.53	26.32
Average			**41.17**	**64.67%**	**10.09**	**30.99**	**3.18**	**1.96**	**25.67**
Residence time group average			**42.19**	**77.33%**	**19.92**	**22.23**	**2.82**	**1.56**	**17.72**
Overall average			**52.10**	**88.33%**	**38.54**	**13.50**	**2.49**	**1.18**	**9.72**

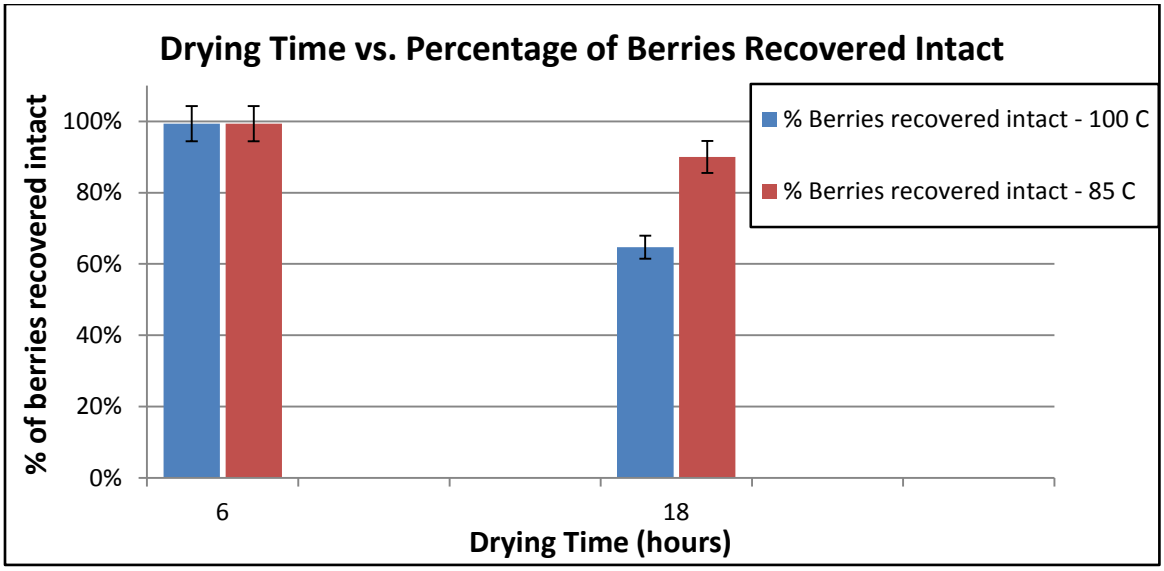

Figure 7.12: Comparison of drying time vs. percentage of berries recovered intact

A distinct relationship between drying time and percentage of intact berries recovered becomes evident when examining table 7.16 and figure 7.12. The percentage of berries recovered intact suffers significantly when drying time is increased from 6 to 18 hours. This decrease in percentage of berries recovered intact is a result of extensive drying creating dry and brittle berries. The dry and brittle berries break apart during the abrasion process and become included in the sepal material. However, when drying residence time is limited to 6 hours the percentage of berries recovered intact is much higher, averaging 99.33%.

A sepal to berry weight ratio was derived by manually hand separating 15 cape gooseberries and weighing the individual berry and sepal separately. This material was dried at 100˚C for 6 hours. The resulting ratio for sepal to berry weight was 0.166. This ratio was then used to determine the expected berry weight and total sepal weight. In addition, this information was then used to calculate the estimated sepal contamination by broken up, crushed berries. Inversely, the amount of sepal material still attached to the intact berries and

stems could also be calculated. The results for this analysis of the initial tests can be seen in table 7.17.

Table 7.17: Estimated contamination of separation materials

Temperature (˚C)	Residence Time (hr)	Expected Berry Weight (g)	Berry weight (g)	Expected sepal weight (g)	Total sepal weight (g)	Estimated Berry material in sepal (g)	Estimated sepal material left on berries (g)
100	6	44.41	47.83	8.81	5.27	0.00	3.42
100	6	41.30	45.82	8.20	3.69	0.00	4.52
100	6	44.81	48.62	8.89	5.06	0.00	3.81
100	18	34.41	10.53	6.83	30.7	23.88	0
100	18	34.15	11.15	6.77	29.66	23.00	0
100	18	34.51	8.6	6.85	32.6	25.91	0
85	6	58.69	65.14	11.65	5.17	0.00	6.45
85	6	56.97	63.52	11.30	4.64	0.00	6.55
85	6	64.24	72.02	12.75	4.85	0.00	7.78
85	18	34.23	26.55	6.79	14.47	7.68	0
85	18	35.91	29.95	7.13	13.15	5.96	0
85	18	38.01	32.72	7.54	12.78	5.29	0

It can be estimated that when a lower residence time was utilized, sepal material was left attached to the berries, and not fully separated. This estimation was confirmed using pictures of the resulting materials after abrasion. During the longer residence times the berries became dry and brittle, allowing them to break up and become fragmented during abrasion. This can be seen as the estimated berry material in sepal in table 7.17. These numbers indicate that berries had broken up into small pieces and become mixed in with the sepal material fractions. A noticeable difference could also be seen between the shorter and longer drying residence times. Berries subjected to the 18 hour residence time became blackened and slightly charred while berries subjected to a 6 hour residence time retained

their original color. This difference in berry color and appearance can be seen in figure 7.13 and 7.14.

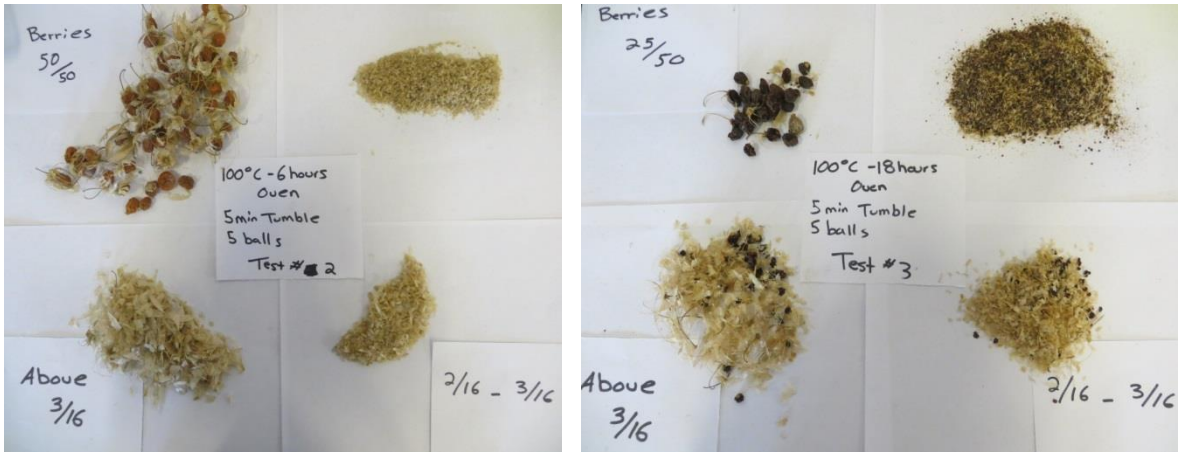

Figure 7.13: Drying and abrasion testing results, 100 C

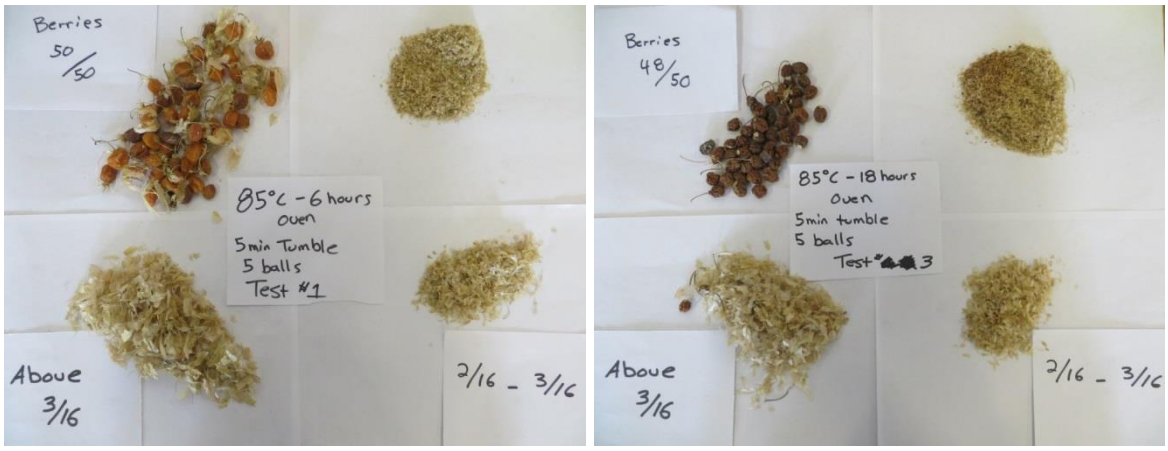

Figure 7.14: Drying and abrasion testing results, 85 C

When analyzing the 100° C drying and abrasion tests, a noticeable difference can be seen in both the percentage of berries recovered intact and also the volume and color of the fine sepal material. The fine sepal material of the 18 hour residence test is darker than the shorter 6 hour residence test. This can be attributed to the darkened berries becoming broken

up and incorporated with the fine sepal material. This fragmentation of the berries and contamination of the sepal material is unacceptable and would undoubtedly have a significant negative impact on extraction efficiency of zeaxanthin.

Several experimental tests were conducted following the completion of the main drying and abrasion DOE. A sample of un-dried cape gooseberries was placed in the durability tester without any rubber balls and allowed to rotate for five minutes. No separation of the sepal from the berries was observed. Rubber balls were then added to sample and the durability tester was rotated for another five minutes. The rubber balls crushed the berries and did not increase separation of the sepal. This testing confirmed that drying of the material is a critical process that must precede abrasion. Cape gooseberries were then dried and placed in the durability tester without rubber balls. After 10 minutes of rotation, minimal separation of the sepal had occurred. This test confirmed that the rubber balls were also critical to separation efficiency.

Overall, the drying and abrasion process has proven to be an effective system to separate sepal material from the berry. While several process parameters remain to be optimized to maximize separation efficiency, this work provides a base to move forward with the optimization.

7.6 Differential Drying and Abrasion Optimization Testing

Proven as an effective method for separation of cape gooseberry material, the differential drying and abrasion system was then optimized using Chinese lantern material. This testing was completed with three goals: (1) validate the system is effective for separating Chinese lantern sepal from berries, (2) determine optimum moisture content

values for chinese lantern berries and sepal to be dried to in order to achieve a high level of separation, and (3) define the relationship between drying temperature, drying residence time and the rate of cis-zeaxanthin formation.

A full set of quantitative results from this testing can be seen in Appendix A, Table A.4. These results include: separation efficiency, % berries recovered intact, berry moisture content, sepal moisture content, as well as the drying and abrasion process parameters. Several relationships become very evident when examining these results. As seen in figure 7.15, berry moisture content has a significant impact on % berries recovered intact. When moisture content of the berries falls below ~ 16.00% berries begin to fragment and shatter, contaminating the separated sepal material. On the upper end of the moisture content range, berries above ~ 45.00 – 50.00% moisture content tend to be too wet and become smashed during the abrasion process.

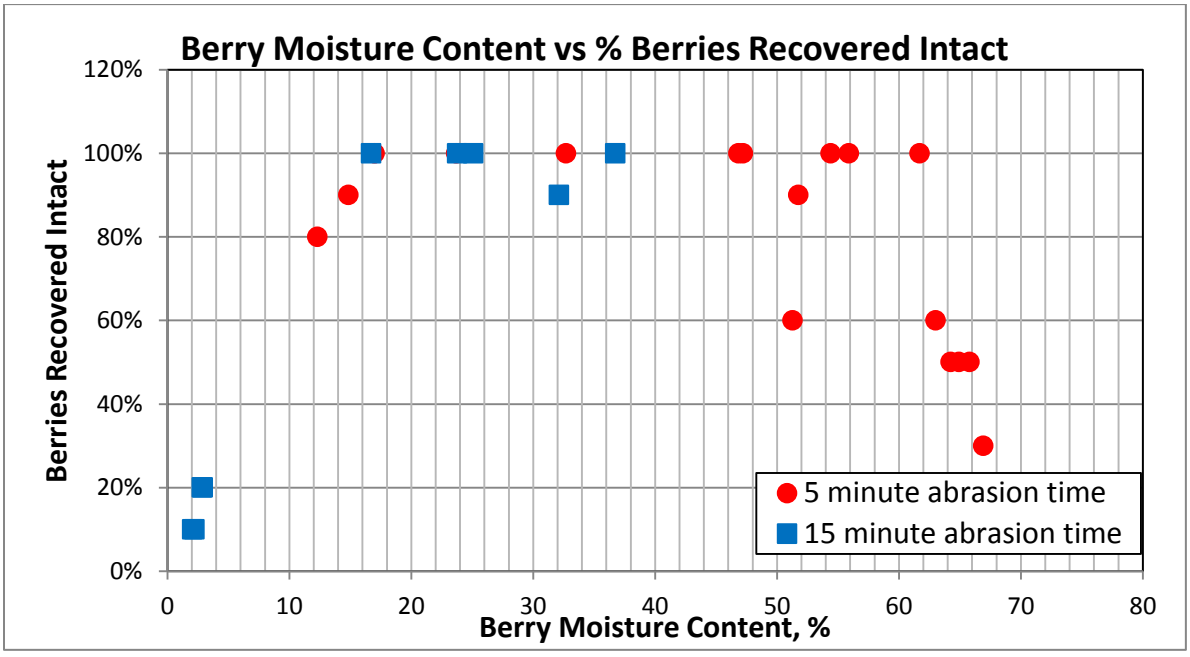

Figure 7.15: Berry moisture content vs. % berries recovered intact, 5 (blue) and 15 (red) minute abrasion times

Moving forward with larger scale testing and commercial processing, the target range for berry moisture content can be conservatively defined as between 20.00 and 35.00 %. Drying berries to this moisture content has minimized berry loss and sepal contamination during the abrasion process.

When analyzing the sepal moisture content and separation efficiency results, a target moisture content can be defined for the sepal. As seen in figure 7.16, separation efficiency is maximized when the sepal is dried below 6.00 % moisture content. However several data points do exist for sepal dried below 6.00% moisture content where separation efficiency suffers and is below ~65.00%. However, these points are for tests that utilized a 5 minute abrasion residence time. It is believed that these separation efficiencies could be increased significantly by increasing the abrasion residence time slightly.

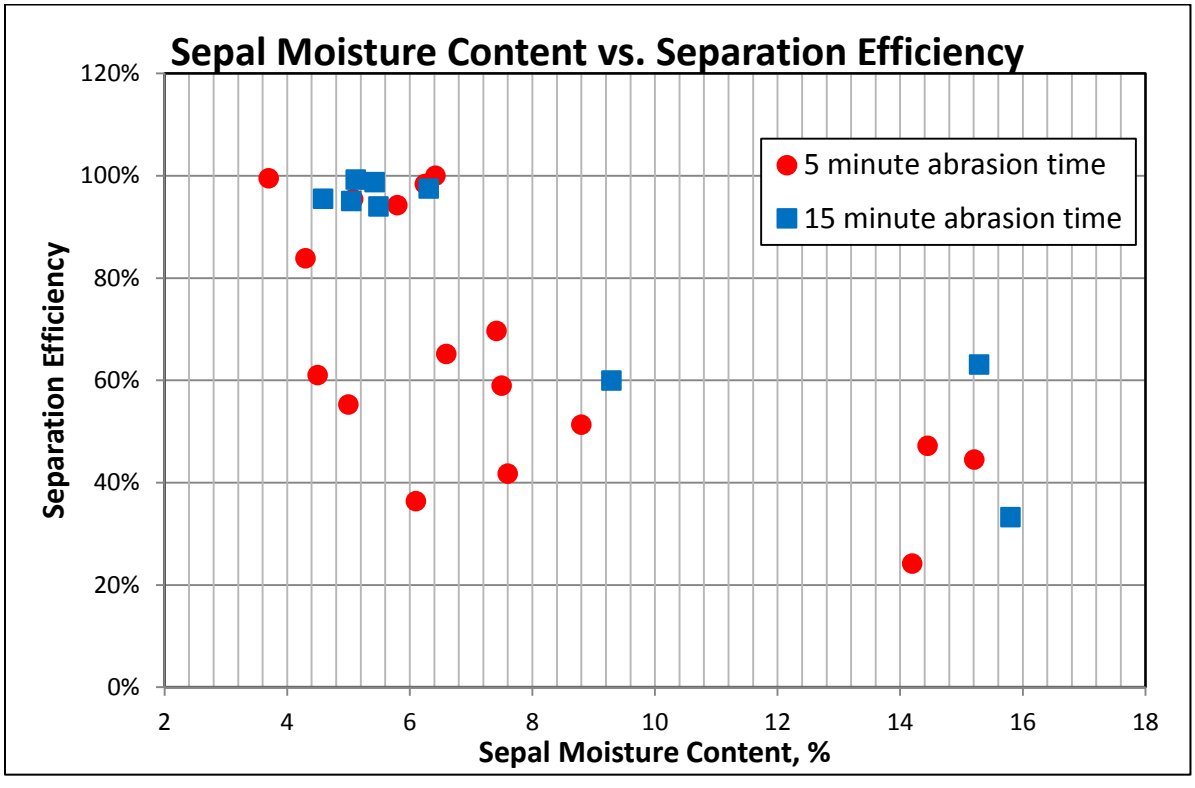

Figure 7.16: Sepal moisture content vs. separation efficiency, 5 (blue) and 15 (red) minute abrasion times

Investigation into the effects of drying temperature and residence time on cis-zeaxanthin formation was completed using a standard least squares ANOVA analysis as well as a T-test for the different temperature and time levels. The results of the ANOVA analysis are displayed in table 7.18. The analysis indicates that drying temperature is the only statistically significant effect on cis-zeaxanthin. This main effect is significant well beyond α=0.05 level. It can also be seen that neither drying residence time, nor the interaction between drying temperature and time has a statistically significant impact on cis-zeaxanthin formation. The conclusion from this testing is that temperature is the main factor that impacts and determines the rate of cis-zeaxanthin formation.

Table 7.18: ANOVA analysis of cis-zeaxanthin formation data

Source	DF	Sum of Squares	F ratio	Prob > F
Temperature (°C)	1	168.0556	58.3867	< 0.001
Residence Time (Hours)	1	2.7222	0.9458	0.3409
Temperature * Residence Time	1	4.9408	1.7166	0.2031

T-tests were completed for each factor, drying temperature and drying residence time, in order to fully understand their effect on cis-zeaxanthin formation. The results from these tests can be seen in tables 7.19 and 7.20. As seen in table 7.19, all levels of drying temperature were proven to have a statistically different impact on cis-zeaxanthin formation.

Table 7.19: T-test analysis, effect of temperature on cis-zeaxanthin formed

Temperature Level	Level	% Cis Zeaxanthin Formed Mean
115	A	17.97
100	B	14.18
85	C	11.86
70	D	3.1667
55	E	-0.06

Table 7.20: T-test analysis: effect of residence time on cis-zeaxanthin formed

Residence Time (hours) Level	Level	% Cis Zeaxanthin Formed Mean
4	A	15.33
6	A	14.72
2	A	13.94

Table 7.20 displays the t-test analysis completed for the effect of the drying residence time levels on cis-zeaxanthin. This analysis confirms the earlier conclusion made from the ANOVA analysis and re-iterates the fact that drying residence time does not have a statistically significant effect on cis-zeaxanthin. No drying residence times were found to be statistically different from any other level.

Further investigation of table 7.19 reveals a direct relationship between drying

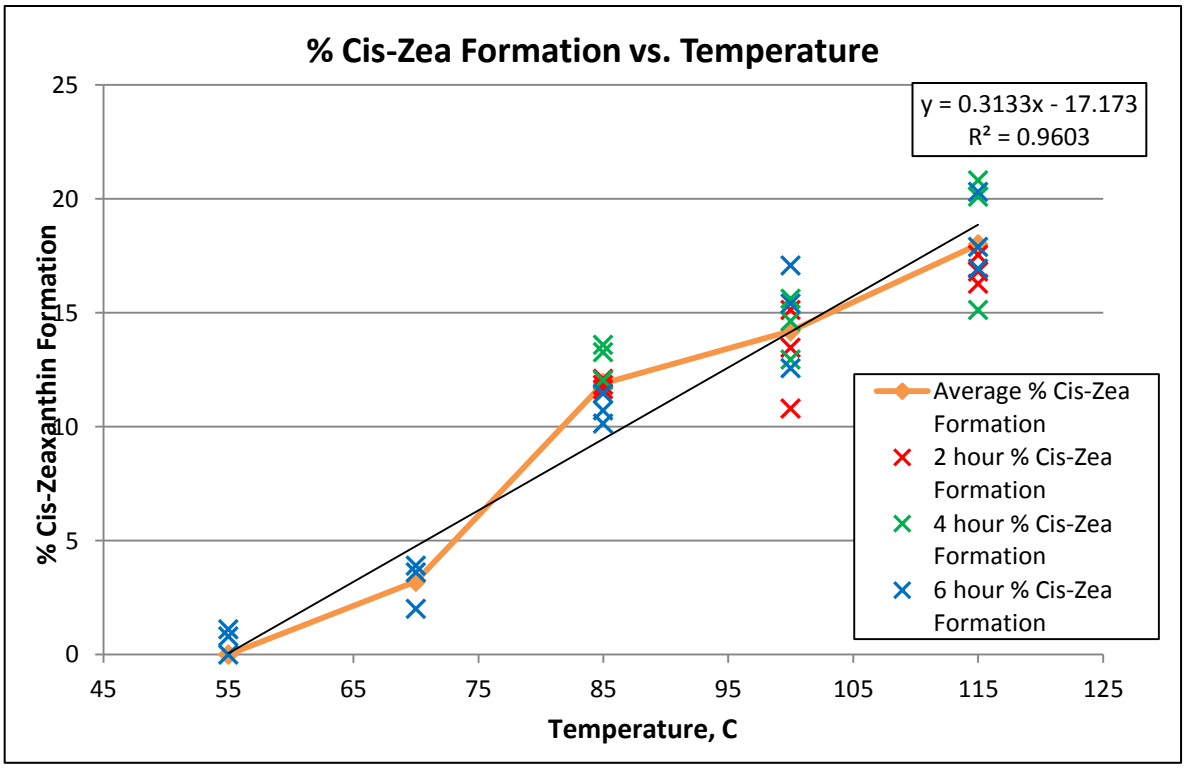

Figure 7.17: % cis-zeaxanthin formation vs. Drying temperature

temperature and cis-zeaxanthin. As temperature increases, cis-zeaxanthin formation increases also. This relationship can be further investigated by examination for figure 7.17. Due to the analysis results' indicating that drying residence time is not a significant factor effecting cis-zeaxanthin formation, data can be averaged at each drying temperature level to create one data point per level. Figure 7.17 was developed using these methods. The relationship between drying temperature and % cis-zeaxanthin formed during drying becomes very evident when examining figure 7.17. It becomes evident that cis-zeaxanthin can be minimized by utilizing drying temperatures below 55˚C

An investigation of the drying rates of both the sepals and berries can be seen in figure 7.18. The initial moisture content of the sepals and berries prior to drying was 40% and 75%, respectively. As seen, a considerable amount of time is required to remove moisture from the berries, while the sepals dry down very quickly. This information validates the differential drying approach to removing moisture from the sepal and berry material, at different rates. It is this difference in moisture removal rates that allows the differential drying and abrasion process to achieve successful separation.

Overall, the differential drying and abrasion system has been proven capable of separating the outer sepal from the inner berry, effectively creating two component streams with minimal to zero cross contamination between components. When material is dried to within the recommended moisture contents, below 5.5% for sepal and between 20-30% for berries, the separation method is capable of achieving separation efficiencies of 98.36%. Degradation of zeaxanthin during the drying process can be minimized by utilizing

temperatures of 55˚C and below.

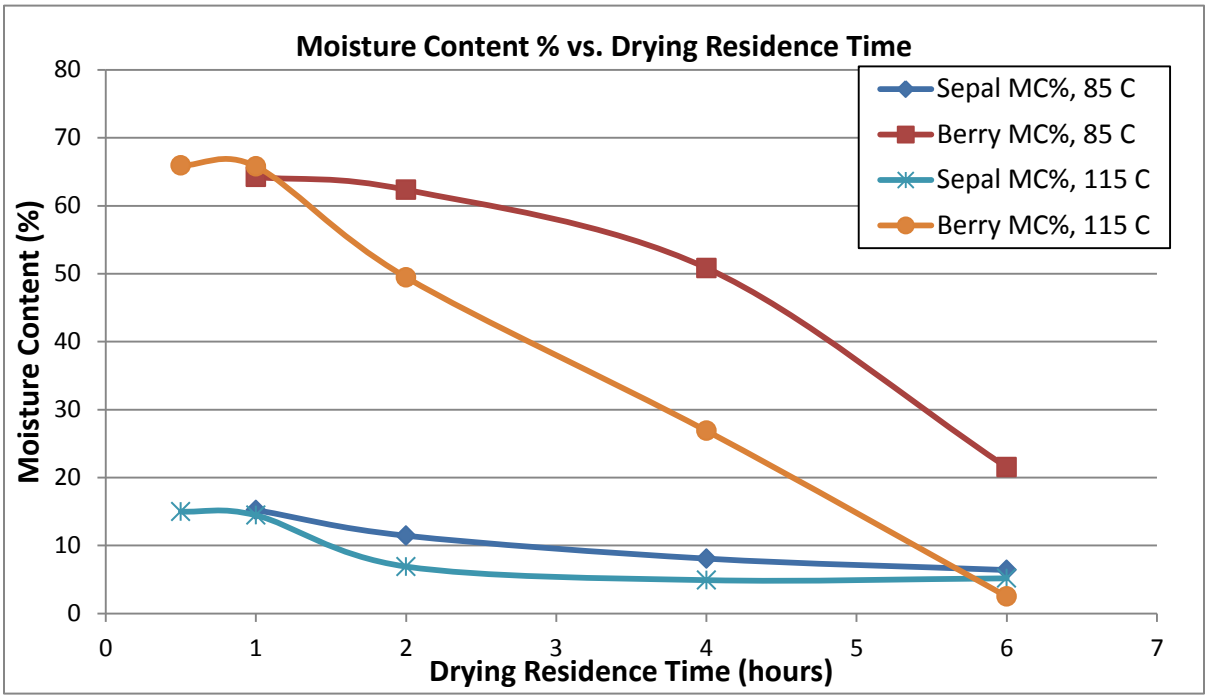

Figure 7.18: Moisture content of sepals and berries vs. drying residence time.

CHAPTER 8: CONCLUSIONS AND RECOMMENDATIONS

8.1 Conclusions

The goal of this research work was the development of a mechanical harvesting and post-harvest processing system for Chinese lantern that will allow for commercial production and advancement of the crop. In order to achieve this goal, several systems and machines were developed, fabricated and tested. Throughout observation and testing, improvements were continuously made to each system in order to maximize performance. Conclusions for both the mechanical harvesting and post-harvest separation systems will be discussed throughout this section

8.1.1 Mechanical Harvesting System

Over the course of two harvest seasons, three mechanical harvesting systems for Chinese lantern were developed and tested. The manual powered rotary harvesting system provided a platform for initial testing of the specifically designed stripping fingers. The results of this testing essentially proved that a stripping method could the utilized to remove Chinese lanterns from plant stems. The stripping fingers performed very well, achieving an average stripping efficiency of 96.71%. However, high collection losses were also observed during testing. The development and testing of the integrated harvesting and collection belt system reduced these collection losses. While challenging crop conditions and differences in plant geometry significantly reduced stripping efficiency, several key observations during testing allowed improvements to be made throughout the entire system. These improvements were utilized in the development and testing of the self-propelled harvesting system.

The self-propelled harvested was tested in dense, second year crop. This crop provided many challenges that drove the development of the guide and pin header system. This system increased harvesting efficiency while stabilizing the finger position and immensely improving header durability.

Overall, the testing of each harvesting system has proven that Chinese lanterns can be successfully harvested using a stripping method. The stripping fingers are capable of combing through Chinese lantern crop and detaching whole lanterns with high efficiency. However, plant geometry and crop density have a significant impact on both stripping efficiency and overall system performance. Crops consisting of SVS are ideal for a harvesting system that utilizes stripping technology to remove wanted material. Branched and low-lying crops reduce stripping efficiency and tend to become entangled in the stripping elements of the header. Both header designs testing throughout this work have shown potential to be highly effective for harvesting Chinese lanterns with minimal additional development. The fundamental result of the harvesting system research is that mechanical harvesting of Chinese lanterns can be accomplished utilizing specifically designed stripping elements and header system.

8.1.2 Post-harvest Separation System

Several methods of removing the sepal from the berry were investigated throughout this research work. Both the frictional roller and the drying and abrasion methods proved to be effective at separating the sepal from the berry.

The frictional roller system was developed very heavily and utilized for separation of the entire 2012 Chinese lantern crop. Very high separation efficiencies can be achieved with the frictional roller method if lanterns are orientated correctly, stem first, when presented to

the rollers. However, separation efficiency suffers greatly when lanterns are delivered to the rollers with a random orientation. A disadvantage of the frictional roller separation system is potential for and rate of berry crushage during separation. This crushage introduces unwanted materials into the separated sepal stream and is unacceptable for further downstream processing. The major limiting factor for this system has proven to be the orientation of the lanterns.

The drying and abrasion method proved to be a highly effective method to separate the sepal from the berry. Separation efficiencies for this system exceeded that of the frictional roller method. The drying and abrasion system offers better process and parameter control when compared to the frictional roller method. Drying parameters; temperature, time, and airflow, can be optimized in order to maximize separation efficiency and minimize berry breakage and fragmentation. The limiting factor for this process involves the effect of drying on the zeaxanthin content of the sepal. However, degradation of the zeaxanthin content can most likely be minimized through the use of drying parameters that minimize the temperature at which the material is exposed to.

Overall, the drying and abrasion method has proven to be the most effective method for separation of the sepal from the berry. When material is dried to the correct moisture content, testing of this system has resulted in separation efficiencies of 98.36% with zero berry fragmentation. The two processes involved in the system, differential drying and abrasion, can be developed to commercial scale and adapted to create a continuous flow process that is necessary to achieve high throughput. The overall conclusion of the separation system research work is that drying and abrasion has been proven to be highly efficient at mechanically removing the sepal from the berry.

8.2 Recommendations

This research work provided a considerable amount of information and insight on both the mechanical harvesting and post-processing of Chinese Lanterns. However, further study is recommended in order to increase the performance and efficiencies of both systems. A full scale DOE is needed to fully analyze and understand the performance of the mechanical harvesting system in regards to machine parameters. The harvesting header and stripping belt movement path could be modified to include the best aspects of the rotary system while retaining the stripping finger belt system to convey harvested material.

Recommendations for further study and improvement of the mechanical harvesting system are as follows:

- Develop two modified header designs for the self-propelled harvester.
    - Large scale rotary header
    - Modified harvesting and collection belt design with guide and pin system
- Complete a full scale DOE to compare the performance of the two headers harvesting in similar crop conditions.
- Investigate the effect of machine parameters on stripping and overall efficiencies.
    - Stripping finger linear speed
    - Forward machine speed
- Utilize a conveyor belt to move material across the header to minimize material wrapping and plugging of the header.
- Utilize standard components for harvesting headers to facilitate scale-up of the system.

- Use of a defoliant on the Chinese lantern crop may reduce the amount of foliage throughout the crop structure. Resulting in a lower load on the harvesting header.

Further investigation of the separation system is necessary to optimize process parameters and increase separation efficiency. Recommendations for further study and investigation of the separation system are as follows:

- Investigate the effects of airflow rate during drying on drying time and subsequent separation efficiency.
- Develop and test a continuous flow drying and abrasion system using moisture content of incoming and outgoing material as a reference to determine drying parameters and achieve maximum separation efficiency.
- Integrate the moisture content guidelines developed throughout this work into a commercial scale separation system.

APPENDIX

Table A-1: Self-propelled harvester hydraulic component list

Hydraulic System Components				
Component	**Manufacturer**	**Part #**	**Quantity**	**Description**
Main hydraulic pump	Sauer Danfoss	LRR025CLS2315NNN3C2 C2BGANKNBNNNNNN	1	Series 45 axial piston pump
Valve block	Sauer Danfoss	157B6530	8	PVG 32 basic module
Valve block	Sauer Danfoss	157B5914	1	Pump side module
Valve block	Sauer Danfoss	157B2020	1	End plate
Valve block	Sauer Danfoss	157B2265	8	Shock and suction valve assembly
Valve spool	Sauer Danfoss	157B7002	4	PVG 32 valve spool
Valve spool	Sauer Danfoss	157B7003	4	PVG 32 valve spool
Cylinder	Maxim	218-306	2	Header lift cylinders
Cylinder	Maxim	218-306	1	Header tilt cylinder
Cylinder			1	Conveyor elevation cylinder
Motor	Char Lynn	104-3099-006	1	Main header belt drive
Motor	Char Lynn	101-1706	1	Header auger drive
Motor	Char Lynn	101-1706	1	Conveyor drive motor
Heat Exchanger	ASA Hydraulics	1B021373	1	Hydraulic fluid cooler

Table A-2: Self-propelled harvester engine and electronic components

Component	Manufacturer	Part #	Quantity	Description
Engine Component				
Diesel Engine	Lombardini	1603 LDW	1	3 cylinder diesel engine
Mobile Electronic Components				
Joystick	Sauer Danfoss	JS7000M1SMNNNNCANJ90TV NNVRB5TRTBTBTYTYNNNNN NNNNNPNSBN	1	Right machine control joystick
Joystick	Sauer Danfoss	JS7000M1SMNNNNCANJ93TV NNVRB5TRTBTBTYTYNNNNN NNNNNPNSBN	1	Left machine control joystick
Display	Sauer Danfoss	DP600SAC2V2KS	1	Operator station display
Microcontroller	Sauer Danfoss	MC088-015	1	Machine microcontroller
Valve Actuator	Sauer Danfoss	157B4735	8	PVE electronic valve actuator

Table A-3: Vibration orientation testing results: tube height, vibration amplitude, percentage of lanterns by orientation

Parameters			Percentage of lanterns											
Test #	Tube Height (cm)	Amplitude (mm)	0° (stem first)	45°	90°	135°	180°	Stuck in tube	Stuck on table	0° (stem first)	45°	90°	135°	180°
1	2.54	0.61	0.0%	4.0%	4.0%	0.0%	4.0%	88.0%	0.0%	0.0%	0.0%	0.0%	0.0%	0.0%
2	2.54	0.61	0.0%	4.0%	0.0%	0.0%	0.0%	96.0%	0.0%	0.0%	0.0%	0.0%	0.0%	0.0%
3	2.54	0.61	0.0%	0.0%	0.0%	0.0%	0.0%	92.0%	8.0%	0.0%	0.0%	4.0%	0.0%	4.0%
4	2.54	0.91	0.0%	4.0%	8.0%	4.0%	0.0%	76.0%	8.0%	4.0%	0.0%	4.0%	0.0%	0.0%
5	2.54	0.91	20.0%	4.0%	32.0%	12.0%	24.0%	8.0%	0.0%	0.0%	0.0%	0.0%	0.0%	0.0%
6	2.54	0.91	20.0%	20.0%	28.0%	12.0%	8.0%	8.0%	4.0%	0.0%	4.0%	0.0%	0.0%	0.0%
7	2.54	1.22	20.0%	16.0%	12.0%	20.0%	20.0%	8.0%	4.0%	4.0%	0.0%	0.0%	0.0%	0.0%
8	2.54	1.22	20.0%	24.0%	20.0%	20.0%	12.0%	4.0%	0.0%	0.0%	0.0%	0.0%	0.0%	0.0%
9	2.54	1.22	20.0%	20.0%	16.0%	32.0%	12.0%	0.0%	0.0%	0.0%	0.0%	0.0%	0.0%	0.0%
10	3.18	0.61	4.0%	4.0%	4.0%	0.0%	0.0%	88.0%	0.0%	0.0%	0.0%	0.0%	0.0%	0.0%
11	3.18	0.61	8.0%	0.0%	8.0%	4.0%	4.0%	76.0%	0.0%	0.0%	0.0%	0.0%	0.0%	0.0%
12	3.18	0.61	24.0%	8.0%	28.0%	12.0%	16.0%	0.0%	12.0%	8.0%	0.0%	0.0%	0.0%	4.0%
13	3.18	0.91	20.0%	12.0%	32.0%	16.0%	8.0%	4.0%	8.0%	0.0%	0.0%	0.0%	8.0%	0.0%
14	3.18	0.91	16.0%	12.0%	20.0%	20.0%	20.0%	0.0%	12.0%	8.0%	4.0%	0.0%	0.0%	0.0%
15	3.18	0.91	16.0%	20.0%	20.0%	16.0%	20.0%	0.0%	0.0%	8.0%	0.0%	0.0%	0.0%	0.0%
16	3.18	1.22	16.0%	8.0%	24.0%	32.0%	16.0%	0.0%	4.0%	0.0%	4.0%	0.0%	0.0%	0.0%
17	3.18	1.22	16.0%	16.0%	28.0%	24.0%	16.0%	0.0%	0.0%	0.0%	0.0%	0.0%	0.0%	0.0%
18	3.18	1.22	12.0%	20.0%	24.0%	16.0%	20.0%	0.0%	8.0%	4.0%	0.0%	0.0%	4.0%	0.0%
19	3.81	0.61	4.0%	0.0%	0.0%	8.0%	0.0%	84.0%	4.0%	0.0%	0.0%	0.0%	0.0%	4.0%
20	3.81	0.61	8.0%	4.0%	4.0%	4.0%	0.0%	80.0%	0.0%	0.0%	0.0%	0.0%	0.0%	0.0%
21	3.81	0.61	0.0%	4.0%	0.0%	4.0%	4.0%	88.0%	0.0%	0.0%	0.0%	0.0%	0.0%	0.0%
22	3.81	0.91	12.0%	24.0%	8.0%	12.0%	12.0%	0.0%	32.0%	4.0%	12.0%	0.0%	4.0%	12.0%
23	3.81	0.91	20.0%	20.0%	44.0%	8.0%	8.0%	0.0%	0.0%	0.0%	0.0%	0.0%	0.0%	0.0%
24	3.81	0.91	20.0%	32.0%	28.0%	12.0%	8.0%	0.0%	0.0%	0.0%	0.0%	0.0%	0.0%	0.0%

Table A-3 Cont.: Vibration orientation testing results: tube height, vibration amplitude, percentage of lanterns by orientation

Parameters			Percentage of lanterns											
Test #	Tube Height (cm)	Amplitude (mm)	0° (stem first)	45°	90°	135°	180°	Stuck in tube	Stuck on table	0° (stem first)	45°	90°	135°	180°
25	3.81	1.22												
26	3.81	1.22	Unable to tell, one group of lanterns falling off vibration table. Not feasible											
27	3.81	1.22												
28	4.45	0.61	8.0%	28.0%	32.0%	12.0%	8.0%	0.0%	12.0%	0.0%	0.0%	8.0%	0.0%	4.0%
29	4.45	0.61	12.0%	8.0%	32.0%	20.0%	4.0%	0.0%	24.0%	12.0%	0.0%	8.0%	4.0%	0.0%
30	4.45	0.61	8.0%	16.0%	48.0%	8.0%	12.0%	0.0%	8.0%	0.0%	4.0%	4.0%	0.0%	0.0%
31	4.45	0.91	12.0%	16.0%	32.0%	20.0%	12.0%	0.0%	8.0%	0.0%	0.0%	4.0%	4.0%	0.0%
32	4.45	0.91	20.0%	16.0%	40.0%	8.0%	8.0%	0.0%	8.0%	0.0%	8.0%	0.0%	0.0%	0.0%
33	4.45	0.91	20.0%	16.0%	28.0%	12.0%	24.0%	0.0%	0.0%	0.0%	0.0%	0.0%	0.0%	0.0%
34	4.45	1.22												
35	4.45	1.22	Unable to tell, one group of lanterns falling off vibration table. Not feasible											
36	4.45	1.22												

Table A-4: Differential drying and abrasion system testing results, optimization tests completed with Chinese lantern material

Test #	Drying Temp (˚C)	Drying Residence Time (hours)	Tumbling Time (min)	Separation Efficiency	% Berries Recovered Intact	Berry MC, %	Sepal MC, %
1	55	6	N/A	N/A	N/A		
2	55	6	N/A	N/A	N/A	65.5	6.3
3	55	6	N/A	N/A	N/A		
4	70	6	N/A	N/A	N/A		
5	70	6	N/A	N/A	N/A	59.4	6.4
6	70	6	N/A	N/A	N/A		
7	85	1	5	44.51%	50.00%	64.23	15.21
8	85	2	5	41.74%	100.00%	61.7	7.6
9	85	2	15	63.04%	60.00%	63.00	15.29
10	85	4	5	69.61%	100.00%	46.85	7.42
11	85	4	5	58.94%	100.00%	54.4	7.5
12	85	4	15	59.93%	60.00%	51.28	9.29
13	85	6	5	98.36%	100.00%	17.01	6.25
14	85	6	5	65.11%	100.00%	32.7	6.6
15	85	6	15	97.47%	90.00%	14.84	6.31
16	100	2	5	61.01%	100.00%	55.9	4.5
17	100	4	5	36.36%	100.00%	23.7	6.1
18	100	6	5	94.20%	80.00%	12.3	5.8
19	115	0.5	5	24.13%	50.00%	64.92	14.2
20	115	0.5	15	33.22%	30.00%	66.92	15.8
21	115	1	5	47.17%	50.00%	65.78	14.45
22	115	2	5	55.24%	100.00%	47.2	5
23	115	2	5	51.32%	90.00%	51.74	8.8
24	115	4	5	95.39%	100.00%	25.08	5.08

Table A-4 Cont.: Differential drying and abrasion system testing results, optimization tests completed with Chinese lantern material

Test #	Drying Temp (˚C)	Drying Residence Time (hours)	Tumbling Time (min)	Separation Efficiency	% Berries Recovered Intact	Berry MC, %	Sepal MC, %
25	115	4	5	83.82%	100.00%	16.7	4.3
26	115	4	15	95.48%	90.00%	32.13	4.59
27	115	4	15	95.00%	100.00%	36.73	5.05
28	115	4	15	93.98%	100.00%	23.78	5.49
29	115	6	5	100.00%	10.00%	2.03	6.42
30	115	6	5	99.46%	20.0%	2.9	3.7
31	115	6	15	99.20%	20.00%	2.82	5.12
32	115	6	15	98.73%	10.00%	2.22	5.43

REFERENCES

ASABE Standards. 2007. S269.5 – Densified Products for Bulk –Definitions and Method. St. Joseph, MI,: ASABE.

Cargill, B.F., 1999. *Fruit and Vegetable Harvest and Mechanization – Technological Implications*, Rural Manpower Center, Michigan State University, Michigan.

Cloud, Norman. Kemin Industries, Personal Communication, June 1, 2011)

Tado, CJM. P. Wacker, H.D. Kutzbach, D.C. Suministrado *Journal of Agricultural Engineering Research, Volume 71, Issue 2, October 1998, Pages 103-112*

Crawford, B. Fruit Husking Machine. Patent 2362356. 7 Nov. 1944.

Den Hartog, J.P., 1985. *Mechanical Vibrations*, London: Dover Publishers

Flores, Tomatillo Husking Machine. Patent 20070212463. 13 Sept. 2007. Print.

Granger, Apparatus for Dehusking Small Fruits. Patent 20020100373. 1 Aug. 2002.

Kepner, R.A., R. Bainer and E.L. Barger, 1987. *Farm Machinery*, CBS Publishers and Distributors, Daya Basti, Delhi.

Kutz, Myer. *Handbook of Farm, Dairy, and Food Machinery*. Norwich, N.Y., U.S.A.,: William Andrew Pub., 2007.

Erickson. Merritt C. Fruit Stripping Rakes. Patent 5,437,146. 1 Aug. 1995. Print

Oliveros Tascon, Carlos Eugenio et al. Coffee Harvest With Portable Stem Vibrators. *Rev.Fac.Nal.Agr.Medellín* [online]. 2005, vol.58, n.1 [cited 2013-01-28], pp. 2697-2708

Papesch J; Dammer S; Fechner WGrain stripper-Capacity and harvesting losses when harvesting grain and linseed]. Landtechnik, 1995, 50(4), 196-197

Peterson, D.L.: Harvest mechanization progress and prospects for fresh market quality deciduous tree fruits. Hort Technology 15(1), 72–75 (2005)

Plebe, Alessio, and Giorgio Grasso. "Localization of Spherical Fruits for Robotic Harvesting."*Machine Vision and Applications* 13.2 (2001): 70-79. *Springer Link*. Springer-Verlag. Web. 28 Jan. 2013.

Sarig Y (1993) Robotics of fruit harvesting – a state-of-the-art review. J.Agric Eng Res 54: 265–280

Shelbourne, Keith H. Crop Strippers and Stripper Toothing. Shelbourne Reynolds Engineering, Patent 6,315,659. 13 Nov. 2001. Print

Thomson, W.T., 1988. Theory of Vibration with Applications, 3rd Ed, New Jersey: Prentice Hall.

Wang, Jaw-Kai. *Equipment for Husking Poha Berries*. Dec. 1966. Technical Bulletin. Hawaii Agriculture Experimental Station, University of Hawaii.

W.E. Klinner, M.A. Neale, R.E. Arnold, A.A. Geikie, R.N. Hobson *Journal of Agricultural Engineering Research*, Volume 38, Issue 1, September 1987, 37-45

Wrigley, G.A.,1988. *Coffee*, Longman, Singapore.